NTNU – Trondheim
Norwegian University of
Science and Technology

Foam for Flow Assurance in Gas-Condensate Pipelines

Thereza Karam

Petroleum Engineering
Submission date: June 2013
Supervisor: Jon Steinar Gudmundsson, IPT

Norwegian University of Science and Technology
Department of Petroleum Engineering and Applied Geophysics

Norwegian University
of Science and Technology

Department of Petroleum Engineering
and Applied Geophysics

Master of Science in Petroleum Engineering

Foam for Flow Assurance in Gas-Condensate Pipelines

Author:
Thereza Karam

Supervisor:
Professor Jon Steinar Gudmundsson

June, 2013

Trondheim, Norway

Abstract

Use of foam in the oil industry is employed for lifting cuttings in drilling operations, for removal of liquid loading in vertical wells and for increasing oil recovery. Limited researches discussed the foam applicability as a flow assurance practice. This study is an initial attempt to investigate the possibility of using foam to remove or reduce liquid accumulations in horizontal gas-condensate pipelines.

The different rheological models of foam had been examined along with the corresponding correlations. Foam was treated as either a Bingham plastic or a Power law flow. The slippage at the wall was also accounted for. Accordingly, the pressure drop, on which sensitivity analysis was applied, was calculated for three different foam qualities. A simplified laboratory experiment was carried out to compare model calculations to measurements. Practical aspects as the use of equipment and foaming agents were suggested.

Based on the results, it can be concluded that foam induction in horizontal conduits leads to great pressure losses compared to multiphase flow. A comparison of the calculated models and the experiments suggested treating foam as a Power law fluid with the consideration of the wall slip layer. According to the practical aspects, foam is classified as an economical and eco-friendly procedure. Regardless of maintaining a continuous production, the uncertainty attributed to foam behavior recommends some further work to be carried out for a better understanding of its effects.

Preface

This master thesis is submitted in partial fulfillment of the requirements for the degree of Master of Science in Petroleum Technology - Petroleum Production in the Department of Petroleum Technology and Applied Geophysics in the Norwegian University of Science and Technology. It is a product of work carried out between January 14 and June 6, 2013.

I hereby declare that this is an independent work according to the exam regulations of the Norwegian University of Science and Technology.

I would like to express my gratitude to my supervisor Jón Steinar Gudmundsson for introducing me to this interesting subject and for the useful comments and the continuous help and support throughout this semester.

Furthermore, I would like to thank Håkon Myhren and Terje Bjerkan for setting up the experiment and for their continuous assistance and help during the process of running the experiments. I would also like to thank Åge Sivertsen for his contribution with the electric part of the experiment. For helping with some of the equipment and design required for running the experiments, I would like to thank for that Roger Overså. Finally, I would like to thank all my family and friends for their support and motivation during this semester.

Contents

List of Figures

List of Tables

Nomenclature

A	Area, m^2
D	Pipe inner diameter, m
D_h	Pipe diameter, m
d	Bubble diameter, m
E	Expansion ratio
E_g	Gibbs elasticity, N/m
f	Friction factor
k	Consistency index, $lb.s^n/ft^2$
L	Pipe length, m
l_p	Pipe Perimeter, m
n	Flow behavior index
ΔP	Pressure drop, Pa
Q	Volumetric Flow rate
q	Flow rate, m^3/s
Re	Reynolds number
r	Pipe radius, m
t	time, s
u	Superficial velocity, m/s
$\overline{u}$	Average velocity, m/s

Greek Letters

Γ	Foam quality, %
$\dot{\gamma}$	Shear rate, s^{-1}
δ	Slip layer thickness, m
ε	Pipe roughness, m
μ	Viscosity, $Pa.s$
ρ	Density, kg/m^3
σ	Surface tension, N/m
τ	Shear Stress
ϕ	Surfactant concentration

Subscripts

e	Effective
f	Foam
g	Gas
l	Liquid
M	Moody
m	Mixture
p	Plastic
w	Wall
y	Yield

Chapter 1

Introduction

Flow assurance has been highlighted considerably as problems associated with production are expanding especially with aging fields and developments in remote areas. The high demands of the market along with the pressure exerted by the government forced oil companies to increase the production rates per day. The operations are then conducted under slug flow regime. The large concentrations of liquid accumulating at the bottom of the low lying sections led to the reduction in production as well as the corrosion of pipes. Solutions to avoid such occurrences have been researched throughout the years in order to enable an efficient and economical optimization of production.

Foam has been introduced in the oil industry a while ago. At first, it has caused some problems with the equipment at the receiving terminals if not controlled. The worst case scenario could result in a shutdown of the line. Afterwards, it has been applied as one of the EOR techniques to increase the oil recovery. It was also used for drilling purposes where its characteristics helped in lifting the cuttings in underbalanced drilling operations. Foam was rarely considered as a flow assurance solution. It might be a good alternative to pigs and slug catchers for removing or limiting liquid accumulations. The scarcity of the data and research about its behavior, which is classified as unpredictable, makes it hard to estimate the pressure drop.

The pressure drop attributed to foam, according to several sources, is relatively higher than that of a multiphase flow. This might cause some operational problems and hazardous situations when inducing it. This study will evaluate the different rheological foam behaviors to estimate the pressure drop and compare it with the statement of a high pressure loss developed with the use of foam. Additionally, a simplified laboratory experiment will be done to somehow mimic the flow conditions and check whether theoretical calculations are consistent with experimental data.

To evaluate the applicability of foam for flow assurance, other parameters have to be emphasized. The foaming agents needed to induce the foam, their concentration, the injection techniques are to be exposed. Furthermore, as the environmental concerns are rising, the biodegradability of foam and foaming agents has to be highlighted. A constant temperature and no expansion of the gas phase imposed some limitations on the development of this study.

Chapter 2

Multiphase Flow in Gas Pipelines

2.1 Flow Patterns in Gas-Condensate Pipelines

Transport of gas from offshore facilities up to land terminals takes place through multiphase flow pipelines. Most of the fields produce more than one fluid phase simultaneously. High pressure in the reservoir causes the gas to dissolve in the oil or the water to dissolve in the gas. As production is initiated, the pressure is reduced and the dissolved gas or water comes out of solution leading to a multiphase flow in pipelines. Similarly, water comes along gas production especially in aging fields where the majority of the hydrocarbons was already produced. Thus, single fluid phase is rarely encountered in real field production.

By definition, a multiphase flow consists of simultaneous flow of materials of different phases or materials of different chemical properties but of the same phase. It is made-up mainly of a continuous phase known as the primary phase and some dispersed phase(s) within the primary phase known as the secondary phase.

Flow pattern understanding is essential for an accurate estimation of the pressure drop in long pipelines. Both the friction pressure drop and the in-situ liquid volume fraction correlations depend on the flow pattern. The total pressure drop estimation should include the hydrostatic head calculated with the mixture density.

Several multiphase flow regimes are represented in horizontal pipelines. A two-phase flow of water and gas in the pipeline is assumed. The phase separation takes place usually when the gravity effect is perpendicular to the pipe axis. Six different flow patterns can occur in the horizontal pipe and are represented in Figure 2.1. These regimes vary as a function of the increasing flow rate velocities. Stratified smooth (SS) pattern represents the most recurrent flow regime in pipes where both gas and liquid streams are being separated. A smooth and parallel interface appears due to gravity. A slight increase in the gas velocity leads to a stratified wavy (SW) pattern where waves form on the gas-liquid interface.

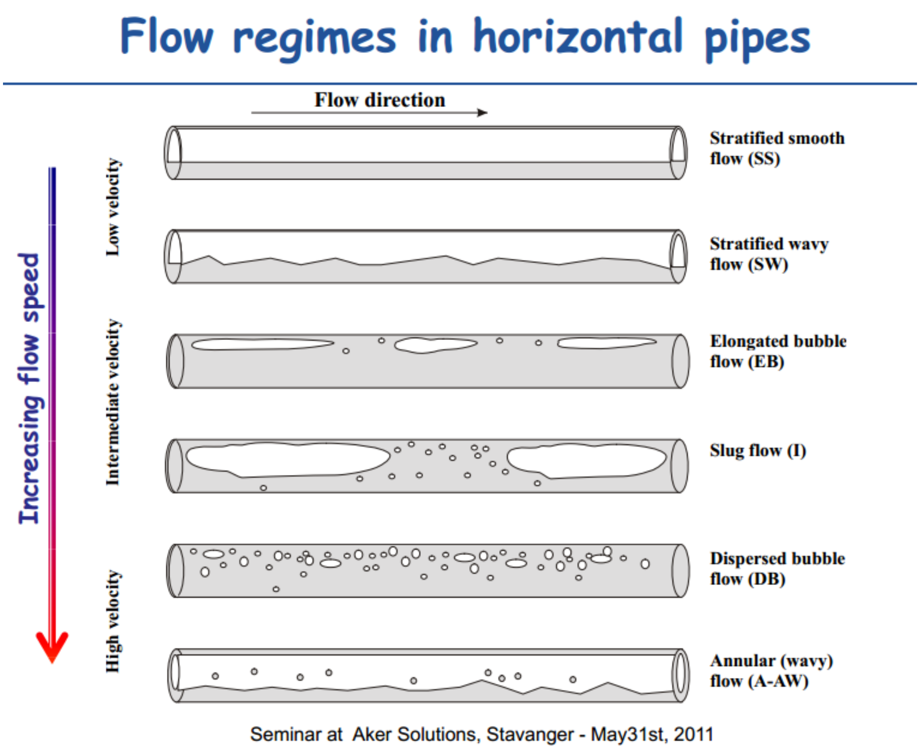

Figure 2.1: An illustration of the six different flow regimes forming in horizontal pipes (Karam, 2012)

More complex flow regimes evolve with the considerable increase in the gas velocity. Elongated bubble flow (EB), also known as plug flow, consists of liquid plugs that are separated by elongated gas bubbles. The liquid phase lies continuously at the bottom of the pipe due to the large diameter of the elongated bubbles. The slug flow (I) arises when the size of the latter increases along with the increasing flow velocity to the point where the bubbles reach a size similar to that of the channel. As a result, some liquid slugs are left behind.

An extensive distribution of the gas phase in the form of bubbles or droplets in the continuous liquid phase leads to a dispersed bubble flow (DB). The highest flow rate induces an annular (wavy) flow (A-AW). Hence, an annular film of liquid will develop around the tube. The film is thicker at the bottom of the tube than at its top. The interface between the liquid film and the gas is disrupted by some small amplitude waves; furthermore, some droplets can emerge in the gaseous phase (Karam, 2012).

2.2 Problems in Multiphase Gas-Condensate Pipelines

Liquid holdup constitutes one of the major problems encountered in long-distance multiphase gas pipelines. It arises when both gas and liquid phases flow with two different velocities within the pipeline. Such an effect takes place when the slug flow regime is dominating. A mixture zone develops due to the faster moving slug front flows compared to the underlying liquid film which will speed up to the same velocity as the slug. Some bubbles will be released in the mixing zone due to the entrainment of a significant amount of gas. These are driven to the bottom of the pipe where they can crash and collapse. Furthermore, liquid water condensates out from the gas condensates and formation water may also be added to the system at the later stages of production.

The effects of such occurrences in the pipe are remarkable. An increase in the corrosion rate and a decrease in the efficiency of corrosion inhibitors result from the bubble collapse. Furthermore, a slug flow in pipes usually leads to a large fluctuation in both gas and liquid flow rates and in large pressure variations. This can be illustrated by a low gas flow rate and low pressure followed by an increase in the liquid and gas rates due to slug development.

Two basic solutions can be implemented to solve such a problem in slug flow regimes. The reduction in production can cause a change of the flow pattern; thus, the slug flow will be replaced with a stratified flow reducing then the corrosion rate. On the other hand, an increase in the gas velocity leads to an annular flow and then to a reduction in the corrosion rate but an increase in the erosion rates.

Scale formation concerns engineers in long distance gas-condensate pipelines. It evolves due to either a chemical or a physical change in the water or the system. It represents a mineral compound mainly composed of calcium carbonates or sulfates but can also be calcium, magnesium carbonates. Scale is inhibited with the presence of water; therefore, it can be deposited wherever water exists and flows. Perforations, casing, production tubing, valves, pumps and downhole completion equipment can be blocked due to scale formation. Near wellbore area can suffer from a reduction in porosity and permeability as the scale blocks the formation pores. The fluid flow is then prevented as the wellbore is clogged (Crabtree et al., 1999). The damage caused by scale formation is enormous, intense and instant.

The rough seabed topography causes some additional challenges that the engineers have to cope with. Sand waves, steep slopes, rock outcrops and glacier scars cause the seabed to be irregular and uneven, thus, challenging production conditions have to be handled. The liquid accumulations intensify at the low lying parts of the pipe. For the pressure drop estimation, all the uphill elevation changes have to be accounted for.

Unlike single phase flow, the net elevation change is not to be considered in the case of multiphase flow. This difference is mainly created by the 'syphon effect'. The latter is commonly known in single phase flow where the hydrostatic head pressure losses in the uphill parts of the pipeline are recovered downhill. Such a recovery is absent in the case of a multiphase flow. As the fluid is flowing uphill, the liquid will fall back and cause an accumulation in the low lying parts. Consequently, the gas velocity increases as well as the friction and the pressure drop. Therefore, a full understanding of the elevation profile is crucial (Gregory and Aziz, 1975).

Liquid accumulations and slugs' removal concentrate the bulk of this study. Expensive solutions have to be implemented to handle the arrival of slugs at the receiving terminals. Buffer volumes, also known as slug catchers, represent one of these solutions due to its large size that can reach the size of a football field. The material used to build such a tool and the money invested in its maintenance explain the high cost associated with a slug catcher. Foam and foam flow, which will be further developed in this thesis, will be tested as an alternative tool to handle liquid accumulations and slugs in gas-condensate pipelines.

Chapter 3

Literature Review

3.1 Foam Characteristics and Overview

Foam make-up and composition have been repeatedly investigated. Foam is known as a colloidal gas emulsion in liquid phase where the continuous liquid phase surrounds and entraps the gaseous phase. The gas bubbles are homogeneously dispersed throughout the liquid phase. Stabilization of foam can come about through the use of surfactants and/or nano-particles. Foam, which is treated as a homogeneous fluid, has varying densities and viscosities. As foam is composed of two different phases one of which is compressible; it can be then considered as the only compressible non-Newtonian fluid. Thus, it is usually classified as a Power Law or Herschel-Bulkley fluid.

Foam is also classified as a colloid. By definition, colloids are particles that are less than 2 microns equivalent of spherical diameter (Schlumberger, 2013). As a matter of fact, the dispersed gas bubbles are larger than 10 μm as they are macroscopic and out of the colloid range. Contrariwise, the thin liquid layer that fills the space between the gas bubbles can be as small as some nanometers in thickness. In addition to that, the behavior and properties of foam rely on colloidal and surface forces along with the interaction between the liquid films separating the gas bubbles. Foam is a non-equilibrium dispersion as a complete segregation of both phases will be reached (Lyklema et al., 2005).

Foam density varies greatly especially due to the thickness of the liquid film separating the bubbles. It can be closer either to the liquid density or to the gas density. Disruption is considered as one of the most common products of gravity difference. The liquid will drain to the bottom while the gas will accumulate at the top. This occurrence continues until the surface tension is exceeded as the bubble walls will not handle it any longer.

Generally, low density and extremely high viscosity characterize foams. Its density is typically lower than that of the liquid phase. Furthermore, the difference in densities between the gas and the liquid phase causes the denser phase, the liquid phase, to separate from the main body. To avoid such an occurrence, the mixture has to be continuously agitated. Since foams are treated as a single phase fluid, its viscosity is to be higher than that of the two phases making it up. Some drilling challenges are solved due to these two features. An efficient cuttings' transport is ensured by the high viscosity while underbalanced conditions are established by the low density (Eren, 2004).

An accurate calculation of the foam density is essential for an accurate analysis of the foam behavior. Some studies have revealed a simplified assumption of the density by neglecting the gas in solution as well as the water-vapor pressure; thus, the gas density was constantly negligible. Hence, the foam density can be expressed as a function of the foam quality as follow:

$$\rho_f = \rho_L(1 - \Gamma) \tag{3.1.1}$$

On the other hand, the foam density is dependent upon the gas density as well as the pressure and temperature. The actual foam density is then calculated based on the following equation:

$$\rho_f = \rho_L(1 - \Gamma) + \rho_g\Gamma \tag{3.1.2}$$

A specific estimation of the foam density is also the basis for an accurate estimation of the friction factor as well as the Reynolds Number. These two are key parameters in determining the pressure loss in a pipe. A lower foam density reflects a lower Reynolds Number and a higher friction loss factor. As a result, the pressure drop due to foam presence can be overestimated (Lord, 1981).

3.2 Foam Stability

The applicability of foam in any system depends mainly on its stability. By nature, foam is thermodynamically unstable. This instability is attributed to the minimal gas surface interface which denotes a surface free energy: naturally, the system tends to reduce its energy level. Both the surface tension and the foam interfacial zone contribute to the calculation of this surface free energy. A decrease in the latter occurs by a breakdown of the foam membrane and a coalescence of the liquid. Hence, foam decomposition into its component's phases is spontaneous. As mentioned earlier, the liquid phase tends to drain from the main body due to its heavy density and a continuous phase is only maintained in case of incessant stirring. Such episode causes the foam instability as physical properties vary with time and height.

For an efficient and functional role, foam must not evolve during operations and experiments. High quality foams consisting of polyhedral gas bubbles tend to break faster than low quality foams made up of spherical gas bubbles. Its stabilization has to be ensured: the films are to be stabilized and the gas bubbles entrapped. Thus, many parameters affecting its stability and structure such as the presence and the type of surfactants used, the gravity effects on the drainage of the liquid phase and the shear stress have to be considered and controlled (Eren, 2004).

For foams with a quality less than 50%, the gas concentration is relatively low, the bubbles are rather dispersed and the liquid film thickness is considerable. Then spherical bubbles and thick liquid wall are characteristics of low quality foams. Such spherical bubbles will transform into polyhedral bubbles due to gravity effects. As a result of drainage, thinning will take place since the wall's bubbles tend to be thinner. Excessive thinning can be prevented by stirring which will redistribute the bubbles. On the other hand, agitation of high quality foams will cause the thinned polyhedral bubbles to break.

Surface tension is the second factor that contributes to the disruption of foam. A gas bubble would collapse due to the surface tension of the liquid in the bubble wall. This is balanced by the pressure within the bubble. The pressure inside a small bubble is higher than that inside a large bubble. This results from the inversely proportional relationship linking the pressure and the bubble size. When two bubbles are in contact, the gas of the smaller one diffuses into the large one. Hence, the smaller bubble shrinks and disappears while the larger bubble grows and the foam coarsens. The effects of the Young-Laplace Law are responsible for such occurrences.

Young-Laplace Law explains the diffusion of gas through a liquid film. It takes place when a curved interface is separating two different fluids. Thus, it explains the pressure drop that occurs at the interface. The latter is expressed by:

$$P_c = P_{gas} - P_{liquid} = \sigma(\frac{1}{R_1} + \frac{1}{R_2}) \tag{3.2.1}$$

P_c represents the capillary pressure or what is known as the pressure difference between the gas and liquid interface. Both R_1 and R_2 represent the two principal radii. This expression shows that the pressure between the gas and the liquid is not uniform at a curved interface when foam is present. A representation of the pressure inside and outside the sphere is shown in Figure 3.1. The ability of the small gas bubbles to diffuse into the larger ones is explained. As a result, a local strain develops and the length of the bubble edges is modified.

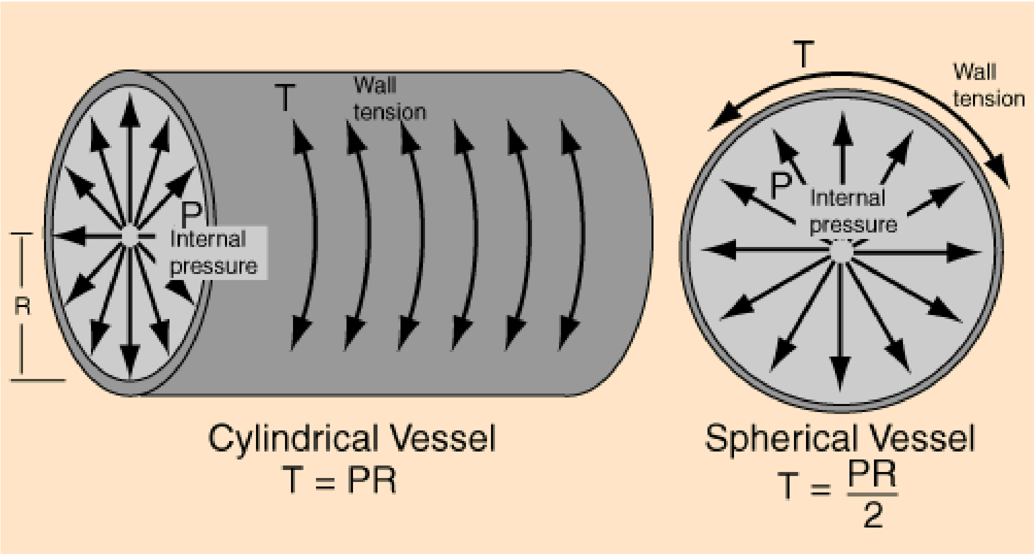

Figure 3.1: A representation of the Young-Laplace law where pressure inside a curved surface is higher than the outside pressure (Nave, 2013)

Two different processes arise from the difference in pressure between the inside and the outside of the gas bubble. To begin with, an unstable structure is attained when the edge of the bubble goes to zero. Then switching with the neighboring edge develops. Such a change in topology is known as a T1 process arising only in case of foam coarsening or if a macroscopic stress was applied to the system. In this case, the 2D rearrangement of the bubble matches up with the dissociation of a fourfold vertex into two threefold vertices, as shown in Figure 3.2. On the other hand, the T2 process takes place when the gas of a bubble is completely diffused to the neighboring bubble leading to the disappearance of the former.

Shear-strengthening surfactants play an important role in the stabilization of foam. When the thinning of the wall's bubbles take place, adding surfactants

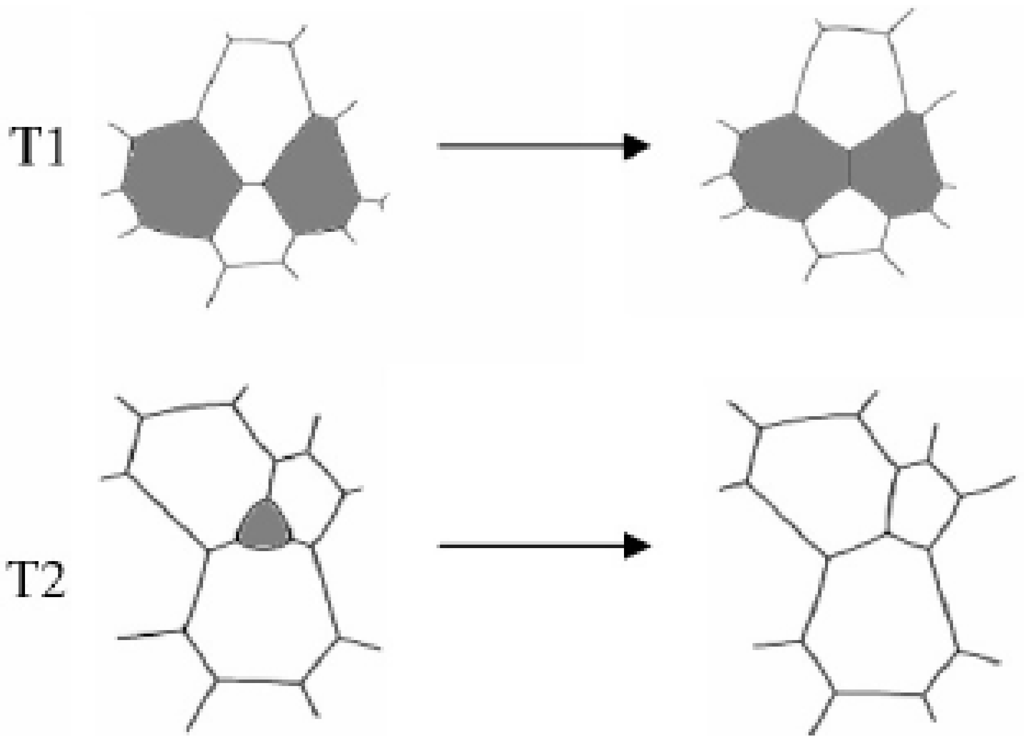

Figure 3.2: An illustration of the T1 and T2 processes in a 2D dry foam. The grey shade represents the bubbles that will combine in case of the T1 process or disappear in the case of the T2 process (Durian, 2002)

can prevent their breakdown, thus, strengthening them and stabilizing the foam. As they are present in different forms, their types affect the degree of stability ensured. A single surfactant would act differently under different conditions: a good stabilizing surfactant under specific conditions would react poorly under a different set of conditions. When an ionic surfactant is added to a system, the electrostatic forces play an important role in foam stabilization whereas structural forces are responsible for such effects when adding an anionic surfactant.

Modeling of foam stability is considered a difficult process. Surfactants, in addition to lowering the surface tension, promote foam formation. Stability cannot be ensured only by reducing the surface tension; many other factors have to be accounted for. Among those is the drainage of the liquid film which is affected, besides gravity, by the bulk and surface viscosity. Moreover, the resistance to mechanical disturbances and the ability to counteract film thinning, which are both controlled by the film elasticity, contribute to foam stabilization (Argillier et al.).

Chapter 4

Foam Characterization

Foam types and rheological characterization vary significantly. The classification and the differentiation of the various foam types are based mainly on its quality. The latter represents the ratio of gas to liquid in the mixture. On the other hand, being a dispersed and naturally unstable system, foam makes its rheological characterization challenging. Therefore, several parameters have to be taken into account when dealing with foam. Among those, we have the foam texture, production method, compressibility and the wall slip effect.

4.1 Foam Quality

Foam quality is a criterion considered for foam classification. It symbolizes the volume fraction of the gas phase. It can be determined by the ratio of the gas volume to the mixture volume. It is represented by the following formula for stationary foam, and it is usually given as a percentage,

$$\Gamma = \frac{V_g}{V_g + V_l}.100 \tag{4.1.1}$$

Since foam is always in motion in pipes, the quality is better expressed as a function of the flow rate. It is defined by the following formula:

$$\Gamma = \frac{q_g}{q_g + q_l}.100 = \frac{u_g}{u_g + u_l}.100 \qquad (4.1.2)$$

The area considered for the calculation of the velocity from the flow rate is represented as follow,

$$A = \frac{\pi D^2}{4} \qquad (4.1.3)$$

The acceptable foam quality range varies mostly between 52 and 96 %. It affects several parameters in the system such as the pressure drop and the volumetric flow rate. On the other hand, it depends on both the pressure gradient and the liquid flow rate in the pipe; it increases with the increase of both the pressure drop and the liquid flow rate.

According to quality, foam is divided into two categories. Low quality foam is known as wet foam since the liquid phase is more abundant and the gas volume fraction is low. Contrarily, high quality foam is known as dry gas as the dominating phase is the dry phase. According to Kuru et al. (1999), in their article 'New Directions in Foam and Aerated Mud Research and Development', low quality foam is recognized by $\Gamma < \Gamma_c$ and high quality foam by $\Gamma > \Gamma_c$. Γ_c represents the critical foam quality. The latter is the value at which the flow behavior of foam is changed from Newtonian to Non-Newtonian. It can vary between 45 and 75 %.

Other studies have showed that wet and dry gas cannot be distinguished by a well-defined criterion. Some others stated that very wet foam is recognized when the gas fraction is 0.63. Dry foam is recognized when the gas fraction surpasses 0.8. Some cases have shown extremely dry foam where the gas fraction exceeds 0.95. Such dryness affects both the mechanical and the rheological properties of the foam. The structure and the shape of the gas bubbles are represented in Figure 4.1 and 4.2.

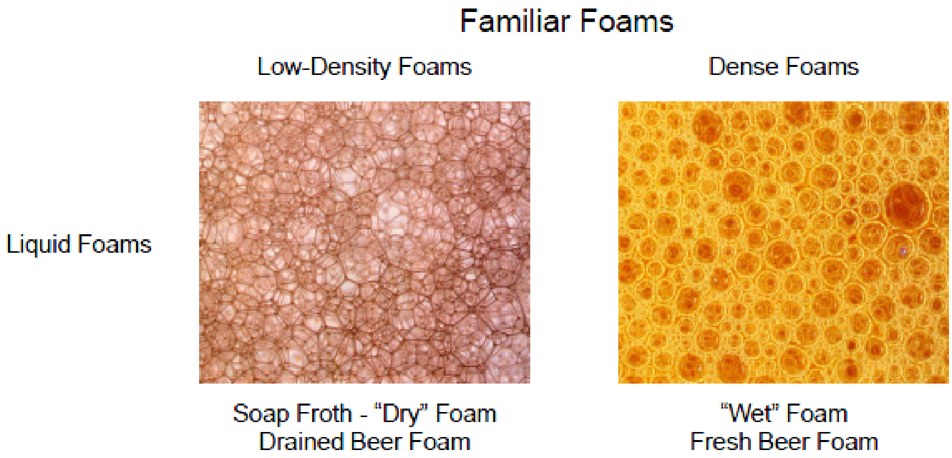

Figure 4.1: A representation of the two different categories of liquid foam with dry foam showing polyhedral bubbles and wet foam showing spherical bubbles (Kraynik et al.)

4.2 Foam Texture and Structure

Texture is the second criterion used to characterize foam. The size and the distribution of the bubbles represent the texture. The shape of the bubbles also contributes to foam characterization. The bubbles can either be spherical or polyhedral in shape. If the bubbles are spherical and are present in large concentrations, then the foam is called sphere foam. If the foam is newly generated, then it is also a sphere foam. On the other hand, a polyhedral foam consists of polyhedral bubbles.

In general, spherical bubbles are more likely to form due to the minimum energy principle. Moreover, spherical foam has a larger portion of liquid phase since randomly packed spheres have a low compaction. The increase of the gas volume fraction will cause the bubbles to compact and form polyhedral structures; thus, a polyhedral foam is a dry foam whereas a spherical foam is a wet foam. In ideal cases, a better foam would consist of polyhedral bubbles. The latter can have up to 12 sides (Lyklema et al., 2005).

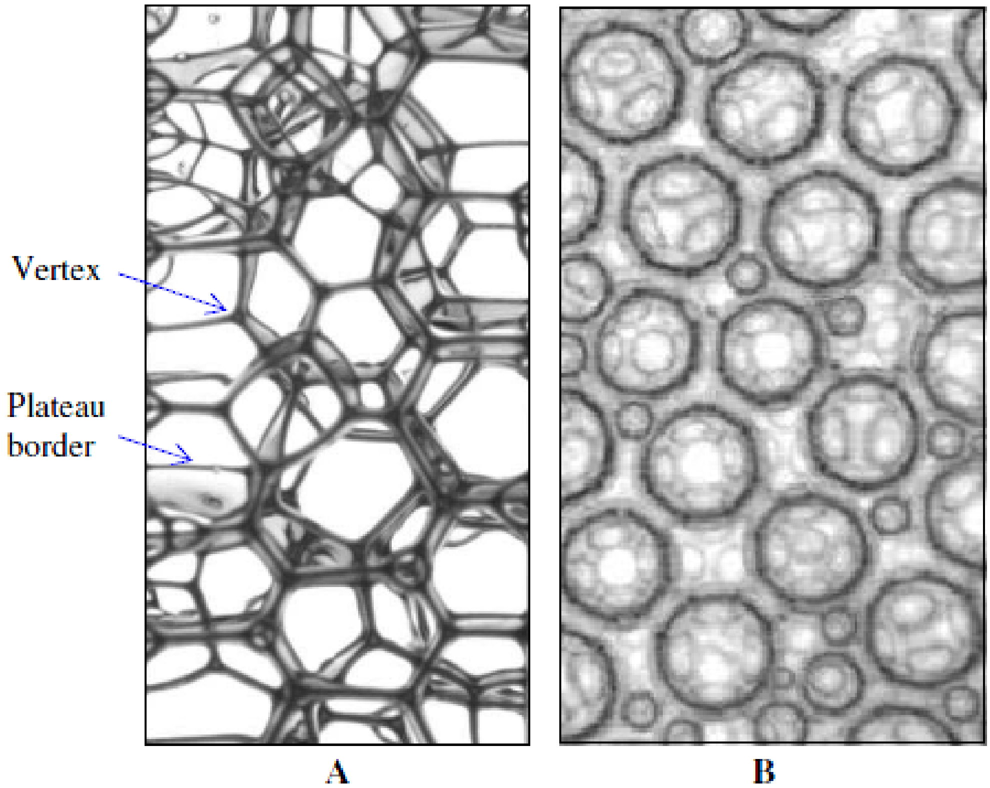

Figure 4.2: A representation of the typical structure of a dry gas (A) and a wet gas (B)(Höhler and Cohen-Addad, 2005)

Another classification of foam can be given according to the degree of coarseness of the bubbles. If the latter are small and spherical, the foam is referred to as fine foam. If they are coarse and polyhydric, then it is known as coarse foam. According to the previous statements, the fine foam is a wet foam while the coarse foam is classified as dry foam.

Foam can also be characterized by four different levels of structures. These levels range from a macroscopic to a molecular scale. The aqueous homogeneous foam represents the macroscopic level. By zooming in, the uniform foam seems to be composed of gas bubbles ranging in size from 10 μm to 1 cm and separated by a thin liquid film of 10 nm to a few μm in size. A smaller scale review of foam examines the liquid and gas interface. Such level operates at a size of 100 nm. Lastly, the molecular scale is the most detailed level at which the foam can be analyzed. It reflects the behavior of both gas and liquid molecules at the interface. Such level operates at a size of 1 nm. The four different levels of structure are represented in Figure 4.3 (Durian, 2002; Höhler and Cohen-Addad, 2005).

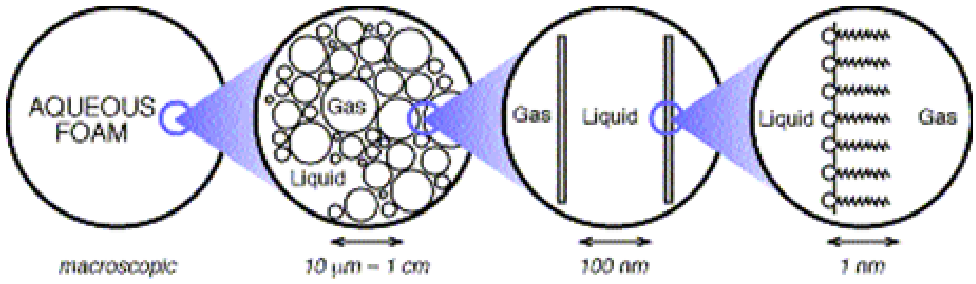

Figure 4.3: A schematic representation of the four different levels of foam structure ranging from macroscopic to molecular scale (Durian, 2002)

Borders between the bubbles are considered in the analysis of foams. In dry foams where the liquid content is too small, the polyhedral bubble edges are called Plateau borders whose junctions are known as vertices. Foam structure is not as random as it seems; the Plateau Law governs partially its behavior. According to this law, three films will join the Plateau borders at mutual angles of 120° when the foam is under equilibrium state and within the dry bounds. Similarly, four films will join to form vertices of a symmetric tetrahedral form. These foam structures provide stability.

Foam loses stability when the number of films exceeds four and the number of vertices and edges is higher than what was described. To gain stability, it dissociates into the stable structures. As the liquid content of the foam increases, the bubbles will take a spherical shape. The foam rigidity is thus lost and a bubbly liquid characterizes the foam behavior (Höhler and Cohen-Addad, 2005).

Plateau's Law can be further analyzed as it explains foam's behavior. It is mainly based on the fact that a bubble always searches, by nature, to surface energy or area minimization. In this case, the bubble immediately takes the mathematical optimum shape. The theory is applicable to one or many bubbles. Coalescence of bubbles in different arrangements is shown in Figure 4.4. The bubbles arranged in three, as previously mentioned, can only be gathered with an angle of 120° whereas bubbles arranged in four can only be gathered at an angle of $cos^{-1}(-1/3) \approx 109°$. At the Plateau borders, and for a mechanical equilibrium, the net force is zero. Similarly, the net force at the vertices is zero. Furthermore, the sum of the pressure difference is zero around a closed loop (Durian, 2002; Morgan, 1994).

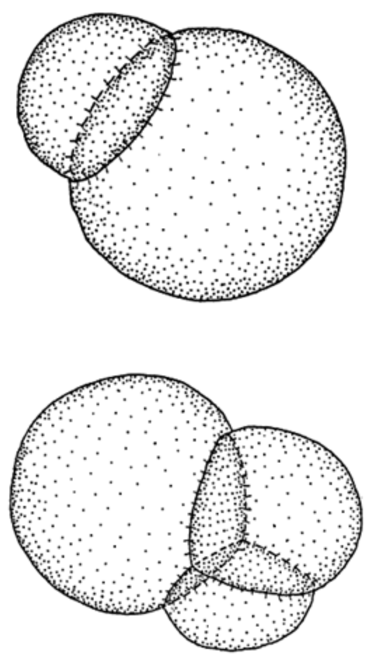

Figure 4.4: Double and triple bubbles searching for the minimum energy surface by merging and separating two or three volumes of air (Morgan, 1994)

4.3 Foam Rheology

The study of foam rheology is essential for the understanding of foam behavior, for an improved handling of foam and for the estimation of the pressure drop in pipes. Foam can expose solid-like or liquid-like mechanical properties regardless of its fluid constituents. This is a matter of the stress applied to the system; the elasticity of foam is represented in Figure 4.5. The graph shows the yield stress curve that separates between a liquid-like and solid-like behavior of the foam when the stress applied to the system is varied. Once a minor stress is applied to a system, the gas-liquid interfacial area increases; similarly, the energy per unit volume will increase. Irreversible bubble arrangement would develop as the applied stress exceeds the yield stress. Therefore, the foam will behave as a viscous, non-Newtonian fluid.

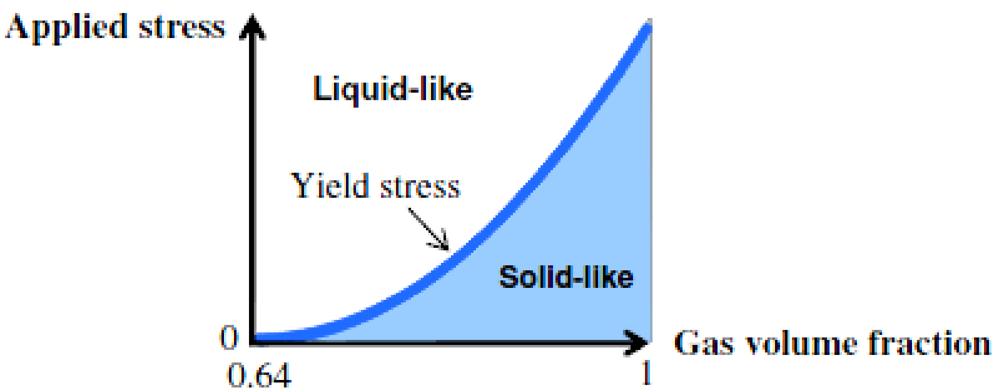

Figure 4.5: A diagram representing the liquid-like and the solid-like behavior of a foam as a function of the applied stress (Höhler and Cohen-Addad, 2005)

4.3.1 Foam Viscosity

Many studies have revealed that the rheological behavior of foam depends mainly on its quality. Einstein and Hatschek (Tisné et al., 2004) have pointed out that the foam has to be treated as a single phase fluid with a viscosity greater than that of any of the components. According to Einstein, foams with a quality smaller than 52 % will behave as Newtonian fluids. In order to calculate the viscosity of the two-phase flow, he considered an energy balance. He assumed that solid particles are suspended in a homogeneous fluid. These particles are identical in volume and diameters and have no weight. Furthermore, the particles are equally spaced and do not touch as well as their surface does not show any slip. As a result, he deduced the foam apparent viscosity which increases with the foam quality. It can be represented in the expression below:

$$\mu_f = \mu_l(1.0 + 2.5\Gamma_{(T,P)}) \tag{4.3.1}$$

On the other hand, foam with a quality ranging between 52 and 74 % are treated differently. The viscosity is calculated based on Hatschek's study (Tisné et al., 2004). He suggested that the foam within this quality range requires additional work to initiate and keep the flow; this is mainly due to the foam's high apparent viscosity. Such foam is known as the bubble interference foam. The viscosity is thus calculated according to:

$$\mu_f = \mu_l(1.0 + 4.5\Gamma_{(T,P)}) \tag{4.3.2}$$

Furthermore, Hartschek (Tisné et al., 2004) added that when the foam quality exceeds 74 %, the foam has to also be treated differently. The bubble texture gets modified with the increased concentration of gas in the fluid. The spherical bubbles will take the form of a dodecahedron and then of a parallelepiped. The latter bubble configuration allows the foam to flow in laminae. In this case, the shear of the fluid between the parallelepiped-shaped bubbles affects the viscosity of the foam which can be calculated from:

$$\mu_f = \mu_l \frac{1}{(1 - \Gamma_{T,P}^{1/3})} \tag{4.3.3}$$

Nevertheless, Mitchell (Tisné et al., 2004) considered that the foam's behavior is compared to a Bingham plastic fluid behavior in laminar flow. He suggested that the foam's quality is disregarded when the foam has a shear rate exceeding 20 000 sec^{-1}. Consequently, a linear relationship links the shear stress to the shear rate. When the shear rate is lower than 20 000 sec^{-1}, foam quality is accounted for and linearization of the relationship between the shear stress and the shear rate is achieved by the subtraction of the apparent yield stress which is illustrated in Figure 4.6 . The shear stress - shear rate relationship for the Bingham plastic foam is expressed, according to Mitchell, by:

$$\tau - \tau_y = \mu_p \phi \tag{4.3.4}$$

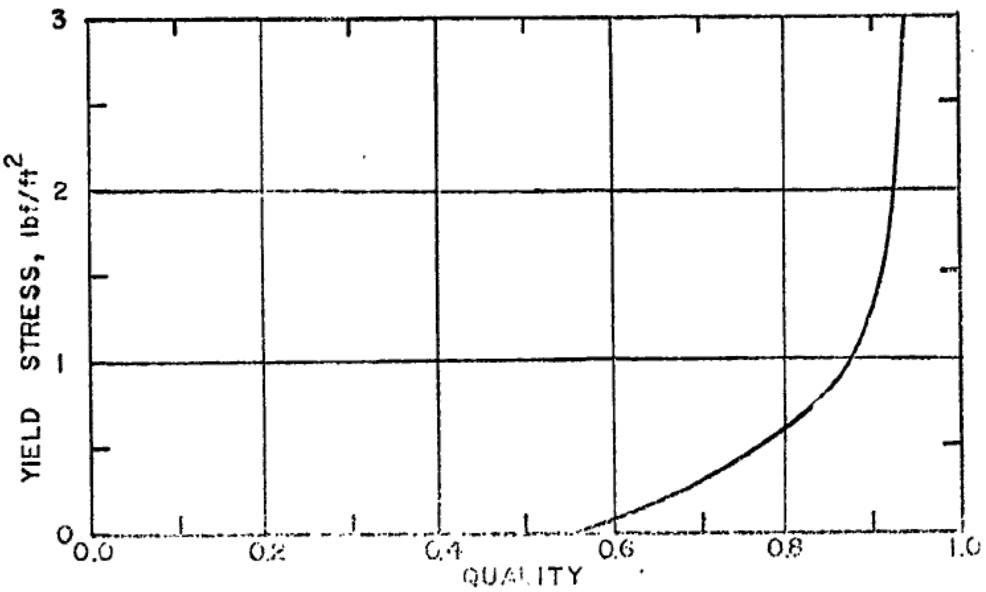

Figure 4.6: Mitchell's yield stress of foam as a function of the foam quality (Blauer et al., 1974)

Shear Rate and Shear Stress

Shear rate is crucial for further analysis of foam behavior in horizontal pipelines. It reflects the intensity at which the shearing action is taking place in the pipe. Similarly it may indicate the change in the velocity between the different fluid layers along the flow path. Depending on foam quality, it can be qualified as a Newtonian or Bingham model fluid. In terms of shear rate, a Newtonian fluid has a constant viscosity for all shear rates. Contrarily, Non-Newtonian fluids have the shear stress dependent upon the shear rate. The general formula for the shear rate is a function of the velocity and the radius and is expressed as follow:

$$\dot{\gamma} = \frac{du}{dr} \tag{4.3.5}$$

In case where the foam is behaving as a Newtonian fluid, the shear rate becomes:

$$\dot{\gamma} = \frac{8u_f}{D} \tag{4.3.6}$$

On the other hand, a foam classified as Bingham model fluid is treated differently. The shear rate depends now on both the yield stress and the plastic viscosity are accounted for and expressed as:

$$\dot{\gamma} = \frac{8v_f}{D} + \frac{\tau_y}{3\mu_p} \tag{4.3.7}$$

The yield stress can also be determined according to foam classification based on Mitchell's proposition (Tisné et al., 2004). For a Newtonian fluid, the shear rate and the shear stress are linearly related by the following formula:

$$\tau = \mu\dot{\gamma} \tag{4.3.8}$$

To determine the shear stress of a Bingham plastic foam, the expression becomes a function of the yield stress as well as the shear rate and the plastic viscosity and is seen below:

$$\tau = \tau_y + \mu_p\dot{\gamma} \tag{4.3.9}$$

The flow curves of these two different models are represented in Figure 4.7 along with the flow curves of two additional rheological models: Power Law and Herschel & Bulkley models. In-depth studies of the relationship between the shear rate and the shear stress have showed that foam, under constant quality, shows two different behaviors. The flow curve slope varies depending on the critical shear rate value. If the shear rate is below the critical shear rate value, then the curve's slope is 1.0 indicating that the flow is laminar. When the shear rate exceeds its critical value, the slope increases and fluctuates around 2. This is an indication of a turbulent flow.

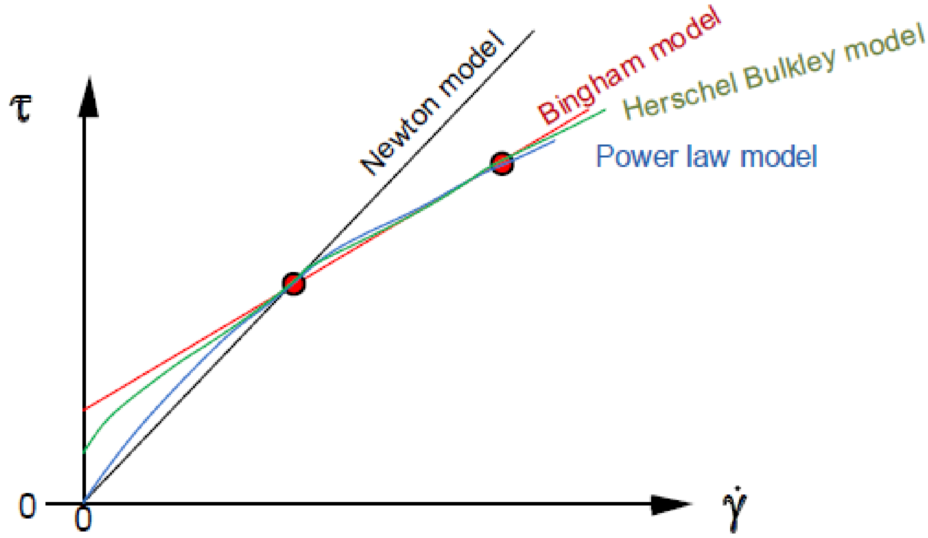

Figure 4.7: The four flow curves (shear stress vs. shear rate) of the four different rheological models including the Newtonian and Bingham models (Skalle, 2011)

4.3.2 Reynolds Number and Fanning Friction Factor

The Reynolds number is an essential parameter to be considered for an analysis of the foam behavior. Reynolds number, a dimensionless parameter, provides a measure of the ratio of inertial forces to the viscous forces. It defines the limits of whether the fluid is flowing in laminar, transient or turbulent flow conditions. A laminar flow is defined by a Reynolds number lower than 2300. On the other hand, a Reynolds number greater than 4000 sets the limit for a turbulent flow. Numbers ranging in between 2300 and 4000 determine the transient flow region. Within this region, both laminar and turbulent flows can occur depending on different parameters such as the pipe roughness. Reynolds numbers is thus calculated by:

$$Re = \frac{u_f D \rho_f}{\mu_e} \tag{4.3.10}$$

In operational conditions, the gas in pipelines has high Reynolds number. The latter's value alters around 10^7. This is mainly due to the high density and low viscosity of the gas at the typical operating conditions with a pressure around 100 bars. Furthermore, the friction factor is indispensable for the analysis and understanding of foam behavior. When operating under laminar conditions with low Reynolds numbers, the friction factor is dependent upon the Reynolds number and is calculated according to:

$$f_{Fann} = \frac{16}{Re} \tag{4.3.11}$$

Contrariwise, when operating under turbulent flow conditions with high Reynolds numbers, the friction factor will mostly depend on the relative roughness (ε/D) of the pipe. The Fanning friction factor can be determined by different expressions in case of turbulent flow. The Zigrang-Silvester equation is mainly used for explicit calculation of the friction factor when both the Reynolds number and the relative roughness are specified. The expression is as follow:

$$\frac{1}{\sqrt{f}} = -4.0log[\frac{\varepsilon/D}{3.7} - \frac{5.02}{Re}log(\frac{\varepsilon/D}{3.7} + \frac{13}{Re})] \tag{4.3.12}$$

A widely used alternative equation, the Haalands equation, has replaced the Zigrang-Silvester equation in case of explicit calculation of the Fanning friction factor in turbulent flow. But it is not favorable to use when a wide range of values of the Reynolds number and the relative roughness are implemented Shankar Subramanian. The Haaland equation is illustrated as:

$$\frac{1}{\sqrt{f}} = -\frac{1.8}{n} log[(\frac{6.9}{Re})^n + (\frac{\varepsilon/D}{3.75})^{1.11n}] \begin{cases} \text{n = 1 for liquid} \\ \text{n = 3 for gas} \end{cases} \tag{4.3.13}$$

Chapter 5

Foam Flow

5.1 Definition

A foam flow develops in a pipe as a result of the introduction of a foaming agent in presence of a hydrocarbon flow, usually gas flow. In this case, more than one phase exists in the conduit; therefore, the flow can be classified as a multiphase flow. Many studies revealed that the classification of foam flow as a multiphase flow is wrong. The foam flow has showed different responses and its natural instability made it hard to anticipate its behavior.

The rheology of the foam in pipes has a major role in affecting its performance. Further rheological studies have shown that pressure contour plots helped detecting two different flow regimes. The former represent the steady-state pressure drops as a function of both the liquid and the gas velocities.

Classification of foam flow regimes is essential for an appropriate and accurate use of foam for flow assurance. The regimes are divided into a high flow regime and a low flow regime separated by a threshold, f_g^*. The latter appears to coincide with the foam quality at which the apparent viscosity is at its maximum value, shown in Figure 5.1, as f_{gth2}. Additionally, the threshold value is not constant according to Gajbhiye and Kam. (2011). On the contrary, it varies concavely with the increasing liquid velocity; this is mainly due to the shear thickening behavior of foam in low quality regime. Furthermore, the foam stability can be affected by the varying the values of the threshold. Both foam quality and total velocity determine the flow regime classification (Gajbhiye and Kam, 2011).

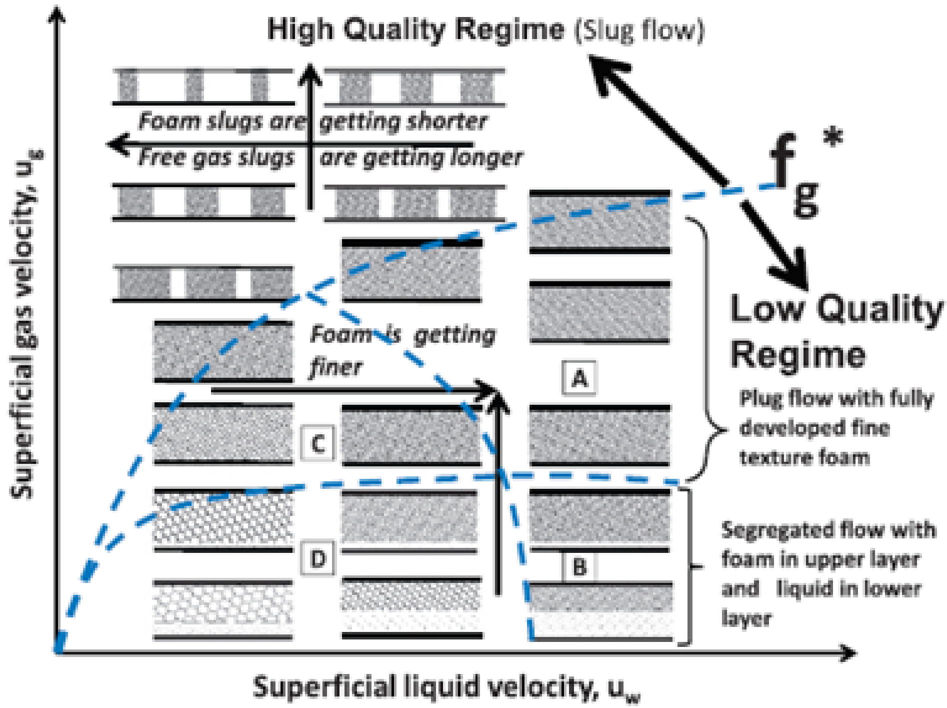

Figure 5.1: A schematic representation of the foam flow regimes in horizontal pipes based on foam textures and flow patterns (Gajbhiye and Kam, 2011)

The two regimes reflect two different properties and characteristics as shown by Gajbhiye and Kam (2011). The high quality regime is known for its oscillating pressure responses. This is due to the slug flow seen through pipes; it is characterized by an alternation of fine-textured foam and free gas. On the other hand, the low quality regime reflected more stable pressure responses; the latter can be represented by one of the two flow regimes. The first is denoted as the plug flow;

it shows homogeneous fine-textured foam with a relatively high f_g where both liquid and gas bubbles flow at nearly the same velocity. However the second is denoted as a segregated flow. It has a layered flow with the slow foam layer overlying the accumulated liquid layer which is flowing at a higher velocity. Here, the f_g is fairly low. The threshold value corresponds to the transition between the plug and the slug flow.

According to Gajbhiye and Kam, both the apparent viscosity and the pressure drop along the pipe following the use of foams are proportional to foam quality. The higher the quality, the higher is the pressure drop and the apparent viscosity and the lower the quality, the lower are both parameters. The threshold value follows also the same trend. Furthermore, he noticed that the pressure drop and the apparent viscosity in very high quality regime decrease with increasing gas velocity for a constant liquid velocity. Contrarily, these two parameters in a low quality regime are not affected by liquid velocity changes but seem to be dependent upon the gas velocity. Both the bubble size and the distribution constitute the base for typifying the foam flow.

The lower flow regime can be further divided into four different sub-categories based on the total injection velocity and the foam quality. A summary of the different regimes and sub-categories can be found in Figure 5.1. The plug flow takes place in regions A and C. This is due to the high foam quality in both and to the high and low total velocities, respectively. On the other hand, the segregated flow appears in sections B and D where the quality is low. It shows that a higher concentration of surfactants would increase the stability and the quality of the foam which, in turn, form a slug flow. As a result, the free-gas portion of the flow expanses and the size of the fine-textured foam shrinks.

Flow patterns have also been classified based on foam quality. Several experiments were held by Briceño and Joseph (2003). They showed that at low foam qualities, a segregated flow is mainly dominant along with some plug flow in the gas bubbles layer. Additionally, segregation of the bubbles was also observed. A further increase in the quality leads to the formation of a plug flow and then to a slug flow. This can be related to the fact that when foam quality is increased, the velocity of gas is increased and thus the velocity of the system is raised. The different flow patterns and their characteristics with respect to the different foam qualities are briefed in Table 5.1.

Table 5.1: Summary of the different foam flow patterns resulting from the variation in the foam quality (Briceño and Joseph, 2003)

Foam Quality [%]	Flow Regime [−]	Flow Regime Characteristics [−]
< 75	Similar to stratified flow	Two distinct layers with the top layer showing a plug flow
$73 < \Gamma < 79$	Early churn flow	Liquid film very thin and bubbles move faster closer to the thin layer Bubble size segregation: smaller at the bottom and larger at the top
$79 < \Gamma < 89$	Mixed or churn flow	One layer observed as slip layer disappeared No bubble segregation
$89 < \Gamma < 97$	Plug Flow	Air bubbles of the same size and no shear Self-lubricated Foam
> 97	Transitional flow between the uniform and the slug flow	Non-homogeneous dispersion
> 98	Slug flow	Slugs retarded by wall friction with gas pockets moving faster than the foam Foam is retarded more at the bottom due to larger gas pockets Gas bubbles coalescence into very large gas bubbles

5.2 Characteristics

The slip layer in pipes characterizes foam flow albeit the disagreements about the need to account for it while calculating the different rheology parameters and pressure drops. Briceño and Joseph (2003) have proposed that the rheology of the foam does not govern its behavior in the case of uniform foams. They suggested that the foam will self-lubricate and move as one rigid whole lubricated by water. Contrariwise, Blauer et al. (2004) have ignored the presence of a slip layer for characterizing foam. The latter is treated as a single-phase Bingham fluid where the effective viscosity is the crucial parameter especially for pressure drop calculations.

The slip layer has become an important parameter when characterizing foams. By definition, a slip layer is a thin layer of water that accumulates and forms due to the migration of the gas bubbles away from the solid boundaries. It is also caused by the tendency of foam to break at the wall of the solid surface when the shear stress in the near-wall exceeds its breaking shear stress. The thickness of this layer is related to the type of flow dominating in the pipe and to the liquid and gas velocities; as well, it affects the friction between the bubbles and between the bubbles and the wall (Zagoskina and Sokovnin, 1999).

For a plug flow, an increase in the liquid velocity leads to a thicker slip layer and to a lower friction which will not affect the pressure drop significantly. This is known as the lubricating effect. On the other hand, for a segregated flow, the increase of the liquid velocity causes the accumulated liquid to move upwards, increasing thus the liquid trapped in the pipe. As a result, the pressure drop will not be affected greatly. This is known as the drainage effect (Gajbhiye and Kam, 2011). The average range thickness of the slip layer in the pipe, shown in Figure 5.2.1, is between 10 and 12 μm for a foam quality greater than 80 %.

The calculation of the thickness of the slip layer has found different tech-

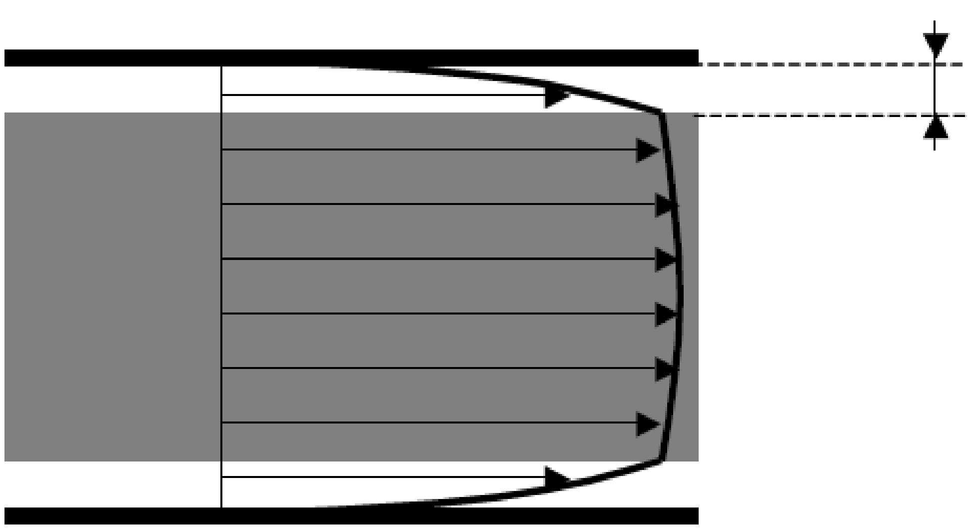

Figure 5.2: A schematic showing the velocity profile of a viscous foam flow lubricated by a thin water slip layer (Peysson and Herzhaft)

niques. It is dependent on the mean diameter of the bubbles and on the liquid fraction of the foam as Calvert et al. (1990) have stated. The expression used for the layer thickness is as follow:

$$\frac{\delta}{d} = \frac{2}{3(E-1)} \tag{5.2.1}$$

where the expansion ratio, E, is given by:

$$E = \frac{u_{foam}}{u_{liquid}} \tag{5.2.2}$$

More recent studies have showed that the thickness is inversely related to the pipe diameter meaning that an increase in the pipe diameter would lead to a decrease in the slip layer thickness. Additionally, the latter is also dependent upon the slip velocity. Further studies held by Tisn*é* et al. (2004) stated that the thickness of this layer is dependent on the shear rate or the wall shear stress. It is inversely proportional to these two parameters. Furthermore, the superficial velocity of the mixture and the liquid viscosity are then both essential. Brice*ñ*o and Joseph (2003) have used the same correlation for the estimation of the thickness.

The slip layer thickness calculation with respect to the shear rate and the wall shear stress when the foam is assumed to be a Newtonian fluid is expressed, respectively, as:

$$\delta = \mu_l \frac{\overline{u}}{\tau_w} \tag{5.2.3}$$

$$\delta = \frac{\overline{u}}{\dot{\gamma}} \tag{5.2.4}$$

When foam is assumed to be a shear-thinning fluid, the Power Law model is implemented. The only difference between the two correlations to calculate the slip layer thickness for Newtonian and shear thinning liquid is the absence of the viscosity of the liquid in the second case. It is replaced by the Power Law consistency index k and flow behavior index n. The expression of the layer thickness for a Power Law foam is the following:

$$\delta = k(\frac{\overline{u}}{\tau_w})^n \tag{5.2.5}$$

5.3 Foam Flow Uses

The foam has been implemented for different disciplines in the industry. Its various applications come as a result of its numerous properties. Besides the characteristically low density and high viscosity, foam has a high capacity of carrying solids and minimizing the filtrate and the circulation losses. Thus, it was applied as one of the improved oil recovery methods, as a tool for removal of liquid loading from wells and in drilling as a tool for hole cleaning in case of drilling underbalanced horizontal wells.

Foam has been practiced as one of the enhanced oil recovery techniques. For EOR purposes, the foam acts on the mobility and the method is currently referred to as foam mobility control. When it is generated in porous media with different permeabilities, fluid will flow from the high to the lower permeability zones since it forms initially in high permeability zones. In case of fractured reservoirs, the foam will flow at the same velocity in both zones due to the capillary contact of the rocks of different permeabilities and to the presence of cross flow between the two zones. Degradation of foam affects the recovery as the resulting surfactants would decrease the interfacial tension between oil and water. Consequently, the wettability is modified and the oil recovery is improved (Skoreyko et al.). The latter can be directly related to the high effective viscosity of foam.

Foam has been employed as a liquid removal tool in vertical wells. The flow rate, liquid viscosity and foam generation techniques play a major role in determining the liquid holdup and the pressure drops. The liquid holdup turns out to be low of low flow rates where the plug flow regime dominates; oppositely, the high flow rate of foam leads to an increase in the liquid holdup. Moreover, an increase in the liquid viscosity leads to an increase in the liquid holdup and thus an increase in the pressure drop as the transition from plug to recirculating flow takes place early and supplementary shear incurs within the foam. A reduction in the foam generation techniques meaning a reduction in the size of the bubbles shows the same effects as the increase in the liquid viscosity (Deshpande and Barigou, 2000).

Underbalanced drilling operations conducted by foam have been extensively used lately for depleted reservoirs. This technique helps in reducing lost circulation, minimizing the formation damage and increasing the penetration rate and the bit life. The tremendous cutting carrying capacity of foam in addition to its ability to handle water influx made it the primary tool applied for proper hole cleaning. Both foam stability and capacity properties made it a desirable drilling fluid. A foam of high quality is mainly required as it has high stability and better cleaning capacity due to the high capacity to carry cuttings. Likewise, foam should be easily broken after use for a fast disposal. Additionally, for UBD, the control of bottom-hole pressure is crucial. Several parameters affect the BHP including the foam velocity, its mode of injection and the reservoir pressure and temperature (Argillier et al.).

5.4 Advantages of Foam Flow

Induction of foam flow in pipes results in many advantages related to production. Liquid accumulations that result from multiphase flow can be removed or reduced. The presence of such water-rich accumulations causes the corrosion of the pipes as well as the reduction of the pipe diameter. Hence, foam flow limits or eliminates the use of corrosion inhibitors usually added, cutting thus on some expenses. Additionally, the pigging activity can be limited. A foam flow flowing through a hydrate region can result in the formation of anti-agglomerating hydrate crystals that avoid any form of deposition and hence explain the reduction in the need for pigging. Furthermore, the foam flow ensures an even distribution of any chemical added to the system resulting also in a cut in the need of pigging.

Another advantage of the induction of foam flow in pipes can take the form of a reduction in the severe slugging. Upstream generation of foam can cause a reduction in the slugging at the risers and can lead to a reduction in the flow velocity causing a change in the flow regime: a slug flow with its fluctuations is replaced by a straight or wavy-straight flow. Continuity in production is then ensured. The downstream separators and other equipment are affected. Therefore, with the reduction of the size of the slugs, the slug catcher's size can be reduced and simpler economical systems can replace the more complex systems at the receiving terminals.

Chapter 6

Foam Flow for Flow Assurance

6.1 Purpose and Effects of Pressure Drop in Foam Flow

Flow assurance, as mentioned earlier, focuses on a successful and economical production of hydrocarbon from the reservoir all the way to the receiving terminals. Optimization of production, by handling of liquid and solid accumulations, constitutes one of the branches of flow assurance. Many techniques have been used to optimize production. Chemical injections in pipelines have always been investigated and used to reduce or avoid corrosion, solid deposition, etc. Very little studies have focused on the foam and its flow for the transport of gas-condensate in pipelines up to the receiving terminals.

The pressure drop calculation will be studied in further details. For a better understanding of the applicability of foam flow in gas-condensate pipelines, different models for the pressure drop measurement will be presented and discussed. These theoretical calculations will later be compared with experimental data. Theoretically, the high viscosity and the low density of the foam cause a reduction in the Reynolds number which fluctuates around 10^7 in gas pipelines. As a result of the lower Reynolds number, the friction factor increases and thus the pressure drop becomes higher when compared to a multiphase flow.

The irregular and hilly topography of the seabed causes a higher pressure drop and additional complications when compared to a perfectly horizontal seabed. This leads to an increase in the wellhead back-pressure which produces a reduction in the flow rates and therefore a reduction in production. A foam flow adds to this pressure drop because of the high viscosity and low density of foam. On the other hand, the foam flow will manage to lift the liquid accumulations and flow in a more regular method than a slug flow which causes a variation in the pressures and rates at the receiving terminals. Additionally, the injection of surfactants through the pipeline is one of the cheapest methods that can be implemented in this aspect (Alvarez and Al-Malki, 2003).

6.2 Pressure Drop Models

A thorough study of the pressure drop models is essential as the large pressure drop associated with foam injection in pipelines is the major difficulty of using this technique for the removal or reduction of liquid accumulations. As a result of several studies, only two major models have been discussed. The first ignores the presence of a thin slip layer forming at the wall of the pipes whereas the other accounts for it. Oppositely to old researches, more recent studies have showed that for a greater accuracy of the pressure drop estimation, the second model is favorable.

According to Einstein and Hatschek (Tisné et al., 2004), treating the foam flow as a single phase flow makes it easy to model the pressure drop. It should not be treated as a multiphase flow since the empirical correlations designed for pressure drop prediction gave erroneous results (Tisné et al., 2004).

6.2.1 Pressure Drop Calculation Without a Slip Layer

A sequence of calculations has to be followed in order to get the pressure drop under the different rheological models attributed to the foam. For Newtonian foam under laminar flow conditions, the Hagen-Poiseuille law is used and represented by the following equations where the first is based on the radius of the pipe while the second is based on the pipe diameter:

$$\Delta P = \frac{8\mu_e LQ}{\pi r^4} \tag{6.2.1}$$

$$\Delta P = \frac{128\mu_e LQ}{\pi D^4} \tag{6.2.2}$$

The diameter, the radius and the length of the pipe are available data. On the other hand, the volumetric flow rate can be calculated with this simple equation:

$$Q = v.A \tag{6.2.3}$$

Similarly, the effective viscosity has also to be determined and it is the same as the foam viscosity determined by Einstein (Tisné et al., 2004) for Newtonian foams. It is represented by formula (4.3.1). Furthermore, the previously stated relationship can be written with respect to the mean velocity of the flow as follow:

$$\Delta P = \frac{32\mu L\bar{u}}{D^2} \tag{6.2.4}$$

When foam is treated as non-Newtonian fluid, many analyses and methods were implemented. According to Mitchell's study (Tisné et al., 2004), the foam behaves as a Bingham plastic flow. There are two different methods to calculate the pressure drop according to the type of flow (laminar or turbulent flow) dominating the pipe. The sequence followed should start with determining the average foam flow; it is the same for both laminar and turbulent flows and can be calculated by the following equation:

$$u_f = \frac{V_m}{4tD^2} \tag{6.2.5}$$

where the total volume of the mixture is the sum of the liquid and gas volumes at flowing conditions and is expressed as follow:

$$V_m = V_l + V_g \tag{6.2.6}$$

Next, the effective viscosity has to be determined as well. It can either be determined from Figure 6.1 or calculated for both laminar and turbulent flow by the following formula:

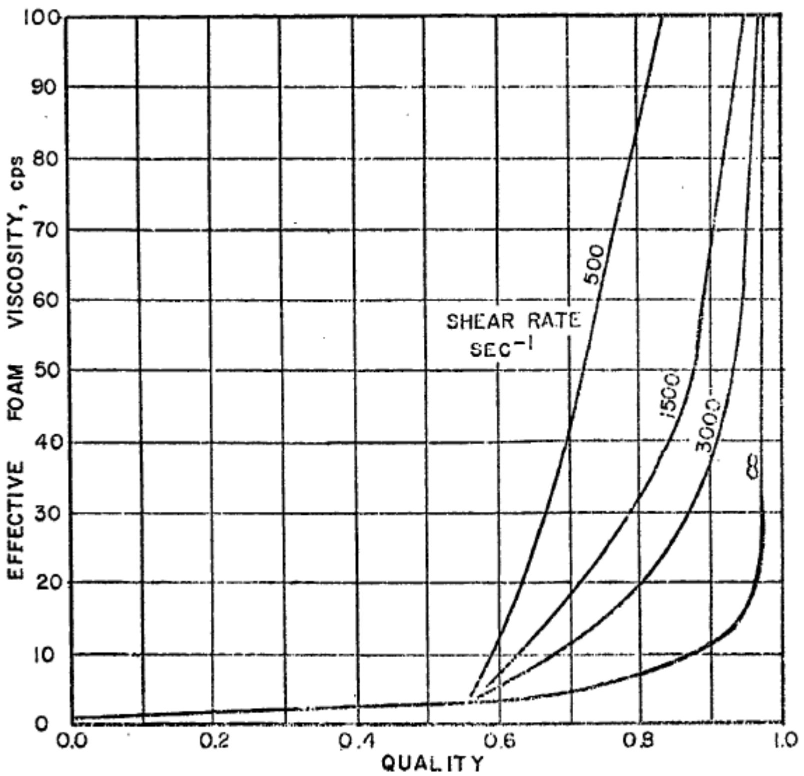

Figure 6.1: A graph representing the effective foam viscosity as a function of quality and shear rate (Blauer et al., 1974)

$$\mu_e = \mu_p + \frac{\tau_y D}{6u} \tag{6.2.7}$$

For the determination of the plastic viscosity, the foam quality has to be known and thus the viscosity is determined from the plastic viscosity vs. the foam quality graph shown in Figure 6.2. The foam quality is calculated according to equation (4.1.2) stated earlier.

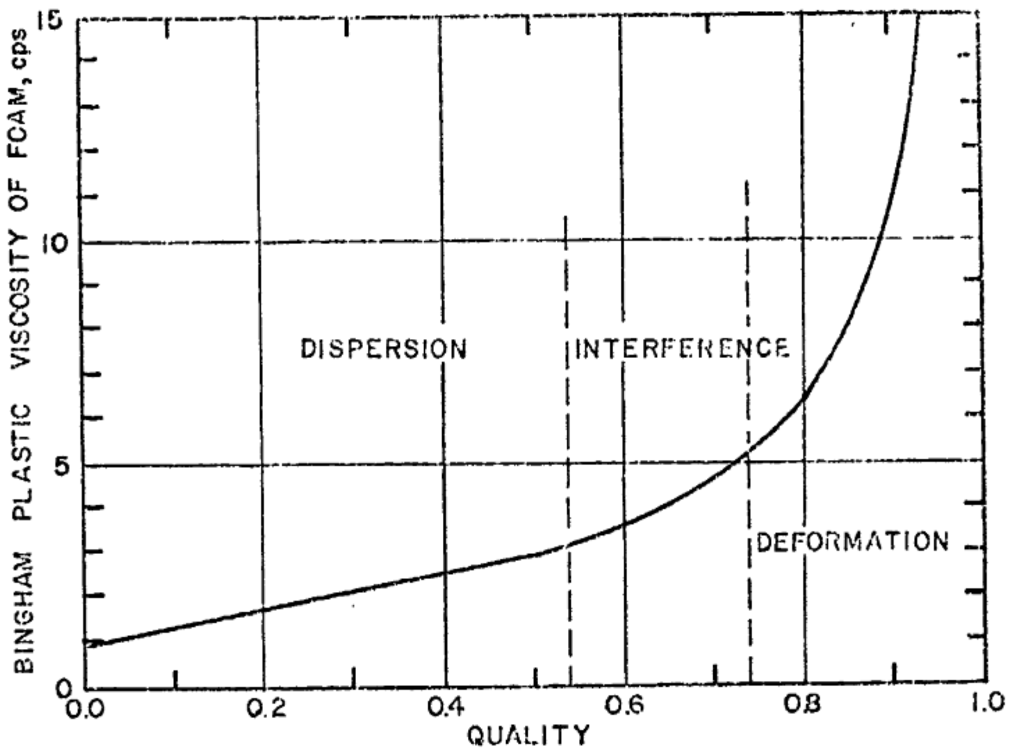

Figure 6.2: Plastic viscosity of Bingham plastic foam as a function of the foam quality (Blauer et al., 1974)

Furthermore, determining the type of flow dominating in the system has is essential; therefore, the Reynolds number should be calculated according to equation (4.3.10). As the flow turns out to be laminar after getting a Reynolds number smaller than 2300, the Fanning factor is inversely proportional to the Reynolds number and can be determined as follows:

$$f_{Fann} = \frac{16}{Re} \tag{6.2.8}$$

On the other hand, if the flow is turbulent, the Fanning friction factor is independent of the Reynolds number and can be calculated through the following formula:

$$f_{Fann} = \frac{2D\Delta P}{L\rho u^2} \tag{6.2.9}$$

Since the pressure drop is the target parameter of the analysis and the Fanning friction factor is not known, the latter has to be determined by some other correlations or expressions. The Moody friction factor which is also known as the Darcy-Weisbach friction factor can be used as a replacement for the Fanning friction factor. The latter is one-fourth the Moody friction factor. The Moody friction factor can also be calculated based on the Haaland equation represented in equation 4.3.13.

Additionally, the Moody friction factor can be determined graphically from the Moody diagram represented in Figure 6.3. It can be estimated based on the knowledge of the Reynolds number and the relative pipe roughness which is the ratio of the pipe roughness, also tabulated in Figure 6.3, to the pipe diameter.

On the other hand, the viscosity was proved not to be the major parameter upon which the foam behavior is dependent. The shear stress and the shear rate seem of a great importance. The pressure drop can be represented for a laminar flow in case of a Bingham fluid, according to the Buckingham-Reiner equation:

$$Q = \frac{\pi \Delta P D^4}{128\mu_p L}[1 - \frac{4}{3}\frac{\tau_y}{\tau} + \frac{1}{3}(\frac{\tau_y}{\tau})^4] \tag{6.2.10}$$

A simplified pressure drop expression has been suggested by Skalle (Skalle, 2011) and can be seen below:

$$\Delta P = \frac{32\mu_p L\bar{u}}{D^2} + \frac{16L\tau_w}{3D} \tag{6.2.11}$$

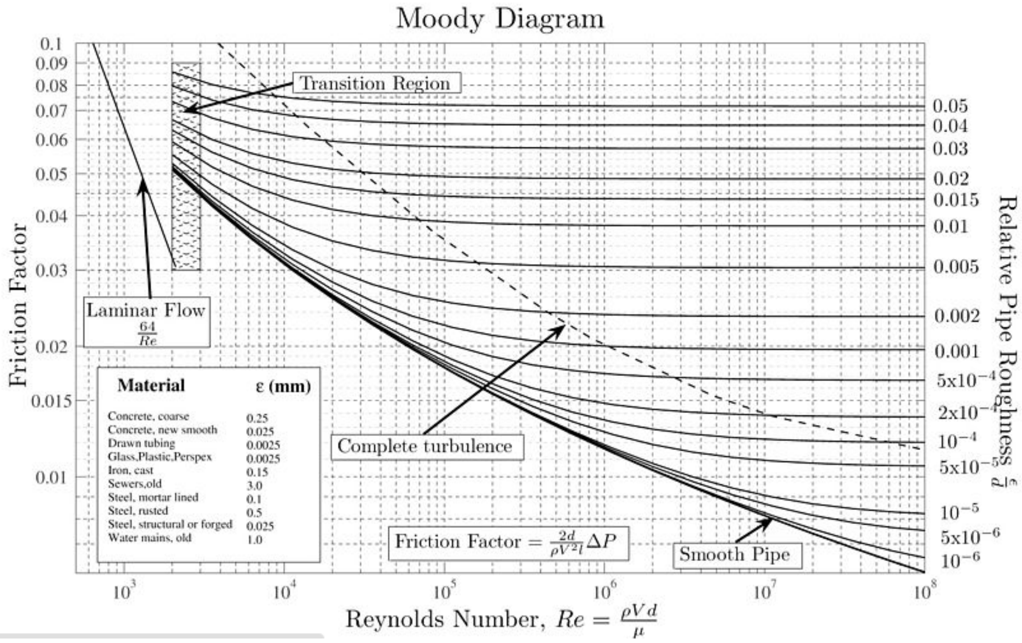

Figure 6.3: Moody diagram showing the relationship between the Moody friction factor, the Reynolds number and the relative pipe roughness

The foam can also be treated as a Power law fluid where the pressure drop is estimated without taking into consideration any liquid slip layer at the wall of the pipe. The consistency index k and the flow behavior index n are now the two major parameters affecting the behavior of the foam. These two can be calculated as a function of the foam quality by the correlation presented by Kuru et al.(2008). The formulas apply to foam qualities smaller than 91.5 % and are denoted as:

$$k = 0.0074e^{3.5163\Gamma} \tag{6.2.12}$$

$$n = 1.2085e^{-1.9897\Gamma} \tag{6.2.13}$$

The Reynolds number which is essential for the calculation of the friction factor and thus for the pressure drop in the conduit depends greatly on the Power law coefficients. The latter can be calculated according to the following general equation:

$$Re = \frac{8^{1-n}\rho u^{2-n} D^n}{k(\frac{3n+1}{4n})^n} \tag{6.2.14}$$

This expression is derived from the general formula of the Reynolds number already presented in equation (4.3.15) but with the replacement of the effective viscosity with the equation below. The latter is also a function of both coefficients of the Power law model.

$$\mu_e = (\frac{8\overline{u}}{D}.\frac{3n+1}{4n})^n \frac{kD}{8\overline{u}} \tag{6.2.15}$$

The friction factor is now calculated based on the Power law correlation designated for turbulent flows. The latter is chosen to mimic operating conditions. The Metzner and Reed correlation is applied unlike the Colebrook which has the same specifications as the former but is applied for rough pipes which is not the case here. The former is mainly a function of the Reynolds number and the flow behavior index. It is represented as follow:

$$f_{Fann} = aRe^{-b} \begin{cases} \text{a} = \dfrac{log(n) + 3.9}{50} \\ \text{b} = \dfrac{1.75 - log(n)}{7} \end{cases} \tag{6.2.16}$$

The pressure drop can therefore be calculated based on the Darcy-Weisbach formula in which the Power law versions of the parameters in question are used. The expression, which is a simple manipulation of equation (6.2.9), is the following:

$$\Delta P = \frac{f}{2}\frac{\Delta L}{D}\rho u^2 \tag{6.2.17}$$

6.2.2 Accounting for the Slip Layer in Pressure Drop Calculation

Foam, according to detailed studies, showed a self-lubricating behavior. This is mainly due to the tendency of foam to break rather than to deform and settle at the wall of the pipe or the conduit. The presence of the slip wall layer has altered the calculations of pressure drop due to foam. The latter advances as a stiff block lubricated by water. The water layer is very thin and uneven. The slip layer's thickness, symbolized by δ, is greatly smaller than the pipe diameter D. It can be compared to the thickness of the inter-bubble film in dry foams which is ranging from 1 to 30 μm.

The lubricating water layer has originated from the foam itself. Thus, its different characteristics and properties along with its thickness are dependent not only on the pipe's roughness and diameter and the shear rate but also on the concentration of surfactants, the bubble size distribution and other foam properties. Further studies have showed that the roughness of the pipe plays an important role in determining the major parameter dominating the flow. In smooth pipes, the slip velocity dominated the foam flow while in rougher pipes, the slip was absent. Moreover, small bubbles collide at the pipe wall limiting the slip until a critical stress value is attained to surpass the barriers. Contrarily, wall roughness cannot trap large bubbles into position.

The slip layer has therefore to be accounted for in the calculations of the foam properties. As a result, the models used earlier cannot be applied and have to undergo some modifications in order to represent a more accurate description of the foam in question. The process begins with a force balance between the pressure drop and the wall shear stress where the latter can be calculated as follow:

$$\tau_w = \frac{A\Delta p}{Ll_p} = \frac{r}{2}\frac{\Delta P}{L} \tag{6.2.18}$$

with $\dfrac{A}{l_p} = \dfrac{r}{2} = \dfrac{D_h}{4} = \dfrac{D}{4}$ The wall shear stress expression becomes,

- for a Newtonian fluid:

$$\tau_w = \mu_L(\frac{\overline{u}}{\delta}) \tag{6.2.19}$$

- for a Power law fluid:

$$\tau_w = k(\frac{\overline{u}}{\delta})^n \tag{6.2.20}$$

The Moody friction factor can be calculated from the following equation, keeping in mind that the Moody friction factor is four times greater than the Fanning friction factor;

$$f_M = \frac{2\tau_w}{\rho_L \overline{u}^2} \tag{6.2.21}$$

By knowing the friction factor either from the Moody diagram or from the calculations, the wall shear stress is computed and then it will be possible by manipulating the shear wall equations, to calculate the thickness of the slip layer. As the latter is known, it will be possible to calculate the pressure drop by using the slip layer thickness equation:

$$\delta = \mu_L \frac{2\overline{u}}{r(-\frac{\Delta P}{L})} \tag{6.2.22}$$

A simpler expression of the wall slip layer thickness shows the dependency of the later on the radius of the conduit. It is expressed by the following:

$$\delta = \frac{2D_h}{3700} = \frac{2D}{3700} \tag{6.2.23}$$

The pressure drop is estimated by substituting equations (6.2.20) and (6.2.23) in equation (6.2.18).

Chapter 7

Practical Aspects

Flow assurance, which aims to ensure a continuous and economical flow of fluids from the reservoir to the receiving terminals, is of great significance in oil and gas production. It encompasses handling of the deposition of liquids or solids as hydrates, slugs, waxes, asphaltenes, etc. Therefore, liquid accumulations resulting from multiphase flow, hydrates and slugs have to be inhibited in pipes to ensure a smooth flow. Specific equipment, as slug catchers, and chemical and mechanical treatments have been implemented to solve production-related problems. Foam induction in pipelines is a prospective solution since production does not have to be shut during the process, maintaining thus a high production efficiency.

7.1 Foam Supply and Removal to and From Pipelines

Foam can sometimes form by itself in pipelines and in case of flow assurance, it has to be induced. Induced foam can either be water-based or oil-based. Hence, a foam generator is required. On the other hand, maintaining foam until the receiving terminal might cause problems to the slug catchers, compressors or any other equipment. As a result, the foam has to be removed before it reaches the processing terminals. In this case we need a de-foamer. Such a cycle used to mitigate flow assurance issues, is known as the 'foam flow process' (Kouba et al., 2008). Furthermore, the process is includes three different steps. Steps one and three are previously mentioned while step two consists of transporting the foam in the pipes. The flow process is represented in a flow diagram as in Figure 7.1.

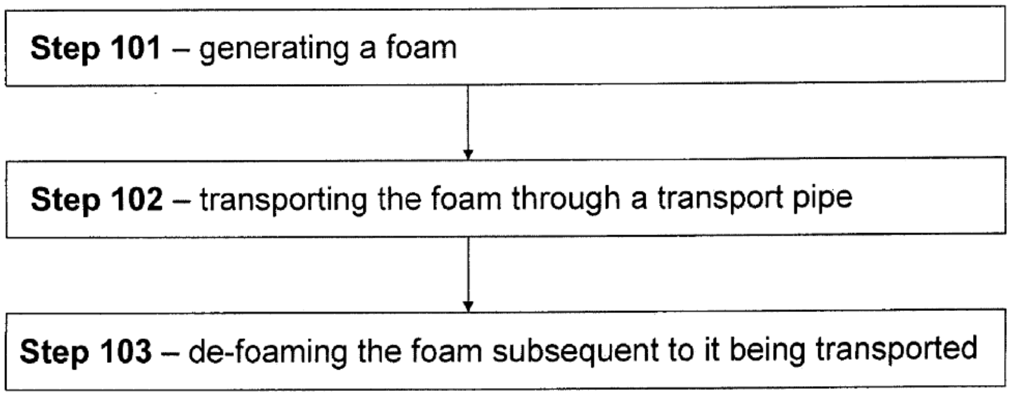

Figure 7.1: A schematic representation of the foam flow process with a brief description of the steps (Kouba et al., 2008)

Foam flow processes can be represented by two simple processes. The first one is known as 'in-situ' process, while the second is known as the 'in-auxiliary side stream' process. Basically the main criterion distinguishing these two processes is the techniques of foam generation and breaking. The transport in the pipe can only take the form of a continuous or intermittent flow for both processes. It should be mentioned that hydrate or corrosion inhibitors or any other additives can be added optionally to the system at the stage where the foaming agents are added.

Different techniques can be used to supply the pipes with foam as well as to remove it. The first technique is known as the 'in-situ' or the 'in-line' method where foam generation is induced by agitation. The latter can take place by a mechanical mixing, a turbulent flow or both. Specific regions are more likely to induce turbulent flow within the system; among those is when the flow goes through a mixer, choke, valve and pump. Additionally, foam generation can result from the addition of foaming agents such as surfactants and foamers.

Foaming agents' introduction to the system takes place in different techniques as well. They can either be injected directly to the main stream in a well-ordered or diluted state or injected in the same state to a separated side stream. Similarly, they can be injected under the same physical state with extra gas injection or they can be injected as pre-mixed concentrated foam.

The same 'in-line' technique used to generate foam can be used to break it. It can take the form of a dilution, thermic application, mechanical forces or chemical injection. The only difference in the latter case is the type of chemical products applied as de-foaming agents are required instead of foaming agents. It should be noticed that this step has to take place following the flow of foam through the conduit. Such methods belong to the 'in-situ' flow process represented in Figure 7.2.

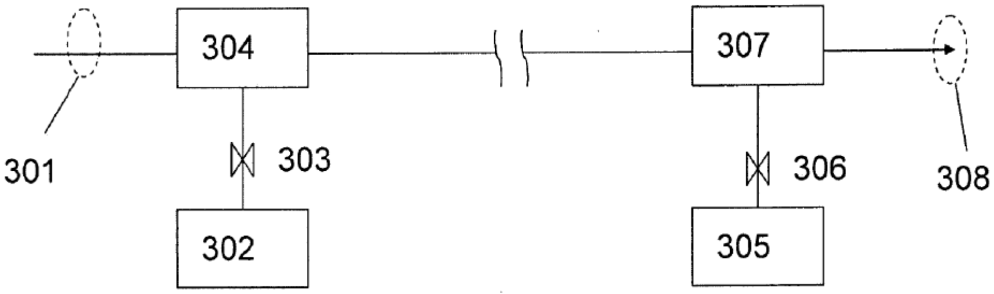

Figure 7.2: 'In-situ' foam flow process with an 'in-situ' generation of foam (304), transport of flow through the conduit and an 'in-line' de-foaming stage (307) (Kouba et al., 2008)

In this case, the foam is generated outside the conduit in a specific means and then injected to the main stream. A valve has to be present to separate the hydrocarbon flow from the foam floe generator as well as to control the flow of foam into the main stream. Similarly, the de-foaming agents are generated out of the main conduit and then injected to it with a valve separating the main conduit from the de-foaming generator. Foam formation and de-foaming means are similar to the techniques previously mentioned.

The second technique used to induce and remove foam from pipes is known as the 'in-auxiliary side stream' method. It is based on the deviation of the main stream through an auxiliary side stream where the generation of foam takes place by addition of foaming agents. The main stream and the side stream are separated by a valve to control the time of deviation of the hydrocarbon fluid. Likewise, a valve is used after the foam generator means to control the entry of the foam flow to the main stream and its continuity.

For elimination of foam from the main stream, a similar procedure is followed but instead of applying foaming agents in the de-foaming means, de-foamers are used. Afterwards, the de-foamed flow is directed to the main stream through a valve. It will be then recovered at the receiving terminals. The 'in-auxiliary side stream' flow process is represented in Figure 7.3.

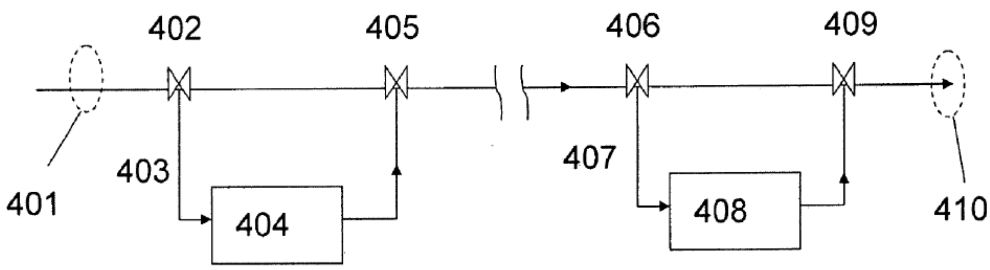

Figure 7.3: 'In auxiliary side stream' foam flow process with a side generation (404) and break of foams (408) through auxiliary side streams (403 and 407) (Kouba et al., 2008)

Transport of foam flow after foam generation and prior to de-foaming is crucial for the sweep efficiency of foam. It can be ensured in two different means: either continuously or intermittently. When the conduit is completely filled with foam, a homogeneous plug flow regime is maintained all along the line. On the other hand, when the conduit is partially filled with foam, intermittent plugs develop and lead to a better sweep of the liquid compared to gas alone. In general, a lower liquid inventory in pipes leads to a lower pressure drop.

7.2 Equipment and Chemicals

Chemical products, also known as foaming agents, added to a hydrocarbon multiphase flow through pipelines are crucial for inducing foam flow. Two types of foaming agents are usually encountered. The first is known as a blowing agent. By definition, the latter, which is a chemical usually added to plastics and resin, generates inert gas and forms the gas of the gaseous phase of the foam. Gas forms by two different techniques: it forms either at the same temperature as that of the foam or as a result of chemical reactions. This type will not be further discussed due to its limited use in the oil and gas area.

Surfactants constitute the second type of foaming agents. They are chemicals that adsorb at the interface of the gas and liquid phases lowering thus the surface tension between the fluids. Additionally, they increase the colloidal stability of the liquid, hindering thus the coalescence of the bubbles. Surfactants have a characteristic structure. The molecule is divided into two major parts: a hydrophilic polar head and a hydrophobic tail. The first is water prone whereas the latter is fat prone and is usually formed of a fatty hydrocarbon chain. The surfactant molecule with both heads is represented in Figure 7.4.

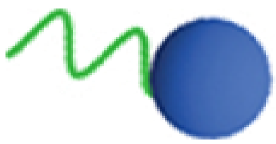

Figure 7.4: A representation of the surfactant molecule with the hydrophilic head (blue) and the hydrophobic tail (green) (Karam, 2012)

The behavior of surfactants is dominated by their structure. They are characterized by their ability to self-orient themselves: the hydrophilic head directs itself towards an aqueous environment while the hydrophobic tail orients itself towards a non-aqueous environment. As a result of this self-orientation, surfactants will concentrate at the liquid-gas interface in foams increasing their stability. A representation of the concentrated surfactants is shown in Figure 7.5.

In case of adding surfactants to an aqueous solution, they will aggregate to form a micelle in a process known as micellation. A micelle is characterized by the hydrophobic tails of the surfactant molecules gathering in a way to direct themselves into the center of the circular micelle, leaving the hydrophilic heads directed towards the polar aqueous environment. The micelle can also take the form of a bilayer. Its size depends on the molecular geometry of the surfactant molecules as well as on the solution conditions such as the surfactant concentration, solution pH and temperature.

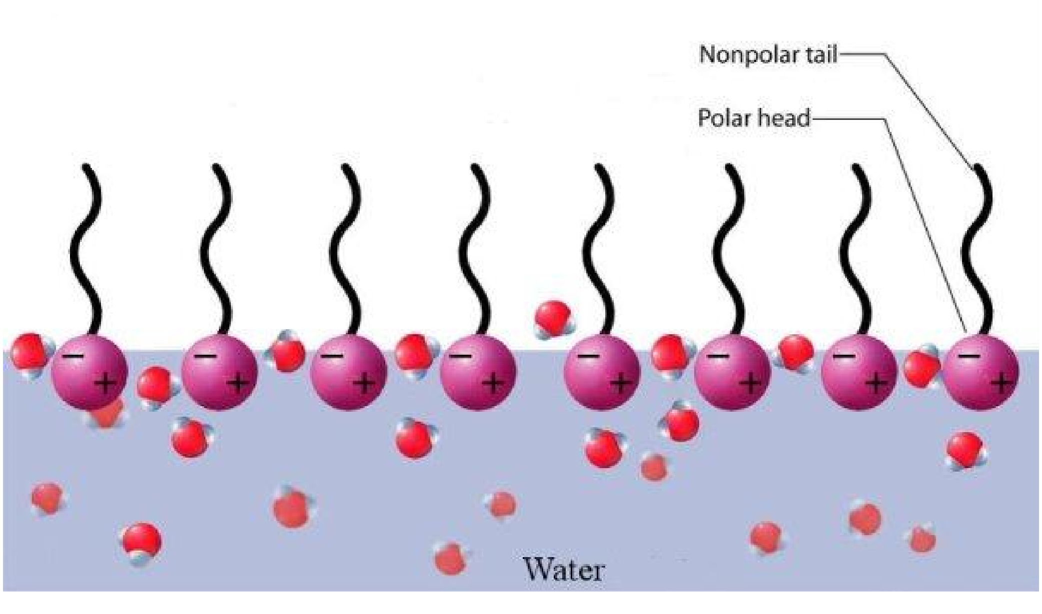

Figure 7.5: Self-orientation of surfactants due to their structure; hydrophilic heads are oriented towards the aqueous environment (water) and hydrophobic tails oriented towards a non-aqueous environment (Karam, 2012)

Critical Micelle Concentration, also known as CMC, constitutes one of the important parameters to be considered for the analysis of the use of surfactants.

It is a measure of the surfactant efficiency. By definition, the CMC represents the concentration of surfactants at which a significant number of micelles start to develop. A low CMC value designates a lower need of surfactant concentration to saturate the interfaces and form a micelle (Dow Chemical Company, 2010).

The quality of surfactants is basically determined by the rate at which the surface tension changes with the surfactant concentration rather than the amount of change. This relationship is expressed by a graph of Figure 7.6 linking the surface tension (σ) to the surfactant concentration (ϕ). Ideally, the surface tension decreases linearly with the bulk concentration until reaching the critical micelle concentration (ϕ_{CMC}) where it stabilizes at a specific surface tension known as the maximally reduced surface tension (σ_{CMC}). As the concentration exceeds the critical micelle concentration, the surfactant does not interfere at the saturated gas-liquid interface. On the contrary, it aggregates with other surfactant molecules to form micelles. The slope of the graph can be determined by

$$\frac{d\sigma}{d\phi} = \frac{\sigma - \sigma_{CMC}}{\phi_{CMC}} \tag{7.2.1}$$

The $d\sigma/d\phi$ ratio determines the speed at which the crucial surface tension gradients develop when stirring the surfactant mixture. The Gibbs elasticity, which will not be discussed in great details in this thesis, is used as a dimensionless expression of the rate of change of the surface tension. Its common expression is as follow:

$$E_g = A\frac{d\sigma}{dA} \tag{7.2.2}$$

Where the ratio $d\sigma/dA$ represents the strain based on the surface area change.

Surfactants are classified into four different categories that affect their behavior. The classification is based on the charge of the hydrophilic head. A surfactant is non-ionic when the hydrophilic head does not have any charge; an example of such surfactant includes polyoxyethylenated non-ionic surfactants. Anionic sur-

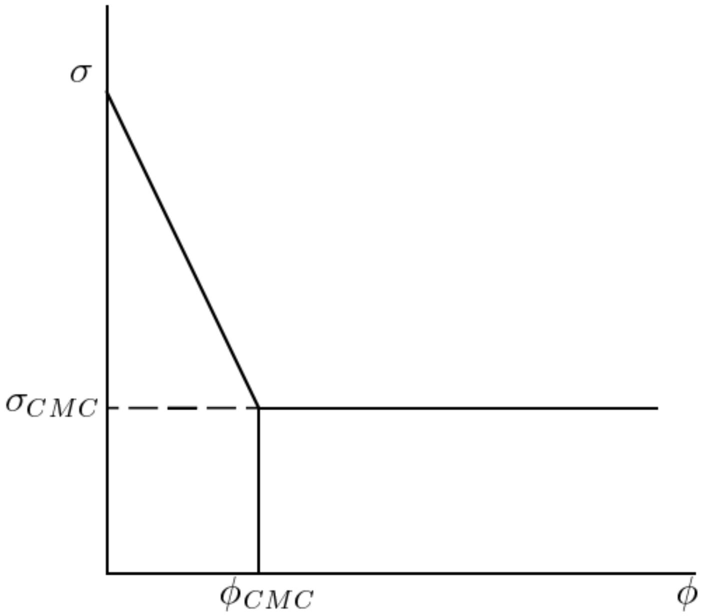

Figure 7.6: Surface tension vs. surfactant concentration to determine the quality of the surfactant. (ϕ_{CMC}) determines the critical micelle concentration and (σ_{CMC}) determines the maximally reduced surface tension (Joseph, 1997)

factants have a negatively charged hydrophilic heads. These include carboxylates, sulfates, sulfonates and phosphates. A positively charged hydrophilic head classify surfactants as cationic. The latter includes long chain amines and quaternary amine salts. Amphoteric surfactants, also known as zwitterionic, constitute the fourth category of surfactants. The hydrophilic head, in this case, has two oppositely charged groups. The different categories of surfactants are represented in Figure 7.7.

Surfactants have different functions and can act either as foaming agents or as de-foamers. The difference between the foaming agent and the de-foamer is the ability to reduce or strengthen the surface tension at the interface between the liquid and the gas phases. Foams, as stated earlier, are unstable by nature and they tend to break due to the surface free energy concept; therefore, foaming agents are added in this case. On the other hand, after inducing foam in pipes,

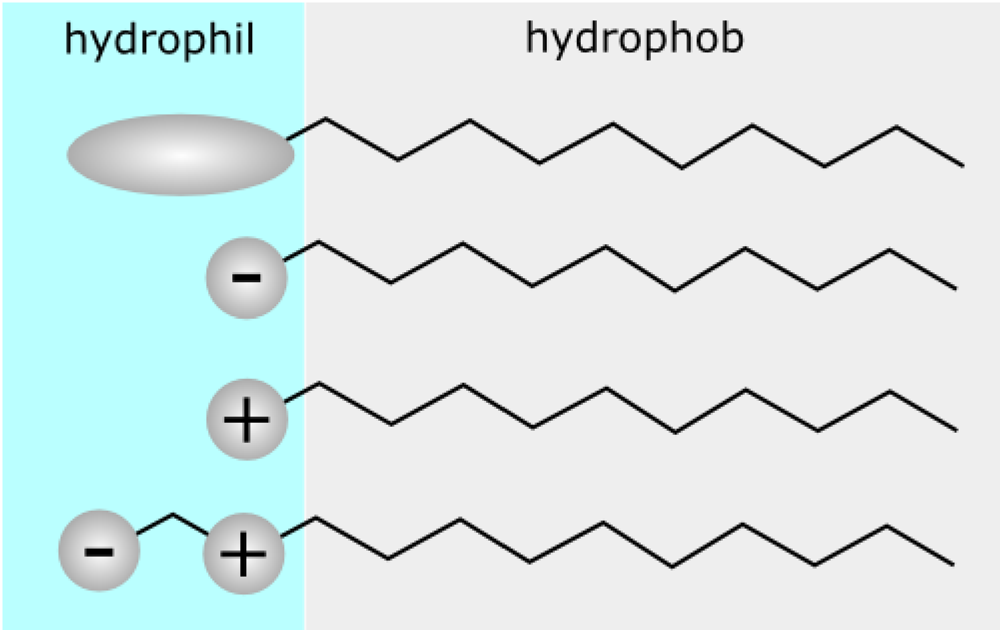

Figure 7.7: Classification of surfactants into four categories based on the charge of the hydrophilic head (Karam, 2012)

it is unfavorable for the foam to remain in the flow that reaches the equipment at the terminals. The latter are not equipped to handle foam; thus, it needs to be deformed or broken before it reaches the equipment. It should be noticed that anti-foams and de-foamers are not similar. The first prevent foam formation while the second destroys it as it forms. In this case, de-foamers and not anti-foams are needed.

De-foamers have the opposite function of foaming agents. A de-foamer is a surface active molecule which provides it with the ability to spread rapidly at any water-air interface. It is used as well to increase the surface tension. Most of the de-foamers include silica or ethylene-bis-stearamide particles in the hydrophobic tail of the molecule. This composition provides these molecules with the ability to pierce foam bubbles' surface leading to bubble coalescence. With gas bubble coalescence, the bubbles will increase in size to the point where they are capable of floating at the water surface before they break. Additionally, the quantity of de-foamer used is crucial as a low quantity leads to a lower drainage performance while large quantities might intensify deposits and deposit problems. Therefore, controlling the concentration is done by monitoring the air content and maintaining it at a minimum acceptable level (Hubbe).

Some of the surfactants used, though they belong to the same category, can perform different functions. In the oil industry, some surfactants have been used more frequently than others. Alfa Olefin Sulfonate, also known as AOS, is an anionic surfactant that showed, by many experiments, its capacity to inhibit hydrate formation. It is completely biodegradable and can be classified as a green chemical that will not present any harm for the environment. Moreover, it is gentle for the skin which makes it easy to handle in laboratory experiments. Nevertheless, it can lead to some skin irritations in case its gamma sultones chlorosultones content is high.

On the other hand, Sodium Dodecyl Sulfate or SDS which is also known to be an anionic surfactant has the capacity to induce hydrate formation. It is also classified as a biodegradable chemical that is perfectly green to be used. Handling of SDS in the laboratory should be done with care due to its dangerous properties. The Cetyl Trimethyl Ammonium Bromite is another foaming agent. CTAB, belongs to the cationic category of foaming agents but has the same function as the anionic SDS in inhibiting hydrate formation.

An Amphoteric surfactant as Ethylene Propylene Glycol Butyl Ether known as Amphoteric Betaines is used as a foam stability enhancer and a corrosion inhibitor. The properties of these four surfactants are gathered from various sources and a summary is represented in Table 7.1. In order to choose the appropriate properties of the foaming agent, the foam with the longest half-life is to be considered. A half-life represents the time needed for half the volume to be consumed.

Table 7.1: Properties of four different foaming agents

	C14-C16 Alfa Olefin Sulfonate	**Sodium Dodecyl Sulfonate**	**Cetyl Trimethyl Ammonium Bromite**	**Ethylene Propylene Glycol Butyl**
Abbreviation	AOS	SDS	CTAB	EGBE
General Formula	$C_nH_{2n-1}SO_3Na$ (n = 14-16)	$C_{12}H_{25}SO_4Na$	$C_{19}H_{42}BrN$	$C_6H_{14}O_2$
Molar Mass (g/mol)	324	288.5	364.45	118
Detergent Class	Anionic	Anionic	Cationic	Amphoteric
Function	Inhibit hydrate formation	Induce hydrate formation	Inhibit hydrate formation	Enhance foam stability
Biodegradability	Rapidly biodegradable	Highly biodegradable (> 90 % within 24 hrs)	Biodegradable	Readily biodegradable

Chapter 8

Experimental Process

The pressure drop estimation in the pipeline where foam was injected is of a great importance in deciding the applicability of foam for removal or reduction of liquid accumulations. Foam flow can induce large pressure drops in the pipelines causing damage into production. A simplified set of equipment was put together to check the pressure drop resulting from a foam flow and compare the results to the calculated pressure drop.

8.1 Experimental Apparatus

The experiments were conducted on a set of equipment including a storage tank, a pump, rotameters, a foam generator, a pipe, a transducer, a multimeter and valves. A schematic of the experimental apparatus is shown in Figure 8.1. The test section consists of a 4 m long acrylic pipe. The latter has an outer diameter of 25 mm and an inner diameter of 23.5 mm. The pump has a maximum capacity of 12.8 m^3/h and can deliver up to 38 % of its maximum capacity. It is used to pump the liquid mixture consisting of both tap water and surfactants from the storage tank up to the pipe passing first through a rotameter measuring the liquid rate.

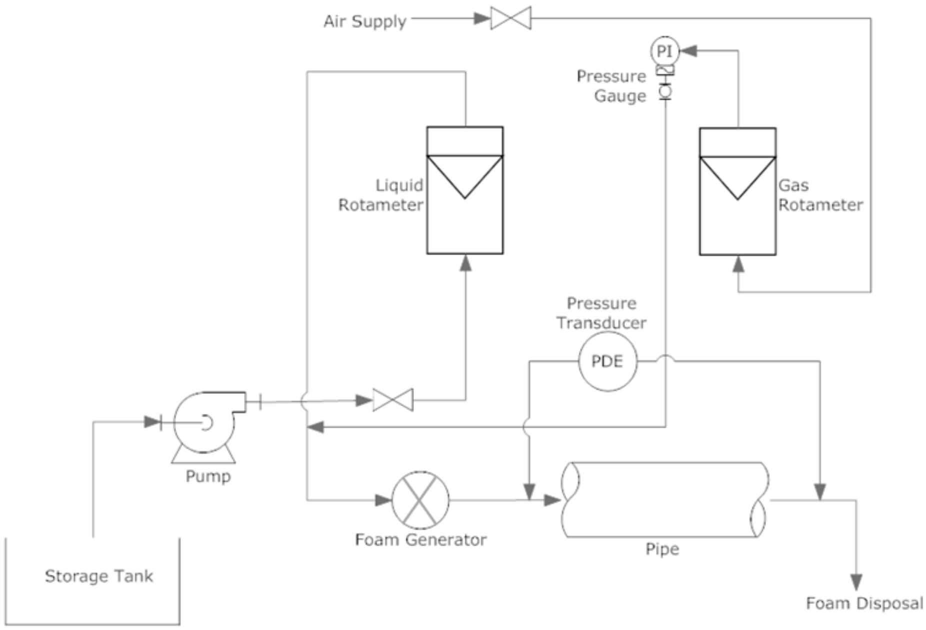

Figure 8.1: Schematic of the experimental apparatus

The air is initiated from the wall under 7 bar pressure. It is mounted to the inlet of the gas rotameter controlling the gas flow rate. The gas rotameter has a maximum capacity of 59 m^3/h and can operate up to 90 % of its maximum capacity. The volumetric flow rates are at atmospheric pressure. Valves are used at the outlet of both rotameters to control the inlet of the flow to the pipe. A MPX5100 SERIES Motorola integrated silicon pressure sensor is used to measure the pressure drop along the pipe. The transducer is mounted on one side at the inlet and the outlet of the pipe and at the multimeter on the other side. An illustration of the transducer is found in Figure 8.2. It is of high accuracy and error varies around 2.5 %. A Brymen BM629 Precision True RMS DMM multimeter is used and regulated to the voltage measurement mode.

Foam generation is provided by the foam generator mounted right before the inlet of the pipe. It is made up of a cylinder filled with stainless steel wires. Its

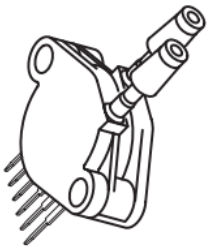

(a)

(b)

Figure 8.2: Illustrations of (a) the MPX5100 SERIES transducer (Motorola, 2001) and (b) the BM629 multimeter used as a voltmeter

function is delimited to ensure a continuous and better mixing of both gaseous and liquid phases. An anionic surfactant, Sodium Lauryl Sulfate, has been used; it is found in many commercial products as in hand soap and many other hygiene and cleaning products. The hand soap used here contain around 10 wt % of SLS. Three different foam qualities have been used: 80 %, 85 % and 90 %. Variations in the liquid and gas flow rates were adapted to the available capacities of both rotameters.

8.2 Experimental Procedure

The test procedure can be divided into a series of steps, which are listed below, to achieve the main goal of pressure drop estimation.

1. The liquid mixture is prepared by adding the hand soap containing the foaming agent (Sodium Lauryl Sulfate also known as SLS) at a 0.1 wt % SLS concentration to tap water and mixing them together in the storage tank. The concentration of SLS in the soap should be taken into account when calculating the amount of SLS added to the system.

2. The pump is put to work and the valve supplying air to the system is opened;

both phases are being mixed and foam is being formed in the foam generator. The flow rates are both being adjusted by the valves in order to get the desired foam quality. The multimeter is turned to the voltage measurement mode.

3. After having the flow flowing through the test section and after stabilization of the flow, an average value of the voltage is read off. The pressure drop is then estimated by converting the voltage into pressure through a graph associated with the MPX5100 SERIES transducer and illustrated in Figure 8.3.

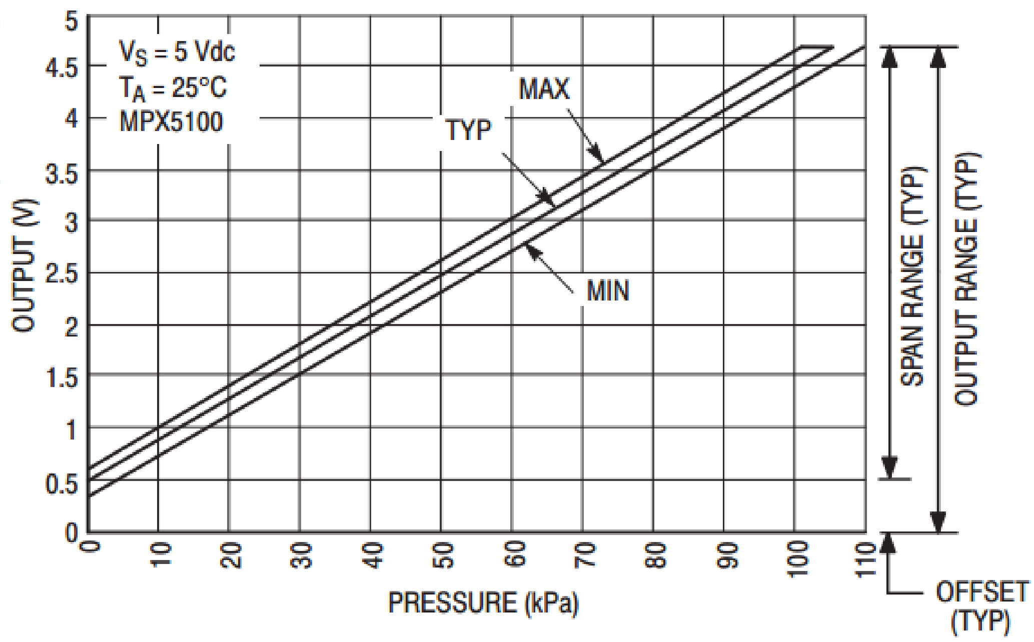

Figure 8.3: The voltmeter output vs. the pressure differential graph (Motorola, 2001)

Chapter 9

Results

9.1 Calculation Results

A series of calculations has been applied on the different pressure drop models possible. The first set of equations considers the foam as a Bingham plastic fluid. Foam will then be treated according to the Power law model. Following that the slip layer is accounted for in the case of a Power law model. By comparing the models, the behavior of the foam can be somehow understood as its rheological behavior is subject to many fluctuations hindering its modeling. Variation in the

Table 9.1: Variables in the calculations

Foam Quality	Superficial Liquid Velocity	Superficial Gas Velocity	Superficial Foam Velocity
%	m/s	m/s	m/s
80	1.7 - 3	6.8 - 11.8	8.6 - 14.7
85	1.7 - 3	9.7 - 16.7	11.5 - 19.7
90	1.7 - 3	15.5 - 26.5	17.2 - 29.5

calculations included the foam quality as well as the gas and liquid flow rates and velocities. The variation range of the factors for the different foam qualities are illustrated in Table 9.1.

It must be remarked that the foam qualities chosen are set as constants. They did not vary with the flow rates since both liquid and gas volumetric flow rates were chosen based on the foam qualities using the foam quality equation represented in equation (4.1.2).

Bingham Plastic Model Calculations

Several parameters affect the outcome of the pressure drop model. The foam density was calculated based on equation (3.1.2) where both the liquid and gas densities are considered. The first set of calculations was based on the assumption that the foam is behaving as a Bingham plastic fluid. Determining the Reynolds number required the knowledge of the effective viscosity since this model is based on the effective viscosity. The latter was calculated based on the graphs and method described earlier in this study. The Reynolds number depicts the type of flow dominating in the conduit. Most of the fields are operated under turbulent flow; therefore the analysis was mainly done under turbulent flow to mimic the field behavior. The use of the high range of velocities for both gas and liquid can be thus explained.

Several methods and equations were found to calculate the friction factor. The latter depends on the type of flow and thus the equations used are modified accordingly. The various expressions were turbulent flow expressions. The latter are dependent mainly on the relative roughness and/or the Reynolds number. A list of the equations implemented is shown in Table 9.2. Haalands equation constitutes one of the mainly used equations in determining the Fanning friction factor under turbulent flow conditions. The variable n in this equation represents the nature of the fluid being used for the analysis; therefore, n = 3 for gases and n = 1 for liquids.

Haalands has also proposed a simplified version of his equation that is used to explicitly calculate the Fanning friction factor in turbulent flow. This equation is only valid when $4.10^4 \leq Re \leq 10^8$ and $0 \leq \varepsilon/D \leq 0.05$ (Welty et al., 2000). Blasius and Moore have also developed very simple correlations.

Table 9.2: Equations for the Fanning friction factor calculation (Shankar Submarian; Skalle, 2001; Welty et al., 2000)

Correlation	Equation
Laminar	$f = 16/Re$
Moore	$f = 0.046Re^{-0.2}$
Blasius	$f = 0.0791Re^{-0.25}$
Haalands (General)	$\sqrt{\frac{1}{f}} = -\frac{1.8}{n}log[(\frac{6.9}{Re})^n + (\frac{\varepsilon/D}{3.75})^{1.11n}]$
Haalands (Explicit)	$\sqrt{\frac{1}{f}} = -3.6log[\frac{6.9}{Re} + (\frac{\varepsilon/D}{3.75})^{1.11}]$

As it is observed from the correlations, the Fanning friction factor requires the knowledge of the Reynolds number determined according to equation (4.3.15). In this case, the foam density is required as well as the effective viscosity. The first is calculated according to equation (3.1.2) while the second is calculated by determining first the plastic viscosity from Figure 6.1 and then by using equation (6.2.7). The yield stress for every foam quality can be retrieved from Figure 4.6. As for the velocity of the foam, it was calculated by the manipulation of the foam quality equation. The relevant pipe properties required for the calculation are summarized in Table 9.3.

Table 9.3: Pipe Properties

Pipe Property	Variable
Length	4 m
Outer Diameter	25 mm
Inner Diameter	23.5 mm
Roughness	0.0015 mm (Chaurette, 2003)

The purpose of the friction factor variation check is based on the necessity of determining as accurately as possible the pressure drop which represents one of the major limitations of the application of foam injection. The Fanning friction factor gave similar results when calculated with the different correlations. The different friction factors were plotted against the Reynolds number as in Figure 9.1. The only divergence from the main trend can be seen for the case when it was calculated for a turbulent flow using the laminar flow equation. For further analysis, any of the turbulent flow correlations can be used for the calculation of the friction factor as the pressure drop estimation will not be affected.

Some other correlations designed for turbulent flow were also available but eliminated as the Metzner and Reed correlation is used in the case of a Power law fluid where the basic parameters a and b depend on the flow behavior index (n). Similarly, the Colebrook equation, which is well known, is mainly used for rough pipes and thus not applicable in this study. These correlations and their coefficients are shown in Table 9.4.

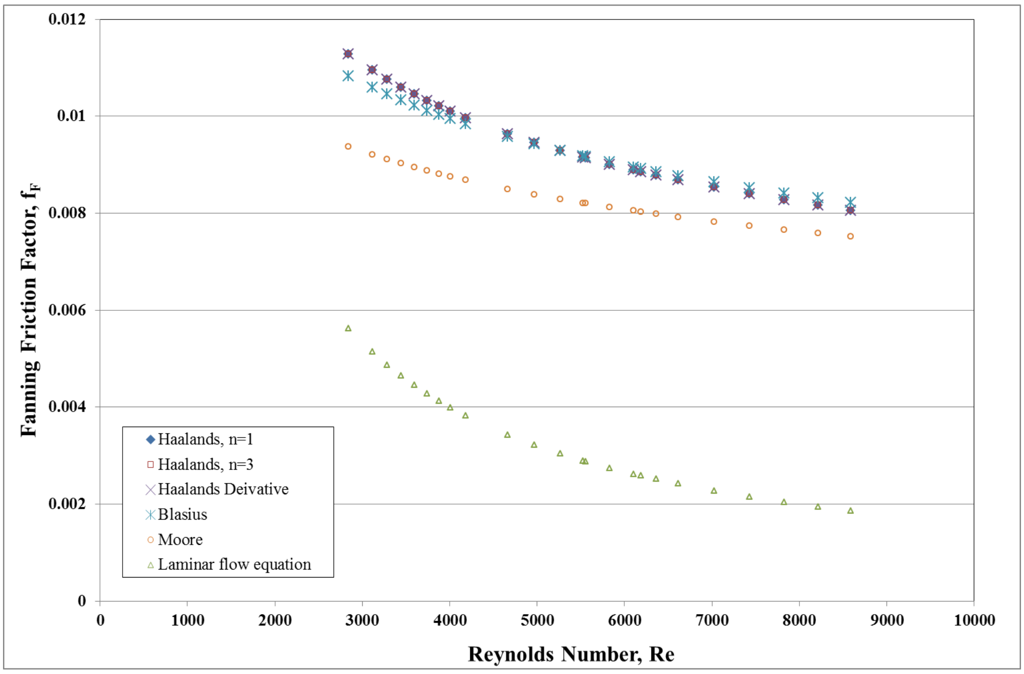

Figure 9.1: The different friction factor correlations as a function of the Reynolds number

Table 9.4: Additional Fanning friction factor correlations (Skalle, 2011)

Correlation	Equation	Coefficients
Metzner and Reed	$f_F = aRe^{-b}$	$a = \frac{log(n) + 3.9}{50}$ $b = \frac{1.75 - log(n)}{7}$
Colebrook	$f_F = c_1 + c_2 Re^{-c_3}$	$c_1 = 0.026(\frac{\varepsilon}{D})^{0.25} + 0.133(\frac{\varepsilon}{D})$ $c_2 = 22(\frac{\varepsilon}{D})^{0.44}$ $c_3 = 1.62(\frac{\varepsilon}{D})^{0.34}$

The pressure drop calculation in the case of a Bingham plastic foam follows the Darcy-Weisbach equation shown in equation (6.2.18). The latter is dependent greatly on the Fanning friction factor, the diameter of the conduit as well as the density and the velocity of the foam through the conduit.

Three major trends result from the calculations of the pressure drop. This is due to the variation in the quality of the foam. Three different qualities were chosen, as mentioned earlier, and accordingly the superficial velocity of the gas and the foam were varied. The results show that an increase in the foam quality implies an increase in the pressure drop. This also corresponds to the increase in the superficial velocity of both the gas and the foam. The results of the Bingham plastic foam are plotted in the graph of Figure 9.2.

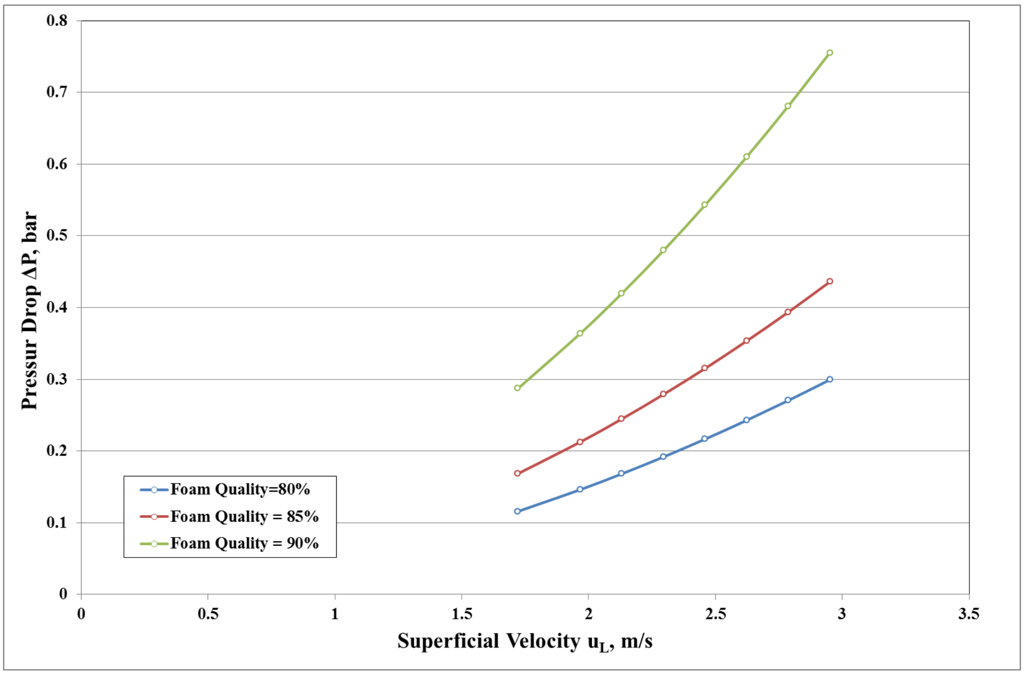

Figure 9.2: The pressure drop in the pipe as a function of the liquid superficial velocity for three different foam qualities in the case of a Bingham plastic model

The diameter of the pipe has also been subject to a sensitivity analysis. The effects of the increase and reduction in diameter size on the pressure drop are to be pinpointed. The pressure drop of a Bingham plastic foam is being calculated with a pipe inner diameter of 10 and 42 mm, respectively, keeping all the other variables constant.

The results have shown that for the same foam quality, the pressure drop increases with the reduction in the size of the pipe. The same trend has been seen for the different foam qualities. This trend conforms to the previous results where the pressure drop increases as a function of an increased foam quality. The pressure drop for the different diameters at the various foam qualities are represented in the graphs of Figure 9.3. A summary of the three different foam qualities variation is also found in Figure 9.3.

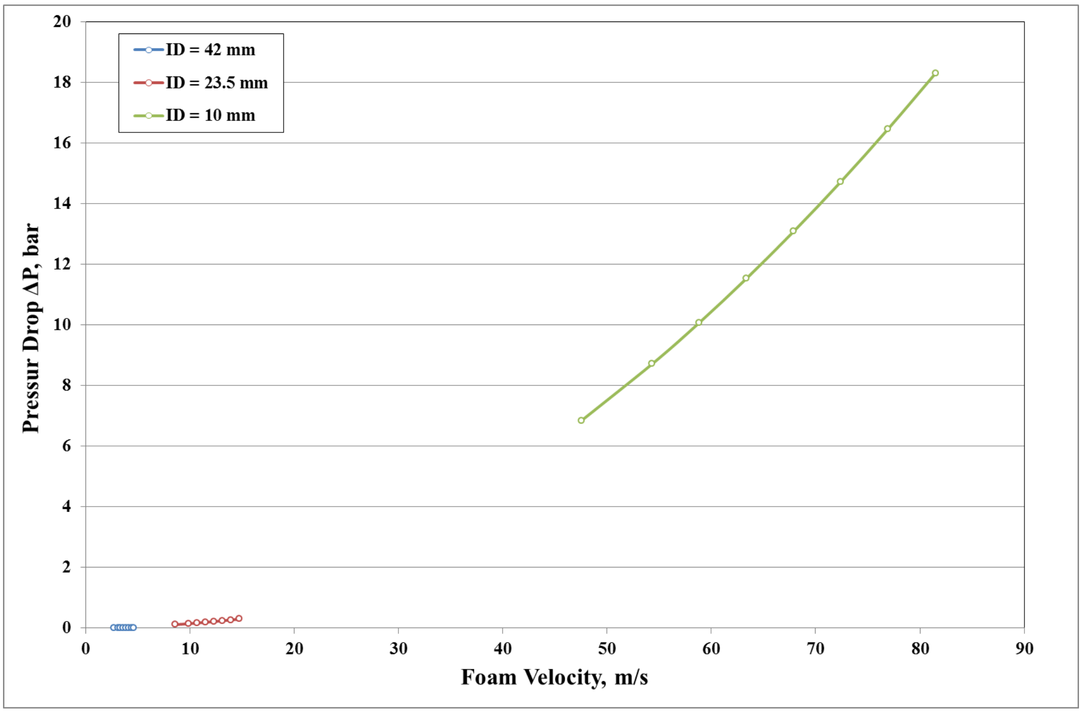
ID = 42 mm
ID = 23.5 mm
ID = 10 mm
Pressur Drop ΔP, bar
Foam Velocity, m/s
0
2
4
6
8
10
12
14
16
18
20
0
10
20
30
40
50
60
70
80
90

(a)

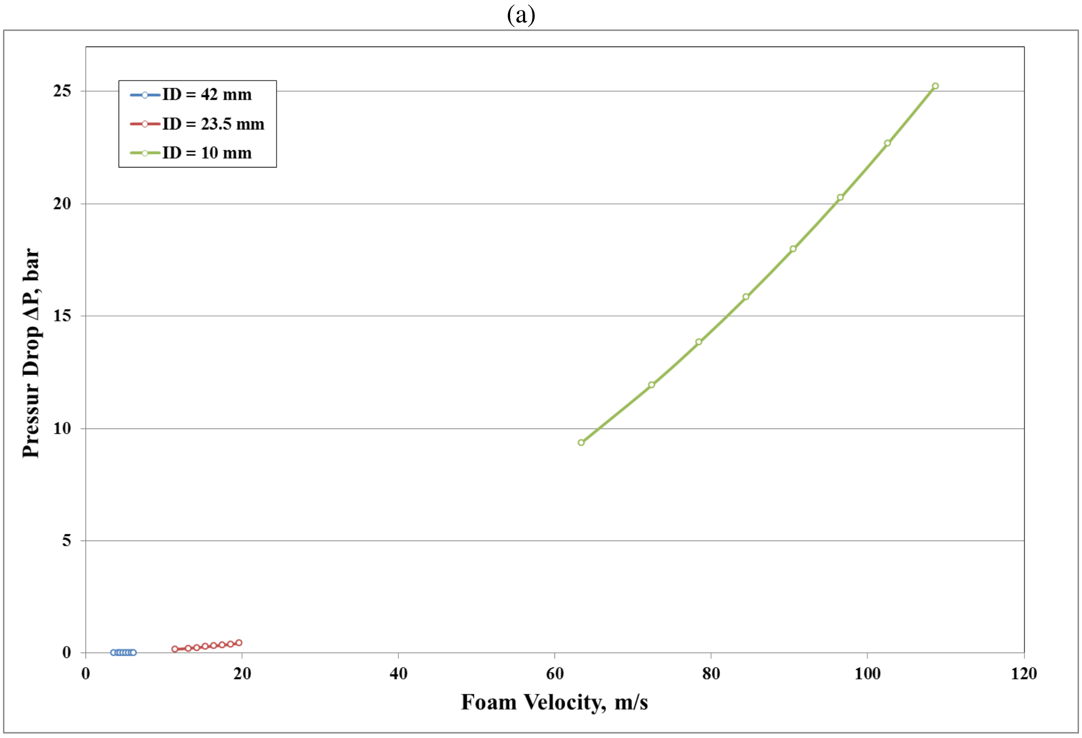
ID = 42 mm
ID = 23.5 mm
ID = 10 mm
Pressur Drop ΔP, bar
Foam Velocity, m/s
0
5
10
15
20
25
0
20
40
60
80
100
120

(b)

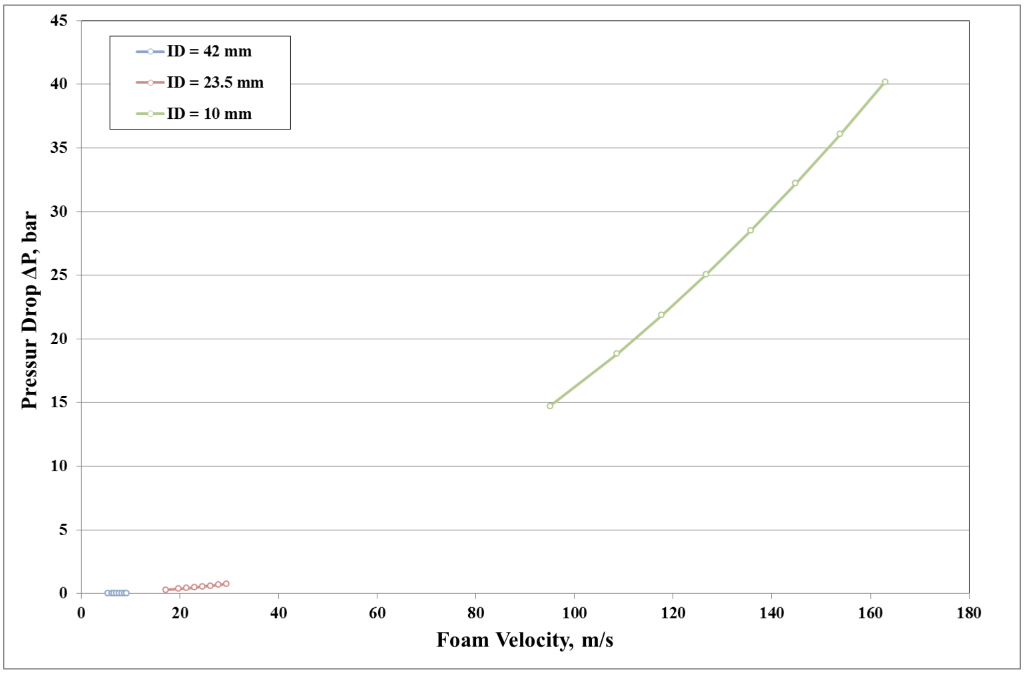

(c)

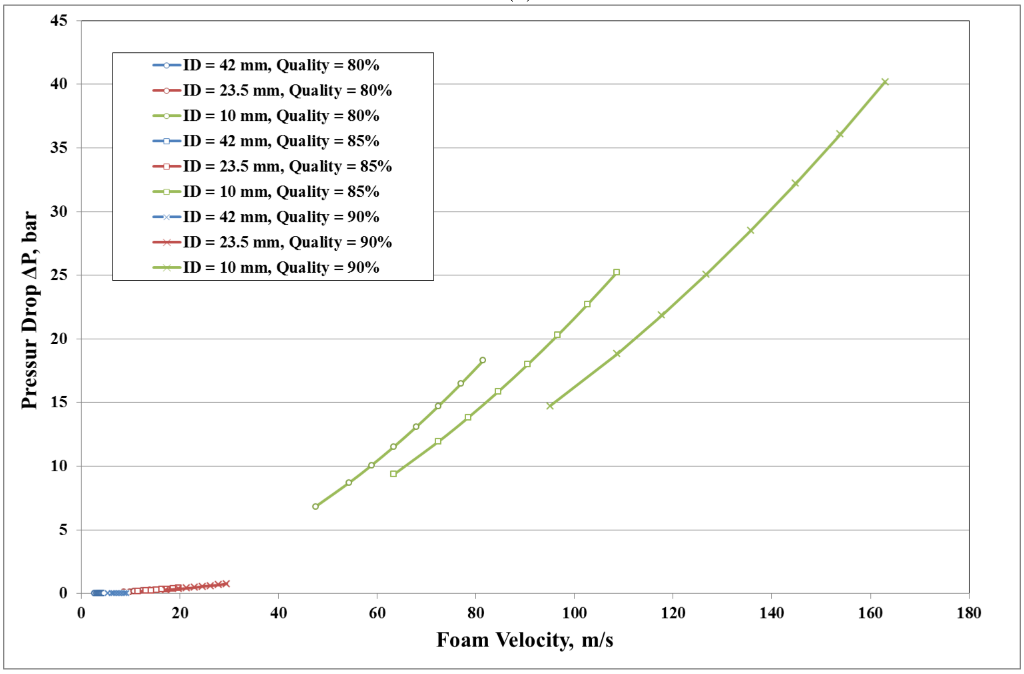

(d)

Figure 9.3: Plots of the pressure drop as a function of the foam velocity for the three different diameters in case of (a) a foam quality of 80 % (b) a foam quality of 85 % (c) a foam quality of 90 %. A summary of all the cases is represented in (d)

Power Law Model Calculations

The foam flow is now being treated as a Power law fluid. The different equations used in the process of the calculation of the pressure drop are represented in Chapter 6. The consistency index and the flow behavior index were calculated for the three different foam qualities used in this study. Following that the Reynolds number and the Metzner & Reed friction factor are computed for the series of velocities presented for every foam quality. The pressure showed a lower overall drop when compared to the Bingham plastic foam but the pressure drop has always showed an increase with the increase in quality. The plot showing the various pressure drop curves for the Power law foam is represented in Figure 9.4.

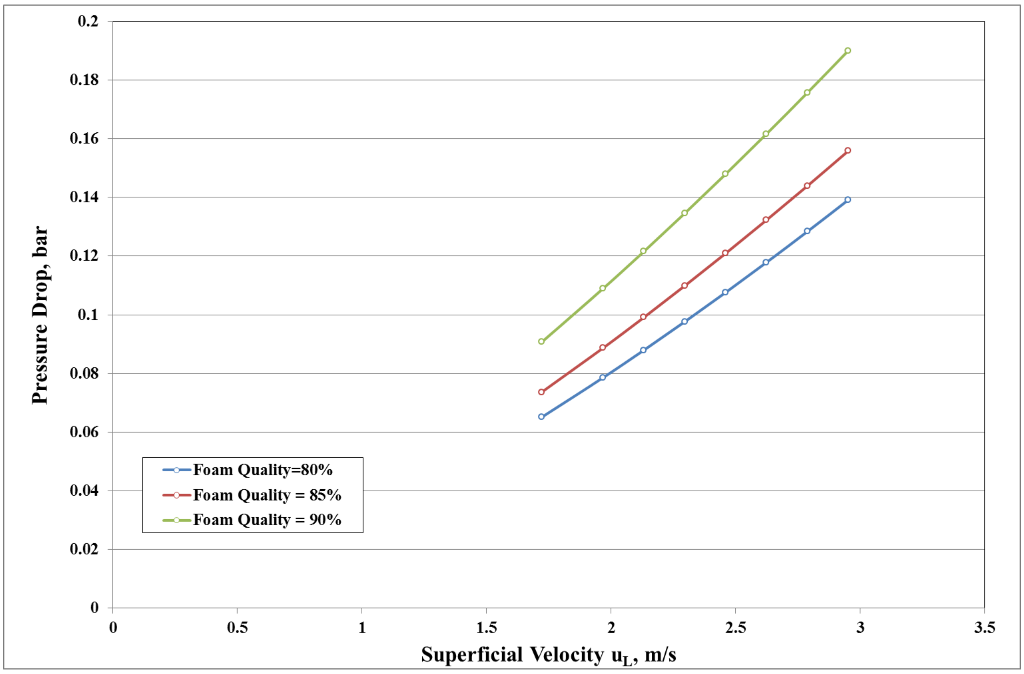

Figure 9.4: The pressure drop in the pipe as a function of the liquid superficial velocity for three different foam qualities in the case of a Power law model

Recent studies have shown that the behavior of foam in pipelines is greatly related to the slip layer that forms at the wall of the pipe. The thickness of the slip layer is determined based on the expression (6.2.25) relating the wall slip layer thickness to the diameter of the pipe. The pressure drop can be then calculated by combining the wall shear stress's equations (6.2.18) and (6.2.20).

The results were plotted on a pressure drop versus superficial liquid velocity graph. The pressure drop shows an increasing slope with the increase in the superficial liquid velocity which implies an increase of the foam superficial velocity. The pressure drop was also calculated for the three different foam qualities. Unlike the Bingham plastic and the Power law without the slip layer models, the pressure drop decreases with the increase of the foam quality. The flow behavior index which decreases with increasing foam quality and the consistency index which increases with an increased foam quality influence greatly the pressure drop within the pipe and explains the observed results.

Similarly to the Bingham plastic case, the diameter of the pipe was subject to a sensitivity analysis to check its effect on the slip layer thickness and on the pressure drop. A larger pipe of 42 mm inner diameter along with a smaller pipe of 10 mm inner diameter was subject to the pressure drop analysis. The latter is inversely proportional to the pipe diameter and thus to the slip layer thickness; the smaller pipe has shown higher pressure drop compared to the larger pipe which had a lower pressure drop. The pressure drop plotted against the superficial liquid velocity for the different pipe diameters is represented in Figure 9.5.

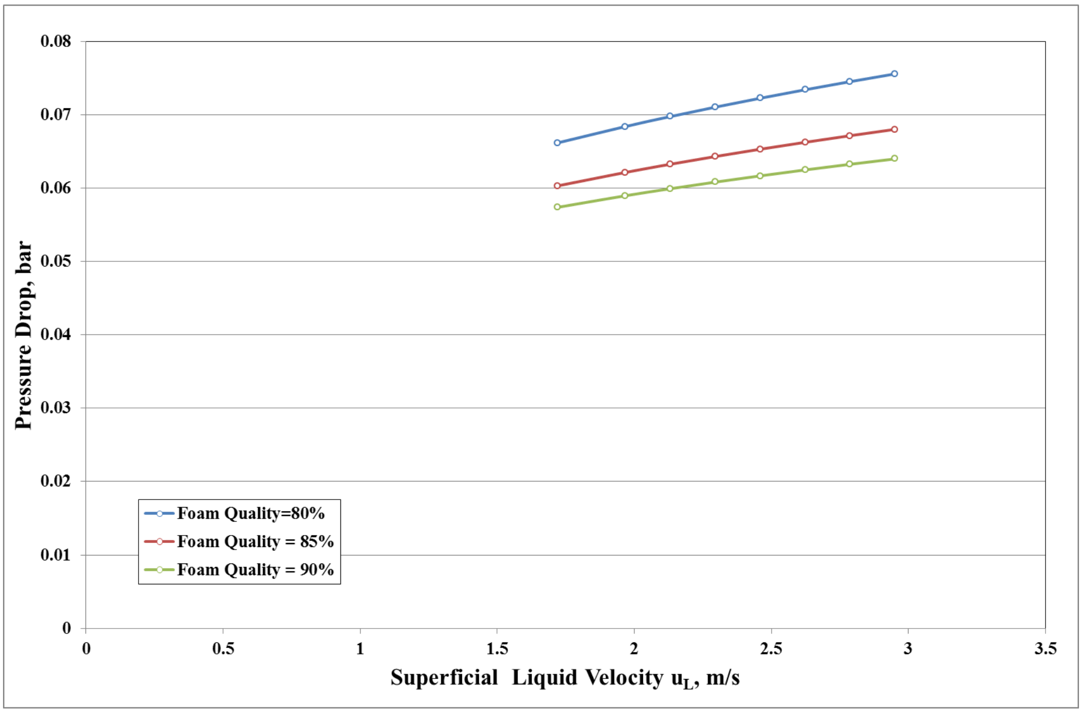

0.08
0.07
0.06
0.05
0.04
0.03
0.02
0.01
0
Pressure Drop, bar
Foam Quality=80%
Foam Quality = 85%
Foam Quality = 90%
0
0.5
1
1.5
2
2.5
3
3.5
Superficial Liquid Velocity u_L, m/s

(a)

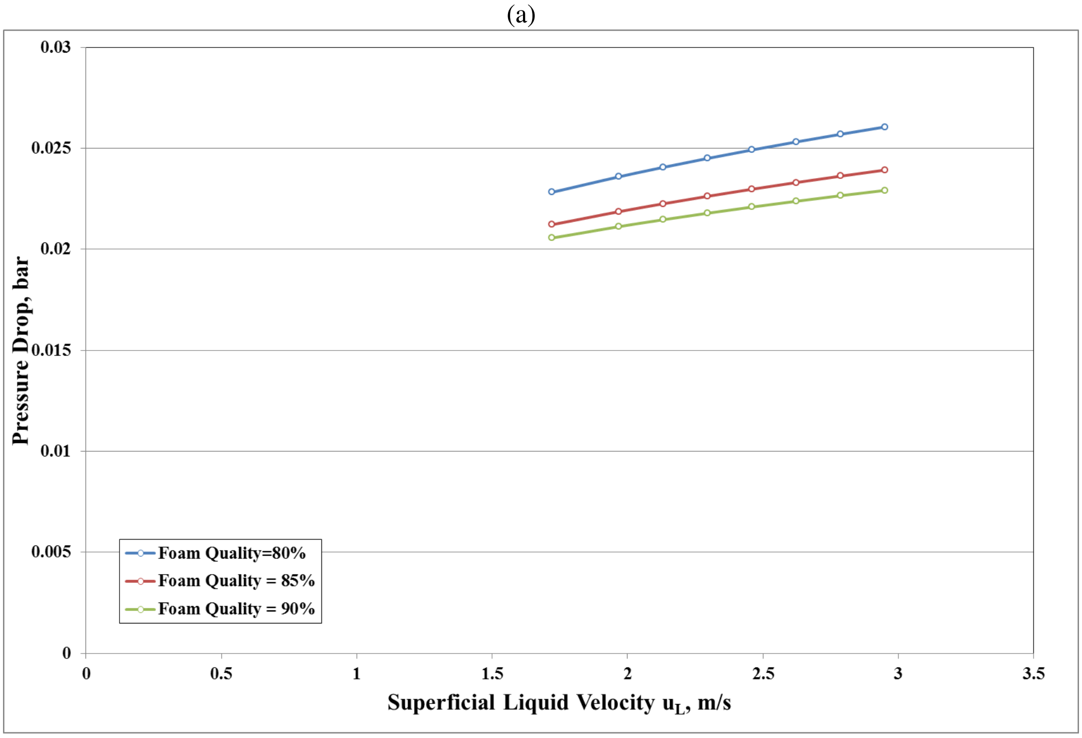

0.03
0.025
0.02
0.015
0.01
0.005
0
Pressure Drop, bar
Foam Quality=80%
Foam Quality = 85%
Foam Quality = 90%
0
0.5
1
1.5
2
2.5
3
3.5
Superficial Liquid Velocity u_L, m/s

(b)

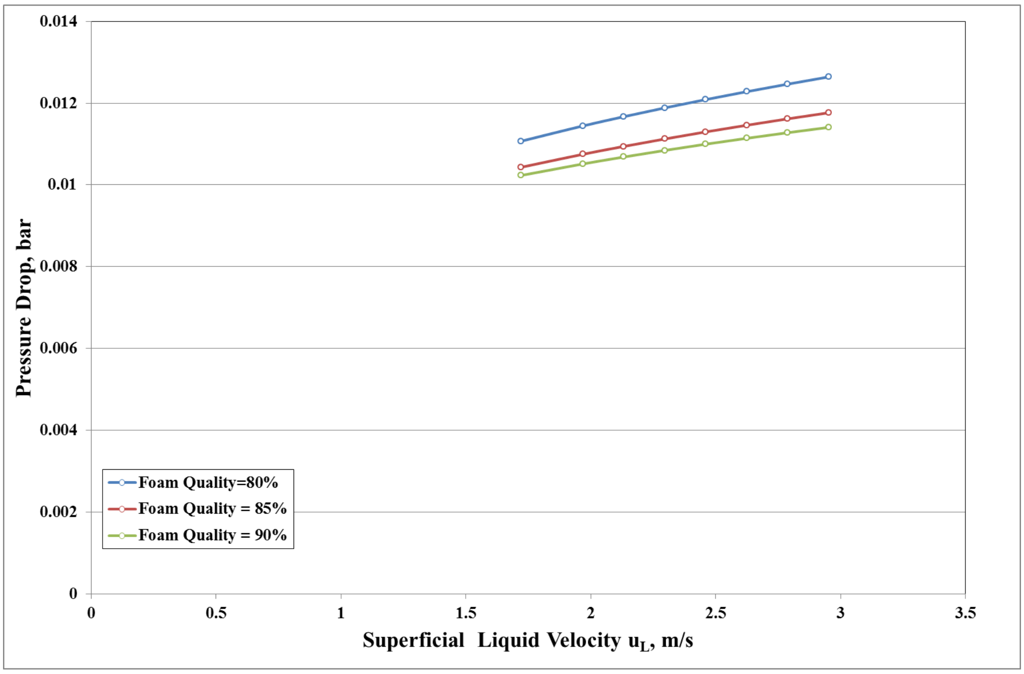

(c)

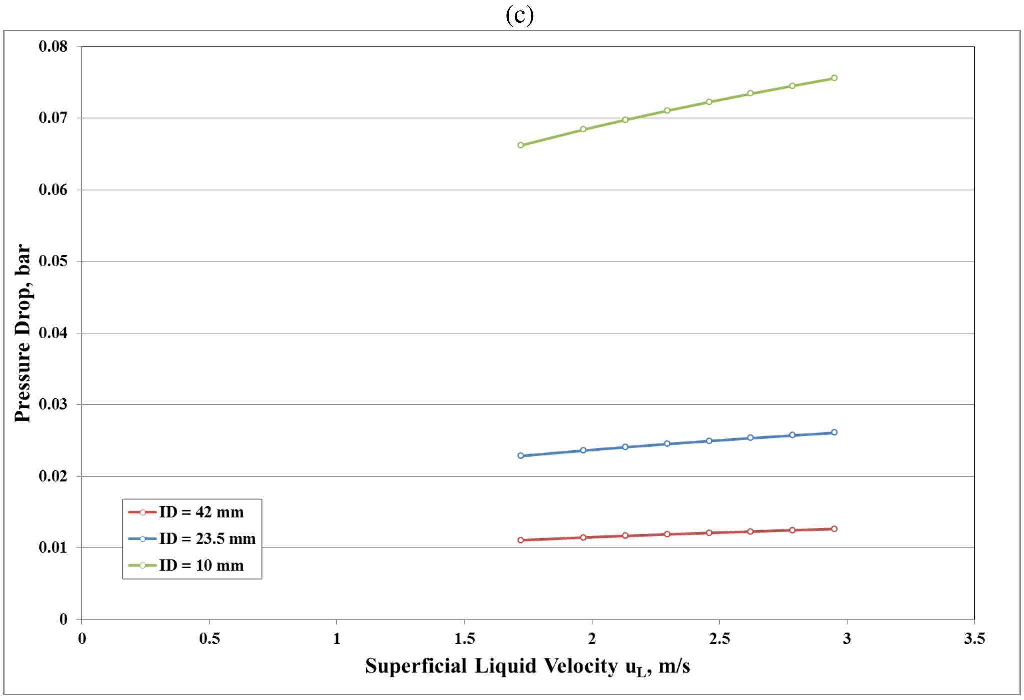

(d)

Figure 9.5: Plots of the pressure drop as a function of the superficial liquid velocity for the three different diameters in case of (a) the 10 mm inner diameter pipe (b) the 23.5 mm inner diameter pipe (c) the 42 mm inner diameter pipe. A summary of all the cases are represented in (d)for a foam quality of 80 %. The Power law model is adopted here.

The various models adopted to determine the pressure drop for a foam flow in pipelines have to be compared. The pressure drop is plotted against the superficial liquid velocity of a foam of an 80 % quality. The foam behaving as a Bingham plastic, Power low without a slip layer and Power law with a slip layer are all represented along with the results of a normal multiphase flow without the presence of any foam. This comparison would allow detecting whether the pressure drop differs with the use of foam.

Similarly, the comparison detects whether the foam flow would increase or decrease the pressure drop in the pipe. It would either refute or confirm the validity of the assumption stating that a foam tends to increase the pressure drop in a conduit. The results, which are represented in Figure 9.6, have shown that foam, no matter what model was attributed to, would result in a higher pressure drop compared to a multiphase flow. The Power law foam with the consideration of the slip layer results in a lower pressure drop compared to that of the multiphase flow at high superficial liquid velocities unlike lower velocities where it is higher.

A comparison of the amount of the change in the pipe diameter and its effect on the pressure drop variation can lead to a better understanding of the system's behavior. A double increase in the pipe diameter caused a small decrease in the pressure drop for a Bingham plastic fluid when compared to base case where the pipe diameter is set to be 23.5 mm. On the other hand, a decrease of the size of the pipe into half led to a large increase in the pressure. The same effects were seen in the case of a Power Law model but with a lower change for the smaller diameter. The diameter ratios and their corresponding pressure drop ratios for every quality are presented in Tables 9.5 and 9.6. The main purpose here is to show how sensitive is the pressure drop to the pipe diameter.

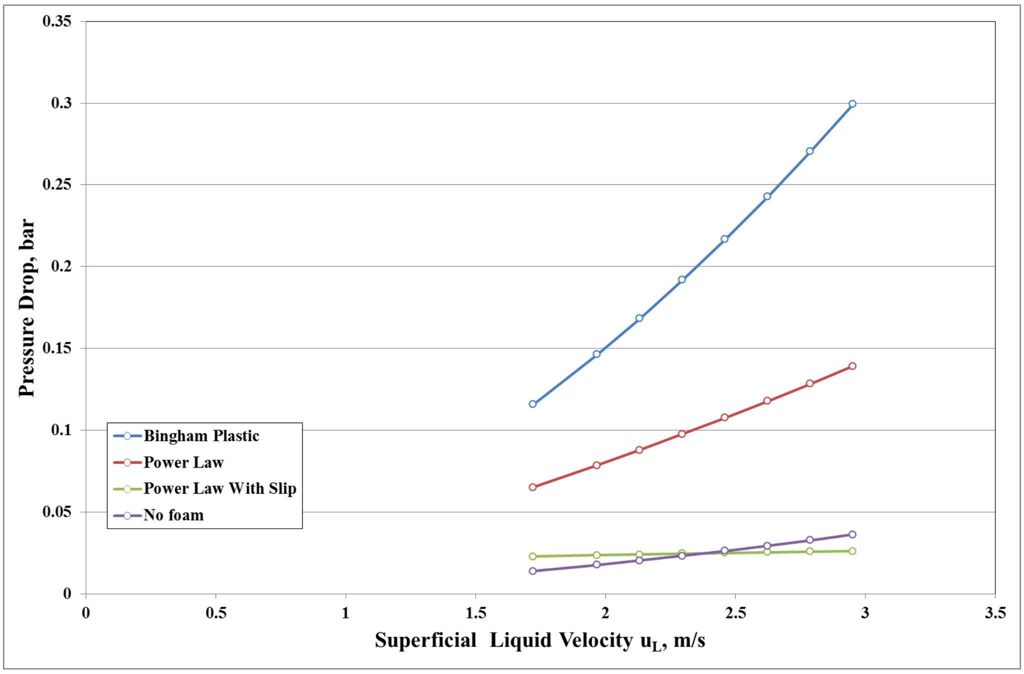

Figure 9.6: The pressure drop in the pipe as a function of the liquid superficial velocity for the different models with a foam quality of 80 %

Table 9.5: Comparison results for a Bingham Plastic Foam

Foam Quality	$D_{42mm}/D_{23.5mm}$	$D_{10mm}/D_{23.5mm}$
80 %	0.063	60.2
85 %	0.059	56.9
90 %	0.052	52.3

Table 9.6: Comparison results for Power Law foam with slippage

Foam Quality	$D_{42mm}/D_{23.5mm}$	$D_{10mm}/D_{23.5mm}$
80 %	0.485	2.89
85 %	0.491	2.84
90 %	0.497	2.79

A similar comparison was made for all the different methods with respect to the multiphase flow. A summary of the average pressure drop for every case was plotted in a histogram to show the variations. These are shown in Figure 9.7.

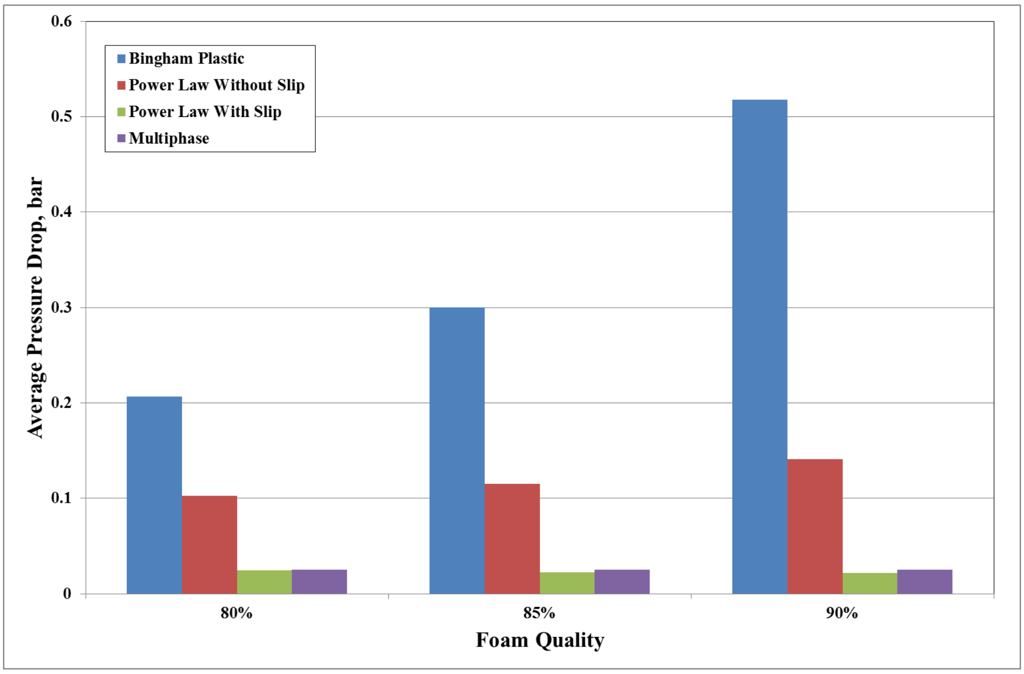

Figure 9.7: A histogram showing the average pressure drop for every model at the three different foam qualities

9.2 Experiment Results

The major purpose of the experiment is to somehow determine what behavior the foam would adopt in a horizontal conduit. Knowing the behavior allows a more accurate estimation of the resulting pressure drop. It should be noticed that the laboratory experiment is very simplified since it is not the main focus of this work. The soap volume needed takes into consideration the small concentration of the SLS surfactant in its composition. The former is estimated accordingly and has to be higher than the concentration of foaming agent required.

The results have shown an increase in the pressure drop compared to a normal multiphase flow with no foam. The values collected from the experiment are plotted in a graph, shown in Figure 9.8, along with the values obtained for the different rheological models. The collected values does show some fluctuations within a small range; therefore, a linear trendline is used to check the slope and compare it to the other models. The results have shown that the pressure drop values lie between those of the Power law model and those of the Power law model with slippage. The trend is closer to trends of the latter and the multiphase flow model. Similarly to the calculations, an increase in the foam quality led to an increase in the pressure drop.

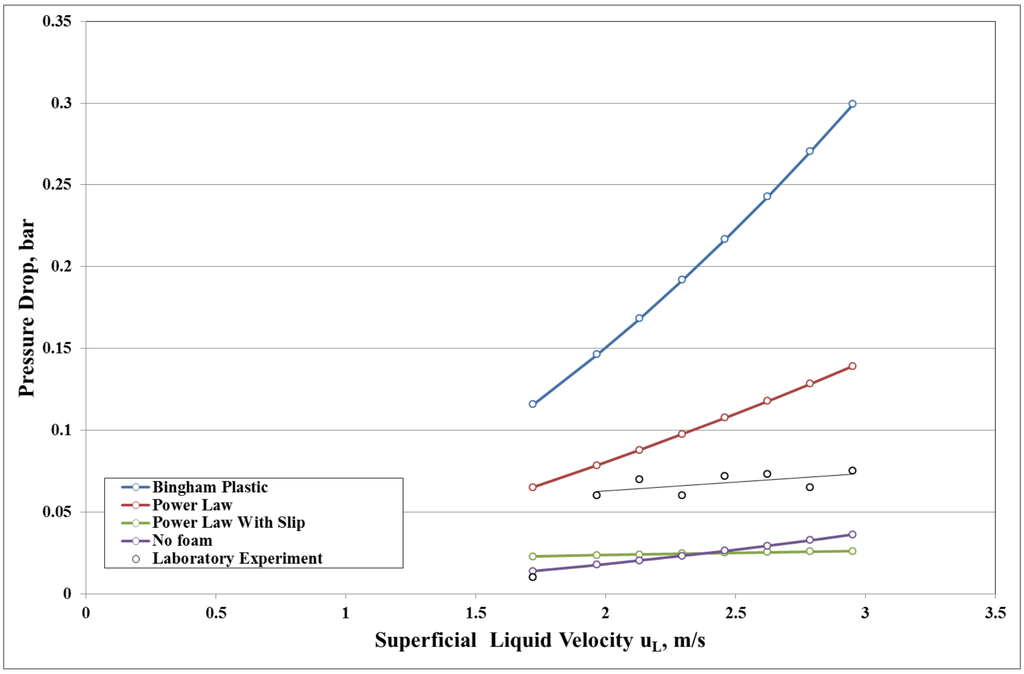

Figure 9.8: A graph showing the pressure drop measurements collected from the laboratory experiment compared to the calculated values for the different models

When plotting the data, the first data point shows a deviation from the rest of the data points; thus, it was ignored when applying the trendline. Such deviation can rise due to the fact that an average value of the voltmeter readings is taken since the values slightly fluctuates. Additionally, the average readings have to be converted to pressure drop data using the graph associated with the device. For small values of readings, the graph does not provide a very accurate conversion which explains such observation.

Chapter 10

Discussion

The main aim of this study is to analyze the applicability of foam as a technique for reduction or removal of liquid accumulations in condensate pipelines. The major concern delaying its application is the scarcity of studies regarding foam's behavior. This is due to the difficulty associated with predicting its behavior. As the pressure in the pipe is reduced along the conduit in the direction of the flow, the gas phase of the foam usually tends to expand. The friction factor shows fluctuations as in incompressible fluids and therefore, the pressure drop remains hard to predict. Moreover, the pressure drop increase associated with a foam flow in the pipe raised concerns.

The foam was studied according to several rheological models: Newtonian and non-Newtonian models. All the models used resulted in an increase in the pressure losses confirming the hypothesis. Furthermore, the pipe diameter and the slip layer thickness play a major role in the pressure drop estimation along with the friction factor. The latter should be estimated according to the corresponding correlation.

Determining the flow conditions under which the experiment is held is essential. The analysis focused on a turbulent flow to somehow mimic the flow conditions in the field where the Reynolds number is around 10^7. The flow prior to foam injection is classified as multiphase flow but as the foam is injected, the flow is treated as a single phase flow where the Reynolds number is lower. It should be noticed that a foam flow cannot be treated as a multiphase flow.

The friction factor effect on the pressure drop estimation is somehow considerable. The friction factor, which is inversely proportional to the Reynolds number, increases leading thus to higher losses in the pressure. Such behavior supports the hypothesis of an increased pressure drop in case of a foam flow. The results have shown a great difference between a friction factor calculated with turbulent flow correlations and that calculated with a laminar flow equation in the case of a turbulent flow. The latter is way smaller which implies smaller pressure drop estimation. This might ensue from the fact that the friction factor is only a function of the Reynolds number in a laminar flow while it is a function of both the Reynolds number and the relative roughness of the conduit. Accordingly, the pressure drop would be underestimated.

The quality of the foam also plays a major role in determining the pressure drop. The results have shown that an increase in the foam quality when foam is treated as a Bingham plastic or Power Law fluid leads likewise to an increase in the pressure drop. High quality foam implies a higher gas fraction. Thus, the gas velocity is increased as well as the liquid velocity. The mixture velocity becomes greater. As the velocity is raised, the flow rate becomes higher and the pressure, which is directly proportional to the foam velocity or flow rate, increases.

On the other hand, Power law foam where the slippage effect is included has shown the opposite. This is mainly due to the fact that the pressure drop is dependent not only on the foam velocity but also on both the flow behavior and consistency indices. The flow behavior index diminishes with the increase of the foam quality; thus, regardless of the increase of the mixture velocity, the decrease of n leads to a lower pressure drop for higher foam qualities.

The experimental measurements have shown that the foam exhibits a higher pressure drop than a multiphase flow through horizontal conduits. Such observation confirms the calculations and the hypothesis. Additionally, the values obtained are ranging between the pressures of a Power law model without slippage, a Power law model with slippage and a multiphase flow. For a better comparison of the results, the slopes of the different models are compared. The Bingham plastic and the Power law models are eliminated as the slopes are very incompatible. The experimental data has a trend lying in between that of a Power law with slippage and that of a multiphase flow.

For that reason, foam can belong to both models. It can be considered as a multiphase flow where the pressure drop is calculated using multiphase correlations. The latter are to be multiplied by a factor that can be called the foam factor, of a value around 2.5. On the other hand, it can also be treated as a Power law fluid with a more accurate estimation of the slip layer thickness.

The pressure drop calculation for a multiphase flow uses the density of every component separately as well as the velocity of each. Contrarily, a foam has only one density and one velocity that have to be used when pressure losses are computed. Other foam parameters, such as foam quality, have to be included in the correlations used for a more precise estimation. Then it is unlikely for foam flow to behave as a multiphase flow. Additionally, treatment of foam as a multiphase fluid in other studies gave an erroneous estimation of the pressure drop.

On the other hand, the Power law model with slippage is more likely to resemble foam's behavior. Anyhow, the trend of the experimental data is closer to the trend of this model rather than that of the multiphase flow. The small variation may be due to the simplifications and assumptions taken into account in the calculations. Gas expansion as well as gas bubbles specifications, though essential, were neglected.

A comparison of all the foam models and a multiphase flow has shown that all the models, as mentioned previously, resulted in a higher pressure drop. The case of a Power law flow with consideration of the slip layer has shown a cross-over which is basically due to the estimation of the slip layer thickness. The latter is of great influence on the pressure drop calculation. The method used in this study focuses on the dependency of the slip layer thickness on the pipe diameter. This layer is most likely to be similar to the inter-bubble lamella thickness; therefore it is dependent on the expansion ratio (E) and the average bubble diameter (d) (Calvert, 1990). Calvert et al. provided a better representation of the slip layer thickness expressed in equation (5.2.1).

The diameter of the pipe affects the pressure drop in foam flow. The latter is inversely proportional to the pipe diameter. This was valid for the various models attributed to the foam. A smaller diameter leads to smaller area and higher velocity leading to a greater friction and a greater pressure drop. The larger diameter results in a reduction in the velocity due to the increase of the area ending with a smaller pressure drop. Most of the pipelines transporting gas condensates have usually large diameters which help in the pressure drop reduction which is considerably high due to the behavior of the foam itself. A variation in the slip layer thickness has the same effect on the pressure drop since the former is directly proportional to the pipe diameter.

The results have shown that a small change in the diameter of the pipe or the slip layer thickness changes considerably the pressure drop. This can form a drawback for implementing the foam technique. The exact knowledge of the behavior of the foam is required to select the exact correlation needed to estimate the pressure drop. A wrong attribution of foam to the correct rheological model can lead to an erroneous pressure drop and thus to an unpredictable series of resulting events.

The proportional relationship between the pipe diameter and the slip wall thickness contradicts what was found in the literature. The reviews have shown that an inverse relationship links the slip layer thickness to the pipe diameter. By calculations, the pressure drop is lower for a large diameter and a large layer thickness. Theoretically, a pipe diameter increase leads to a reduction in the slip layer and the pressure losses. Such difference can be explained by the simplicity in the estimation of the slip layer thickness. The latter should develop more with a higher friction. The latter implies a higher drop in the pressure and thus a higher velocity and a smaller diameter.

The expansion of the gas phase is of great importance when dealing with a foam flow. While running the experiment, the foam was generated in the big tank and maintained while flowing through the pump, the flow meter and the inlet of the pipe. Following that, it was breaking easily. The sudden expansion of the gas phase of the foam due to the reduction of the pressure drop along the pipe can be one reason of the foam breakdown. The pipe is open at the outlet and the pressure is at atmospheric pressure of 1 bar which is lower than that of the inlet of the pipe. Such occurrence confirms the unpredictable behavior of the foam; thus, a meticulous study of the foam and the operating conditions is essential.

The foam breakdown due to the sudden expansion can be explained by the Gibbs-Marangoni effect. A stable foam undergoing a sudden expansion will cause an increase in the surface area which leads to an increase in the local surface tension. Thus, a surface contraction is formed and the resistance to further expansion causes the continuous film thinning to break (Guzmán). The Gibbs - Marangoni effect, represented in Figure 10.1, develops a force that opposes the film breaking which is crucial for de-foaming.

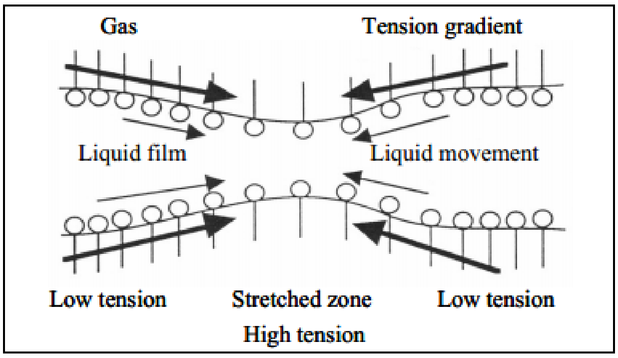

Figure 10.1: An illustration of the Gibbs-Marangoni effect (Guzmán)

The use of low concentrations of the foaming agent in the experiment can be another reason for the early breakdown of foam. Such low concentrations prevent the chemicals to reduce the surface tension as expected and then stability of foam is reduced. It should be noticed that the soap used in the experiment contain a minor percentage of the essential component required, the SLS also known as SDS. This should be accounted for when calculating the percentage of surfactant and soap to be added.

High pressure drops through pipelines can be somehow controlled and reduced by the use of an internal coating of the pipe. The latter helps in the reduction of the friction formed from the contact between the fluid and the surface of the pipe. Similarly, an internal coating leads to a greater mass rate. Additionally, a smaller concentration of foaming agents used helps in the reduction of the pressure drop. The desirable foam characteristics must be fulfilled by the critical foaming agents' concentration; this means using a foaming agent with the longest half-life and at the minimal concentration.

Some additional benefits can be acquired from the use of foam in condensate pipelines. The foam flow reduces the surface tension, the liquid droplets' density and the required critical velocity. The multiphase flow at high velocities usually has a slug flow pattern; the use of the foam reduces the flow velocity and then leads to a change in the flow pattern governing the conduit. The flow pattern is replaced by either a plug or a more stratified flow regime. The outcome is a continuity in the production along with a maintenance of production. But on the other side, the total production diminishes.

The amount of slug usually retained from a multiphase flow is large and requires buffer volumes at the receiving terminals to handle it. The foam flow, as mentioned earlier, modifies the flow pattern and by that can eliminate or at least reduce the amount of slug. Hence, the buffer volume at the receiving terminal can be avoided or can be designed with a smaller size since the latter depends on the volume of the slug expected to form. Such advantage of the foam cuts the expenses associated with slug catchers.

The use of slug catchers is a quite expensive solution applied in the oil industry. This equipment requires large areas as they have to handle large volumes of slugs; some of the slug catchers can reach the size of a football field. The material used to build slug catchers is costly as well as the transportation costs and installation cost. Furthermore, the number of workers required to put the pieces together represents some additional costs. The time needed to put together the equipment is long and can thus stop production for several days.

Table 10.1: Costs associated with slug catchers (Contreras et al., 2007)

Characteristic	Finger Type	Vessel Type
Equipment Cost	1.22 million $	1.87 million $
Installation Cost	0.107 million $	0.058 million $
Area Required	88 meters square	41 meters square
Installation Time	30 days	10 days

The high costs apply for both types of slug catchers: the vessel type and the finger type. A summary of the costs associated with both types are represented in Table 10.1. The high price of the equipment material, its installation costs and the area required represents an incentive to find and implement other techniques to handle slugs and liquid accumulations.

Pigging activity is sometimes required in gas-condensate pipelines. It is used to clean the pipelines from hydrates and other possible products that might block or impede production. It is also classified as an expensive solution as it requires a pig trap arrangement with the pig launcher and receiver. The associated price ranges between 7 120 and 8 420 $ per pig; and a pig is usually launched at least once per month. Additional costs may also be considered for disposing large quantities of pig trash and all the contaminating components that can come along. The pigging activity does not stop production for a long time: it might require 16 hours for a round trip in the pipeline along with two hours to set it up. Therefore, this might cut on the company's profits. Foam, when used, can reduce the pigging activity.

Foam in pipelines is a cheaper substitute to the previously stated techniques. The foam needs to be generated by mixing the surfactant and the flow in a foam generator. The average price of the installation of a foam generator ranges between 500 and 9 800 $. As for the annual cost of the foaming agents, it is 6 000 $ (EPA, 2011). The appropriate choice of surfactants with the lowest CMC helps in getting better results with smaller concentrations. Moreover, the simplicity in the application of this technique as mentioned in earlier chapters adds to the advantages associated with the use of surfactants and foam.

A simple comparison of the various costs associated with a slug catcher, pigging and foam is shown in Table 10.2. Foam seems to outweigh both techniques in feasibility. But this also depends on the size of the field, the production rate and different operating conditions that should be considered.

Foam and foaming agents represent a zero emission solution for removal of

Table 10.2: Cost summary for the different techniques of liquid removal

Costs	Slug Catcher	Pig	Foam
Installation	1.2 - 1.9 million $	5 000 - 10 000 $	500 - 9 880 $
Operational	Maintenance Costs	7 120 - 8 420 $ per pig	500 $ per month

liquid accumulations in pipelines. As it was shown earlier, most of the foaming agents that can be used are biodegradable and environmentally friendly. They can be classified as green components. Such property prioritize the use of foam compared to the other techniques. Moreover, the water contact with the steel will be reduced by foam flow and the corrosion will diminish and so the need for corrosion inhibitors. This reduces the harm that might be associated with the use of other less biodegradable and green chemicals. Additionally, the foaming agents should be applied only in small concentrations with which the experiment was consistent.

Foaming in the system can cause some problems and de-foamers have been used frequently to eliminate the foam. The platform can be shut down in case the foam activity is not controlled appropriately. The flooding at the downstream equipment such as scrubbers and compressors can occur due to the liquid carry-over in the gas outlet. Furthermore, higher compression might be required in case of liquid carry-under. Hence, de-foamers have to be applied, as mentioned earlier, before the pipeline outlet to avoid the damage of the downstream equipment. Moreover, the minimal use of surfactants is justified.

To decide whether the foam is applicable as a flow assurance technique, a comparison between the advantages and the disadvantages of its use is crucial. A simplified citation of the pros and cons of foam is listed in Table 10.3. The costs associated with a plugged or shut pipeline can be summarized by billions of dollars per day; therefore, a continuous production is always required. Foam can be one closer step to a greener and more effective production of multiphase condensate pipelines, only if handled and studied thoroughly.

Table 10.3: Advantages and disadvantages of foam

Advantages	**Disadvantages**
Reduction of surface tension	Higher pressure drop than multiphase flow
Continuity of production	Reduction in production rate
Reduction of flow velocity	Loss pump efficiency and capacity
Change in flow regime	Foam breakdown due to sudden expansion
Reduction of slugs' volume	Reduction in separator efficiency
Prevention of liquid accumulation in law lying pipes	Difficulty in foam behavior prediction
Reduction in the size of slug catchers	Reduction in the effective volume available for gas/liquid separation in primary separators
Use of small percentage of foaming agents	Fluid carryover in gas flowlines
Simple and cheap	
Environmentally friendly	

Chapter 11

Conclusion

Flow assurance has driven the attention of the oil industry for a long time now. The problems associated with the transportation of gas condensates to receiving terminals have led to the development of many new techniques. Furthermore, the topography of the terrains on which the long pipelines are lying are causing further liquid accumulations especially in the low lying parts. Most of the solutions developed are expensive or cannot completely prevent a shut down of the pipeline. Foam has been in use in different disciplines and has very distinguishing characteristics that allow it to be considered for eliminating or preventing these liquid accumulations in multiphase pipelines.

Foam behavior is unpredictable and can cause a variety of hazardous events. Pressure loss is very common throughout any conduit, the gas phase is therefore expected to expand leading to a variation in the friction factor calculation. The pressure drop due to the presence of foam becomes then hard to predict. Another drawback of the foam is the sudden breakdown due to gas phase expansion. This has been encountered during the experiment. Such an occurrence ratifies the existence of a large pressure drop when the foam is induced in a conduit.

The pressure drop depends largely on the foam rheological behavior. Therefore, many calculations were done to check the difference in the pressure loss for the various models. The comparison with the experimental data suggests the necessity of treating foam as a Power law fluid with a slippage. The calculations also aimed to check whether the foam flow would result in a higher pressure drop than the multiphase flow. They have confirmed the hypothesis and avoiding such a high pressure drop can be applied by using an internal coating in the pipe which will reduce the friction or by using a minimum concentration of foaming agents. If applied, the foam should maintain a quality ranging between 80 and 87 % as the higher the quality, the higher the tendency for a slug flow pattern to dominate.

A slip layer can develop in a foam flow at the wall of the pipe. The prediction of the thickness of this layer is crucial for the pressure losses' estimation. The calculations showed an inversely proportional relationship between the thickness of the slip layer and the pressure drop. It should be mentioned that the estimation of the slip layer, on which the bulk foam is flowing, represents a challenge since it develops from the foam itself. Therefore, the thickness and the viscosity of this layer are highly dependent on the properties of the foam which are of high uncertainty.

Foam can be considered as an economic and clean solution for the reduction or the elimination of liquid accumulations by maintaining a continuous flow in the conduit. The change in the flow pattern dominating in the pipe is responsible for the stability of the flow. The equipment required to inject surfactants are cheap compared to slug catchers and pigs. The latter can be then reduced in size and frequency, respectively. Similarly, the costs of surfactants per year are minimal due to the small percentage supposed to be used. Additionally, the majority of the foaming agents to be used have a high biodegradability and are considered environmentally friendly.

The careful handling of foam in horizontal conduits might be the future solution of removal of liquid accumulations in horizontal pipelines. The problems associated with foam flow are known and further studies can be carried out by estimating the exact slip layer thickness. The effect of both the bubble size and distribution along with the expansion ratio, which were neglected in this study, on the behavior of the foam should be accounted for. Foam can be summarized as an economic and eco-friendly solution that ensures a continuity in flow.

Chapter 12

Recommendations

This study has shown several limitations due to the simplifications attributed to the calculations and the laboratory experiment. The expansion ratio and the bubble size and distribution were neglected. This might shape differently the behavior of foam. The foam behavior and rheological properties are posing a considerable amount of uncertainty in pressure loss estimation.

- Further studies can evaluate the pressure drops taking into consideration both the expansion ratio as well as the bubble size and distribution to mimic the situations encountered in the field.

- A meticulous study of the foam behavior and rheology can assist in the elimination of ambiguity.

- Developing a program that would calculate the pressure drop throughout a horizontal and inclined conduits can facilitate the calculation of the pressure drop and provide a better handling of larger amount of data.

- Applying this program on real field data would provide a better understanding of the difference between field and experimental results.

Bibliography

C.J. Alvarez and S.S. Al-Malki, Saudi Aramco. Using gas injection for reducing pressure losses in multiphase pipelines. In *âĂć*, Denver, Colorado, October 2003. SPE Annual Technical Conference and Exhibition, Society of Petroleum Engineers.

J.F. Argillier, Institut Francais du Petrole, S. Saintpere, TOTAL Exploration Production, B. Herzhaft, Institut Francais du Petrole, and A. Toure, CENERGYS: Consultant for TOTAL. Stability and flowing properties of aqueous foams for underbalanced drilling. In *âĂć*, New Orleans, Louisiana, September . SPE Annual Technical Conference and Exhibition, Society of Petroleum Engineers.

R.E. Blauer, B.J. Mitchell, and C.A. Kohlhaas, Colorado School of Mines. Determination of laminar, turbulent, and transitional foam flow losses in pipes. In *âĂć*, San Francisco, California, April 1974. SPE California Regional Meeting, Society of Petroleum Engineers.

M.I. Briceño and D.D. Joseph. Self-lubricated transport of aqueous foams in horizontal conduits. *International Journal of Multiphase Flow*, (29), 2003.

J.R. Calvert. Pressure drop for foam flow through pipes. *International Journal of Heat and Fluid Flow*, Volume 11(Issue 3):236–241, September 1990. Department of Mechancal Engineering, University of Southampton, Southampton SO9 5NH, UK.

J. Chaurette. Pipe roughness values, February 2003. URL `http://www.pumpfundamentals.com/download-free/pipe_rough_values.pdf`.

V. Contreras, M. Alfredo, and N. Foucart. Selection slug catcher type. In *âĂć*, number SPE 107293, Buenos Aires, Argentina, April 2007. Latin American & Caribbean Petroleum Engineering Conference, Society of Petroleum Engineers.

M. Crabtree, D. Eslinger, P. Fletcher, M. Miller, A. Johnson, and G. King. Fighting scale - removal and prevention. *Oilfield Review*, 1999.

N.S. Deshpande and M. Barigou. The flow of gasâĂŞliquid foams in vertical pipes. *Chemical Engineering Science*, Volume 55(Issue 19):4297–4309, October 2000.

The Dow Chemical Company. Surfactant basics - definition of critical micelle concentration (cmc), January 2010. URL `www.dow.com`.

D.J. Durian. The physics of foam. Technical report, Boulder School for Condensed Matter and Materials Physics, UCLA Physics & Astronomy - Los Angeles, CA 90095-1547, July 2002.

EPA. Options for removing accumulated fluid and improving flow in gas wells. *United States - Environmental Protection Agency*, 2011.

T. Eren. Foam characterization: Bubble size and texture effects. Master's thesis, The Graduate School Of Natural And Applied Sciences Of Middle East Technical University, September 2004.

R.N. Gajbhiye and S.I. Kam. Characterization of foam flow in horizontal pipes by using two-flow-regime concept. *Chemical Engineering Science*, Volume 66 (Issue 8):1536–1549, April 2011.

G. Gregory and K. Aziz. Design of pipelines for multiphase (gas-condensate) flow. *Journal of Canadian Petroleum Technology*, Volume 14(Number 3), July-September 1975.

N. M. Guzmán. *Foam Flow In Gas-Liquid Cylindrical Cyclone (GLCC*. PhD thesis.

R. Höhler and S. Cohen-Addad. Rheology of liquid foam. *Journal of Physics: Condensed Matter*, Volume 17(Number 41), September 2005.

M. Hubbe. Mini-encyclopedia of papermaking wet-end chemistry - additives and ingredients, their composition, functions, strategies for use, âĂć. URL `http://www4.ncsu.edu/~hubbe/DFOM.htm`.

D.D. Joseph. Understanding foams & foaming. *Journal of Fluids Engineering*, May 1997. To appear in the column entitled Significant Questions in Fluid Mechanics.

T. Karam. Slug catchers in natural gas production. Technical report, Norwegian University of Science and Technology, 2012.

G. E. Kouba, A. Montesi, and L. D. Rhyne. Foam for mitigation of flow assurance issues in oil and gas systems. *United States Patent Application Publication*, (US 2008/0099946 A1), May 2008.

A. Kraynik, Sandia National Labs, D. Reinelt, Southern Methodist University, F. Van Swol, Sandia National Labs, and S. Hilgenfeldt, Northwestern University. Foam structure and rheology: The shape and feel of random soap froth - foam microrheology. Technical report, Sandia National Laboratories, âĂć.

E. Kuru, SPE, S. Miska, SPE, M. Pickell, SPE, N. Takach, and M. Volk, The University of Tulsa. New directions in foam and aerated mud research and development. Caracas, Venezuela, April 1999. Latin American and Caribbean Petroleum Engineering Conference, Society of Petroleum Engineers.

D.L. Lord, Halliburton Services. Analysis of dynamic and static foam behavior. *Journal of Petroleum Technology*, Volume 33(Number 1):39–45, January 1981.

J. Lyklema, V. Bergeron, and P. Walstra. Fundamentals of interface and colloid science: Soft colloids. chapter 7 - foams. *Elsevier*, 2005.

F Morgan. Mathematicians, including undergraduates, look at soap bubbles. *The American Mathematical Monthly*, Volume 101(Number 4):343–351, April 1994.

Motorola. Integrated silicon pressure sensor on-ship signal conditioned, temperature compensated and calibrated. *Motorola, Inc.*, 2001. Semiconductor Technical Data.

R. Nave. Hyperphysics-laplace law, 2013. URL `http://hyperphysics.phy-astr.gsu.edu/hbase/ptens.html`.

O. Osunde and E. Kuru. Numerical modelling of cuttings transport with foam in inclined wells. *The Open Fuels and Energy Science Journal*, 1:19–33, 2008. School of Mining and Petroleum Engineering, The University of Alberta, Canada.

Y. Peysson and B. Herzhaft, Institut Francais Du Petrole. Lubrication process at the wall in foam flow - application to pressure drop estimation while drilling ubd wells. In *âĂć*, number ISBN 978-1-61399-112-1, Calgary, Alberta, June 7 - 9 . Canadian International Petroleum Conference, Society of Petroleum Engineers [successor to Petroleum Society of Canada].

Schlumberger. Schlumberger oilfield glossary, 2013. URL "`http://www.glossary.oilfield.slb.com/en/Terms/c/colloid.aspx`".

R. Shankar Subramanian. Fanning friction factor for turbulent flow through circular pipes. Technical report, Department of Chemical and Biomolecular Engineering - Clarkson University, âĂć.

P. Skalle. Drilling fluid engineering. 3 - drilling fluid viscosity control. *Pål Skalle and Ventus Publishing ApS*, 2011. Available on bookboon.com.

F. Skoreyko, Computer Modelling Group, A. Villavicencio Pino, Pemex E & P, H. RodrÃŋguez Prada, Independent Consultant for Pemex, and Q.P. Nguyen, University of Texas at Austin. Understanding foam flow with a new foam eor model developed from laboratory and field data of the naturally fractured cantarell field. In *âĂć*, Tulsa, Oklahoma, USA, April . SPE Improved Oil Recovery Symposium, Society of Petroleum Engineers.

P. Tisné, L. Doubliez, and F. Aloui. Determination of the slip layer thickness for a wet foam flow. *Colloids and Surfaces A: Physicochemical and Engineering Aspects*, Volume 246(Issues 1-3):21–29, October 2004.

J. Welty, C. Wicks, R. Wilson, and Rorrer G. *Fundamentals of Momentum, Heat, and Mass Transfer*, chapter Chapter 13 - Flow in Closed Conduits, pages 170–175. John Wiley & Sons, Inc., 5^{th} edition, March 2000.

N. V. Zagoskina and O. M. Sokovnin. Conditions for foam flow and breaking. *Theoretical Foundations of Chemical Engineering*, 35(1):95–98, April 1999. Vyatka State Technical University, Moskovskaya ul. 36, Kirov, 610601 Russia.

Appendix A

Rheological Calculations

The calculation of the rheological parameters can be done in the laboratory using the VG viscometer to determine the shear rate and the shear stress. By knowing those two parameters, a rheogram can be built and the wall shear stress can be determined by extrapolating the curve until the shear rate is zero. The slope can be used to determine the plastic viscosity in the case of the Bingham model and the flow behavior index n in case of Power law and Herschel-Bulkley models.

A sample from the foam resulting from the pipes can be tested in the laboratory. It has to be added in the 350 ml cup of the VG rheometer where readings, noted as θ, are taken at six different RPMs. From the latter, the true shear stress can be determined by multiplying the readings by a correction factor of 1.06. The true shear stress unit in this case is $lb/100ft^2$ and can be converted to Pascal by multiplying the first by 2.088. The shear rate is then easily calculated by multiplying the RPM value by 1.703.

The different formulas for the different rheological models relating the shear stress and the shear rate can be summarized as follow:

- for a Newtonian fluid:

$$\tau = \mu\dot{\gamma} \tag{A.1}$$

- for a Bingham plastic fluid:

$$\tau = \tau_w + \mu_p \dot{\gamma} \tag{A.2}$$

- for a Power law fluid:

$$\tau = k\dot{\gamma}_n \tag{A.3}$$

- for a Herschel-Bulkley fluid:

$$\tau = \tau_w + k\dot{\gamma}_n \tag{A.4}$$

The calculation process is very simple for the Newtonian fluid where the viscosity can be determined by knowing the true shear stress and the shear rate. As for the Bingham plastic model, it is based on a 2 data point model with a standard approach where the plastic viscosity is calculated from the slope of the rheogram curve by the following formula:

$$\mu_p = \frac{\tau_{RPM1} - \tau_{RPM2}}{\dot{\gamma}_{RPM1} - \dot{\gamma}_{RPM2}} \tag{A.5}$$

The RPM1 is equivalent for example for an RPM of 600 (or 300) and RPM2 is equivalent for an RPM of 300 (or 200). The wall shear stress can now be calculated from:

$$\tau_w = \tau_{RPM1} - \mu_P \dot{\gamma}_{RPM1} \tag{A.6}$$

If the data were to be calculated with the oil field approach, the results are almost the same with an error margin of 1 %. The power law model shows that the flow behavior is calculated from the slope of the logarithmic version of the graph. The expression used becomes:

$$\mu_p = \frac{log\tau_{RPM1} - log\tau_{RPM2}}{log\dot{\gamma}_{RPM1} - log\dot{\gamma}_{RPM2}} \tag{A.7}$$

The consistency index k is calculated by manipulating the main formula for the Power law model resulting in:

$$k = \frac{\tau}{\dot{\gamma}^n} \tag{A.8}$$

The analysis of the Herschel-Bulkley model is more complex and requires a 3 data point analysis. The oil field approach is the easiest to estimate the parameters and can be done by reading the yield shear stress from the graph at a zero shear stress or by assuming that this value is equal to the shear stress associated with the lowest RPM of 3. The n can be also found from the slope of the log-log plot of the shear stress and shear rate. As for the k value, it is determined by:

$$k = \frac{(\tau_2 - \tau_y)}{(\dot{\gamma}_2 - \dot{\gamma}_y)^n} \tag{A.9}$$

On the other hand, the calculation of those parameters in the case of a standard approach is more complex and requires an iterative process since three data points are to be used resulting in 3 equations that need to be solved simultaneously (Skalle, 2011).

Appendix B

Pressure Drop Calculations

Tables summarizing some of the input and output data for the calculations of the pressure drop are illustrated in this appendix.

Table B.1: General input for the three models

Property	Input	Unit
Pipe Roughness	0.0015	*mm* (Chaurette, 2003)
Pipe ID	23.5	*mm*
Area	0.00043	m^2

Table B.2: Additional input for the Power law model

Foam Quality	n	k	Shear Stress
[%]	$[-]$	$[Pas^{-}]$	$[Pa]$
80	0.246	0.123	1.416
85	0.223	0.147	1.436
90	0.202	0.175	1.480

Table B.3: Pressure drop calculation for the Bingham plastic model

Foam Quality [-]	Liquid Flow Rate [m^3/s]	Mixture Flow Rate [m^3/s]	Gas Flow Rate [m^3/s]	Gas Velocity [m^3/s]	Mixture Velocity [m^3/s]	Liquid Velocity [m^3/s]	Foam Density [Kg/m^3]	Effective Viscosity [cP]	Effective Viscosity [Pa.s]	Reynolds Number [-]	Flow Type [-]	Fanning Friction Factor	Pressure Drop [Pa]	Pressure Drop [bar]
0.8	0.0007	0.0037	0.0030	6.886	8.607	1.721	200.6	7.349	0.0073	5521.244	Turbulent	0.0092	11579.43	0.116
0.8	0.0009	0.0043	0.0034	7.870	9.837	1.967	200.6	7.499	0.0075	6183.874	Turbulent	0.0089	14624.04	0.146
0.8	0.0009	0.0046	0.0037	8.525	10.657	2.131	200.6	7.599	0.0076	6611.105	Turbulent	0.0087	16830.52	0.168
0.8	0.0010	0.0050	0.0040	9.181	11.477	2.295	200.6	7.699	0.0077	7027.246	Turbulent	0.0085	19176.86	0.192
0.8	0.0011	0.0053	0.0043	9.837	12.296	2.459	200.6	7.799	0.0078	7432.724	Turbulent	0.0084	21661.93	0.217
0.8	0.0011	0.0057	0.0046	10.493	13.116	2.623	200.6	7.899	0.0079	7827.942	Turbulent	0.0083	24284.74	0.243
0.8	0.0012	0.0060	0.0048	11.149	13.936	2.787	200.6	7.999	0.0080	8213.287	Turbulent	0.0082	27044.42	0.270
0.8	0.0013	0.0064	0.0051	11.804	14.756	2.951	200.6	8.099	0.0081	8589.122	Turbulent	0.0081	29940.18	0.299
0.85	0.0007	0.0050	0.0042	9.755	11.477	1.721	150.8	9.722	0.0097	4182.153	Turbulent	0.0100	16840.61	0.168
0.85	0.0009	0.0057	0.0048	11.149	13.116	1.967	150.8	9.968	0.0100	4661.661	Turbulent	0.0096	21269.13	0.213
0.85	0.0009	0.0062	0.0052	12.078	14.209	2.131	150.8	10.132	0.0101	4968.398	Turbulent	0.0095	24480.48	0.245
0.85	0.0010	0.0066	0.0056	13.007	15.302	2.295	150.8	10.296	0.0103	5265.365	Turbulent	0.0093	27897.09	0.279
0.85	0.0011	0.0071	0.0060	13.936	16.395	2.459	150.8	10.460	0.0105	5553.021	Turbulent	0.0091	31517.54	0.315
0.85	0.0011	0.0076	0.0064	14.865	17.488	2.623	150.8	10.624	0.0106	5831.796	Turbulent	0.0090	35340.59	0.353
0.85	0.0012	0.0081	0.0069	15.794	18.581	2.787	150.8	10.788	0.0108	6102.097	Turbulent	0.0089	39365.16	0.394
0.85	0.0013	0.0085	0.0073	16.723	19.674	2.951	150.8	10.952	0.0110	6364.303	Turbulent	0.0088	43590.3	0.436
0.9	0.0007	0.0075	0.0067	15.493	17.215	1.721	100.9	14.358	0.0144	2842.991	Turbulent	0.0113	28717.54	0.287
0.9	0.0009	0.0085	0.0077	17.707	19.674	1.967	100.9	14.981	0.0150	3114.098	Turbulent	0.0110	36399.05	0.364
0.9	0.0009	0.0092	0.0083	19.182	21.314	2.131	100.9	15.396	0.0154	3282.655	Turbulent	0.0108	41990.92	0.420
0.9	0.0010	0.0100	0.0090	20.658	22.953	2.295	100.9	15.811	0.0158	3442.362	Turbulent	0.0106	47957.58	0.480
0.9	0.0011	0.0107	0.0096	22.133	24.593	2.459	100.9	16.226	0.0162	3593.899	Turbulent	0.0105	54297.68	0.543
0.9	0.0011	0.0114	0.0102	23.609	26.232	2.623	100.9	16.641	0.0166	3737.876	Turbulent	0.0103	61010.09	0.610
0.9	0.0012	0.0121	0.0109	25.084	27.872	2.787	100.9	17.056	0.0171	3874.845	Turbulent	0.0102	68093.84	0.681
0.9	0.0013	0.0128	0.0115	26.560	29.511	2.951	100.9	17.471	0.0175	4005.307	Turbulent	0.0101	75548.09	0.755

Table B.4: Pressure drop calculation for the Power law model

Foam Quality [-]	Liquid Flow Rate [m^3/s]	Mixture Flow Rate [m^3/s]	Gas Flow Rate [m^3/s]	Gas Velocity [m^3/s]	Mixture Velocity [m^3/s]	Liquid Velocity [m^3/s]	Foam Density [Kg/m^3]	Reynolds Number [-]	Flow Type [-]	Fanning Friction Factor	Pressure Drop [Pa]	Pressure Drop [bar]
0.8	0.0007	0.0037	0.0030	6.886	8.607	1.721	200.6	117647.4	Turbulent	0.00129	6510.80	0.065
0.8	0.0009	0.0043	0.0034	7.870	9.837	1.967	200.6	148696.1	Turbulent	0.00119	7858.49	0.079
0.8	0.0009	0.0046	0.0037	8.525	10.657	2.131	200.6	171108.6	Turbulent	0.00113	8796.61	0.088
0.8	0.0010	0.0050	0.0040	9.181	11.477	2.295	200.6	194860.4	Turbulent	0.00109	9764.73	0.098
0.8	0.0011	0.0053	0.0043	9.837	12.296	2.459	200.6	219927.1	Turbulent	0.00104	10761.56	0.108
0.8	0.0011	0.0057	0.0046	10.493	13.116	2.623	200.6	246286.6	Turbulent	0.00100	11785.95	0.118
0.8	0.0012	0.0060	0.0048	11.149	13.936	2.787	200.6	273918.5	Turbulent	0.00097	12836.87	0.128
0.8	0.0013	0.0064	0.0051	11.804	14.756	2.951	200.6	302804.1	Turbulent	0.00094	13913.39	0.139
0.85	0.0007	0.0050	0.0042	9.755	11.477	1.721	150.8	148962.3	Turbulent	0.00109	7365.99	0.074
0.85	0.0009	0.0057	0.0048	11.149	13.116	1.967	150.8	188862.0	Turbulent	0.00101	8868.38	0.089
0.85	0.0009	0.0062	0.0052	12.078	14.209	2.131	150.8	217734.2	Turbulent	0.00096	9912.11	0.099
0.85	0.0010	0.0066	0.0056	13.007	15.302	2.295	150.8	248386.6	Turbulent	0.00091	10987.66	0.110
0.85	0.0011	0.0071	0.0060	13.936	16.395	2.459	150.8	280789.8	Turbulent	0.00088	12093.62	0.121
0.85	0.0011	0.0076	0.0064	14.865	17.488	2.623	150.8	314917.2	Turbulent	0.00084	13228.73	0.132
0.85	0.0012	0.0081	0.0069	15.794	18.581	2.787	150.8	350744.1	Turbulent	0.00081	14391.88	0.144
0.85	0.0013	0.0085	0.0073	16.723	19.674	2.951	150.8	388247.8	Turbulent	0.00078	15582.03	0.156
0.9	0.0007	0.0075	0.0067	15.493	17.215	1.721	100.9	206638.5	Turbulent	0.00089	9070.94	0.091
0.9	0.0009	0.0085	0.0077	17.707	19.674	1.967	100.9	262725.8	Turbulent	0.00082	10894.37	0.109
0.9	0.0009	0.0092	0.0083	19.182	21.314	2.131	100.9	303401.7	Turbulent	0.00078	12158.68	0.122
0.9	0.0010	0.0100	0.0090	20.658	22.953	2.295	100.9	346655.5	Turbulent	0.00074	13459.70	0.135
0.9	0.0011	0.0107	0.0096	22.133	24.593	2.459	100.9	392449.1	Turbulent	0.00071	14795.75	0.148
0.9	0.0011	0.0114	0.0102	23.609	26.232	2.623	100.9	440747.1	Turbulent	0.00068	16165.34	0.162
0.9	0.0012	0.0121	0.0109	25.084	27.872	2.787	100.9	491517.3	Turbulent	0.00066	17567.15	0.176
0.9	0.0013	0.0128	0.0115	26.560	29.511	2.951	100.9	544729.5	Turbulent	0.00064	18999.96	0.190

Table B.5: Pressure drop calculation for the Power law model with a wall slip layer

Foam Quality [-]	Liquid Flow Rate [m^3/s]	Mixture Flow Rate [m^3/s]	Gas Flow Rate [m^3/s]	Gas Velocity [m^3/s]	Mixture Velocity [m^3/s]	Liquid Velocity [m^3/s]	Pressure Drop [Pa]	Pressure Drop [bar]
0.8	0.0007	0.0037	0.0030	6.886	8.607	1.721	2282.7	0.023
0.8	0.0009	0.0043	0.0034	7.870	9.837	1.967	2359.0	0.024
0.8	0.0009	0.0046	0.0037	8.525	10.657	2.131	2405.9	0.024
0.8	0.0010	0.0050	0.0040	9.181	11.477	2.295	2450.1	0.025
0.8	0.0011	0.0053	0.0043	9.837	12.296	2.459	2492.1	0.025
0.8	0.0011	0.0057	0.0046	10.493	13.116	2.623	2532.0	0.025
0.8	0.0012	0.0060	0.0048	11.149	13.936	2.787	2570.0	0.026
0.8	0.0013	0.0064	0.0051	11.804	14.756	2.951	2606.4	0.026
0.85	0.0007	0.0050	0.0042	9.755	11.477	1.721	2122.2	0.021
0.85	0.0009	0.0057	0.0048	11.149	13.116	1.967	2186.3	0.022
0.85	0.0009	0.0062	0.0052	12.078	14.209	2.131	2225.6	0.022
0.85	0.0010	0.0066	0.0056	13.007	15.302	2.295	2262.7	0.023
0.85	0.0011	0.0071	0.0060	13.936	16.395	2.459	2297.7	0.023
0.85	0.0011	0.0076	0.0064	14.865	17.488	2.623	2331.0	0.023
0.85	0.0012	0.0081	0.0069	15.794	18.581	2.787	2362.7	0.024
0.85	0.0013	0.0085	0.0073	16.723	19.674	2.951	2392.9	0.024
0.9	0.0007	0.0075	0.0067	15.493	17.215	1.721	2056.1	0.021
0.9	0.0009	0.0085	0.0077	17.707	19.674	1.967	2112.2	0.021
0.9	0.0009	0.0092	0.0083	19.182	21.314	2.131	2146.6	0.021
0.9	0.0010	0.0100	0.0090	20.658	22.953	2.295	2178.9	0.022
0.9	0.0011	0.0107	0.0096	22.133	24.593	2.459	2209.4	0.022
0.9	0.0011	0.0114	0.0102	23.609	26.232	2.623	2238.3	0.022
0.9	0.0012	0.0121	0.0109	25.084	27.872	2.787	2265.9	0.023
0.9	0.0013	0.0128	0.0115	26.560	29.511	2.951	2292.1	0.023

Appendix C

Laboratory Apparatus

Some pictures showing the experimental setup and the equipment used throughout the experiment are gathered in this appendix.

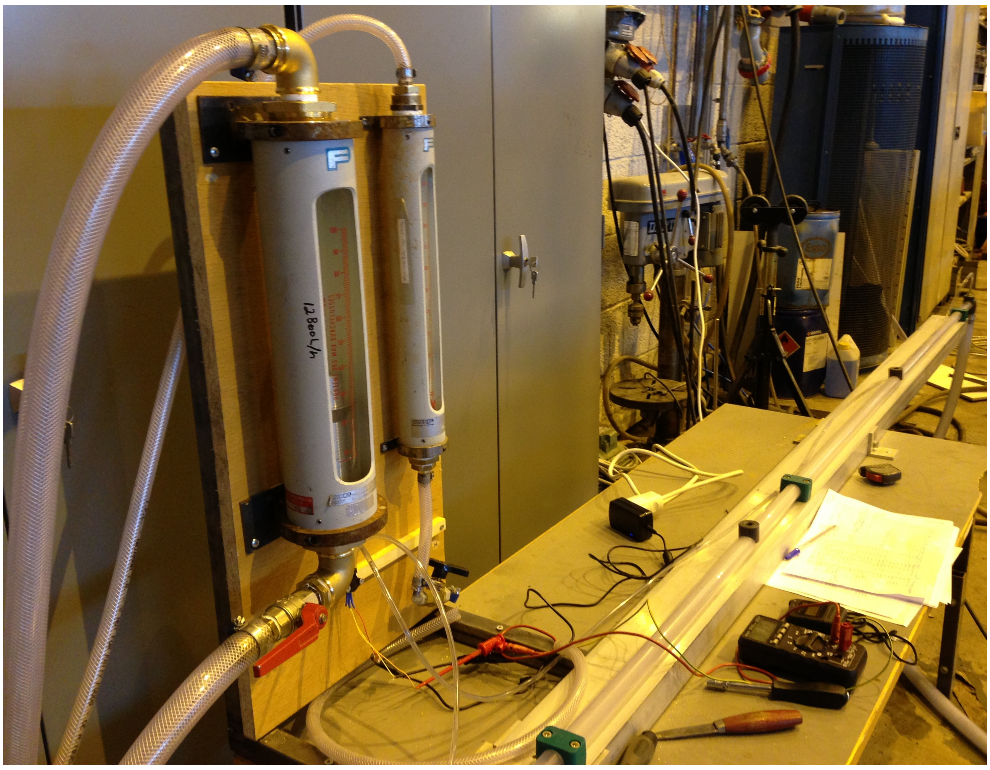

Figure C.1: Experimental setup showing the pipe, the rotameters and the voltameter

Figure C.2: Experimental setup showing the pipe, the rotameters and the tank

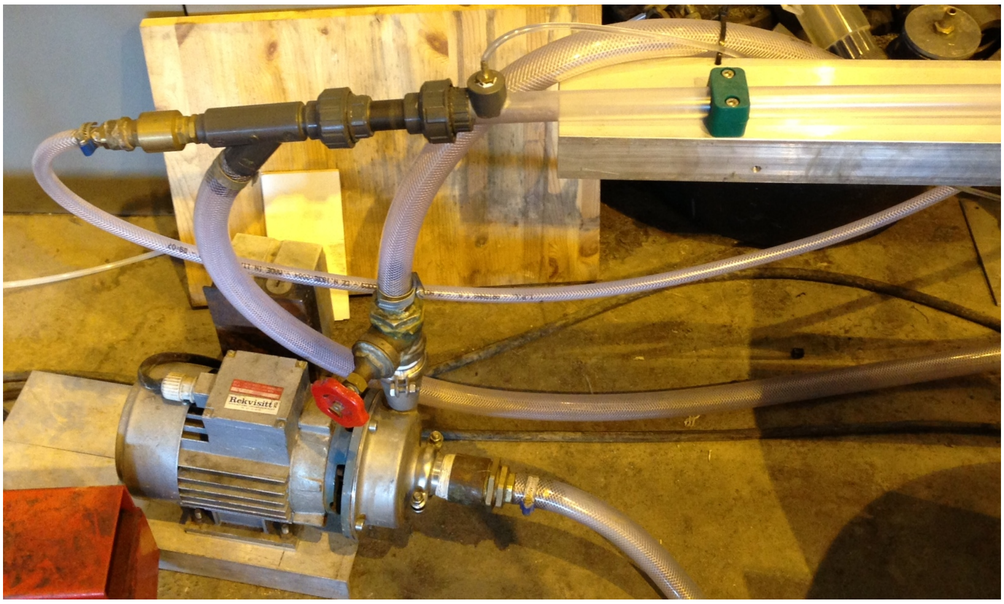

Figure C.3: A close up view of the pump, the pipe inlet with both gas and liquid inlets and the foam generator

Figure C.4: A close up view of rotameters and the pressure gauge

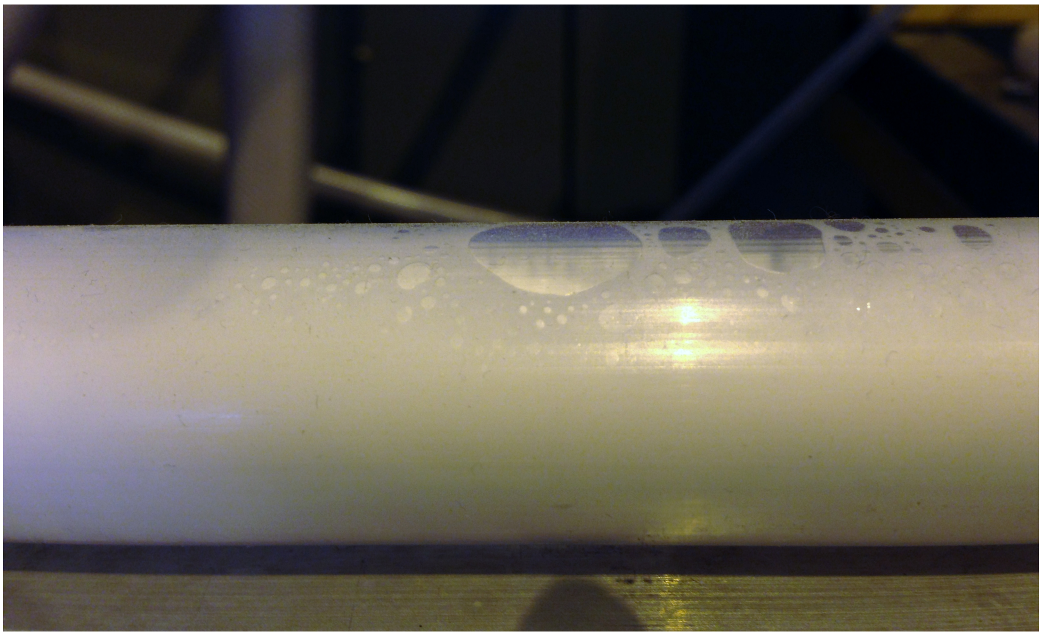

Figure C.5: A closeup view of the foam generated in the pipe

Appendix D

Flow Pattern Maps

As the experiment was set and since a multiphase flow was dominating the pipe, an additional test was conducted. The flow patterns governing the pipe are compared with the calculated operating points plotted on a flow pattern map for a multiphase flow. The calculations were made in an Excel sheet where the flow patterns were digitized by Shell DEP. Some of the flow pattern maps generated by the Excel sheet are represented in Figure D.1. The input data to excel and the resulting flow patterns are summarized in Table D.1. The blue dot represents the operating point at which the experiment is taking place. Both calculations and measurements have shown a similarity in the outcome.

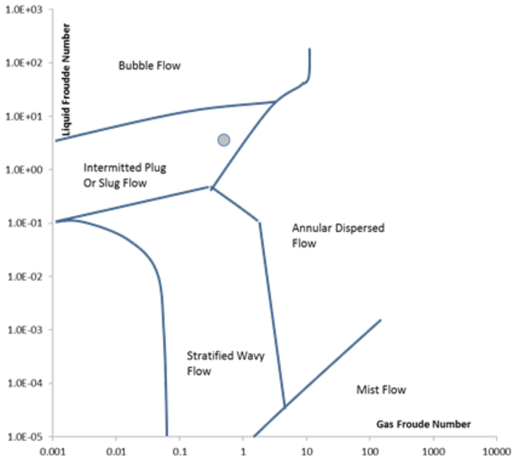

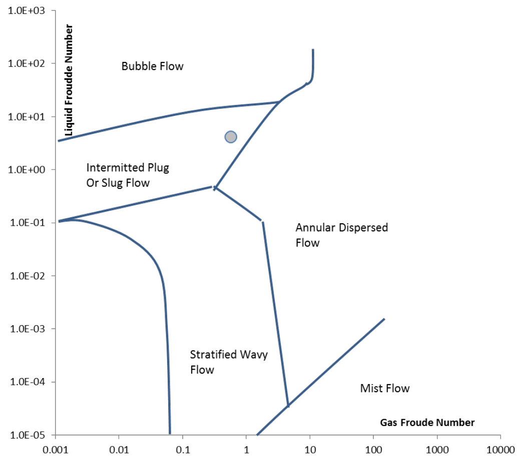

(a) Case 1

(b) Case 2

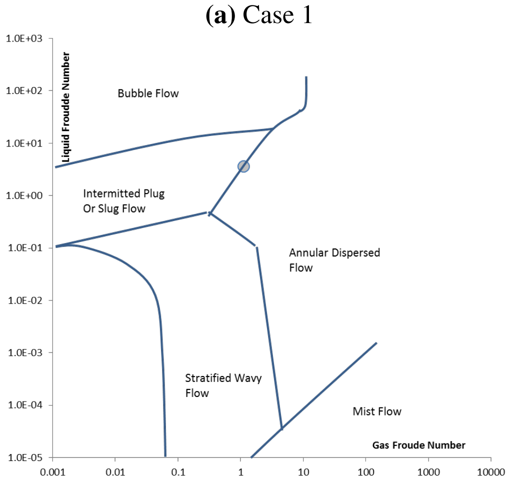

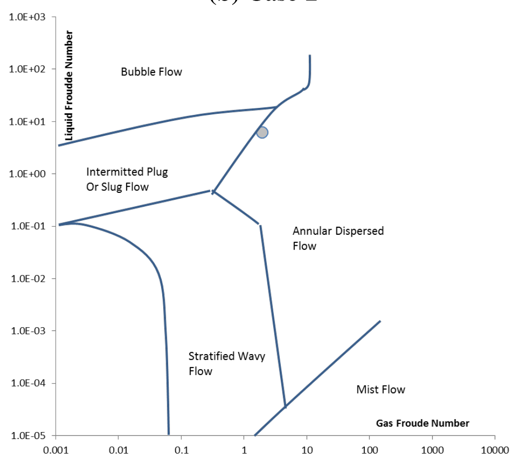

(c) Case 17

(d) Case 24

Figure D.1: Flow pattern maps of some of the cases, where the gas Froude number is plotted against the liquid Froude number, are represented. The operating points vary according to the modification of gas and liquid velocities

Table D.1: Summary of the input and output data of the Excel sheet

Case Number [−]	Liquid Flow Rate $[m^3/h]$	Gas Flow Rate $[m^3/h]$	Flow Pattern [−]
1	2.688	10.752	Intermittent Plug or slug flow
2	3.072	12.288	Intermittent Plug or slug flow
3	3.328	13.312	Intermittent Plug or slug flow
4	3.584	14.336	Intermittent Plug or slug flow
5	3.840	15.360	Intermittent Plug or slug flow
6	4.096	16.384	Intermittent Plug or slug flow
7	4.352	17.408	Intermittent Plug or slug flow
8	4.608	18.432	Intermittent Plug or slug flow
9	2.688	15.232	Intermittent Plug or slug flow
10	3.072	17.408	Intermittent Plug or slug flow
11	3.328	18.859	Intermittent Plug or slug flow
12	3.584	20.309	Intermittent Plug or slug flow
13	3.84	21.760	Intermittent Plug or slug flow
14	4.096	23.211	Intermittent Plug or slug flow
15	4.352	24.661	Intermittent Plug or slug flow
16	4.608	26.112	Intermittent Plug or slug flow
17	2.688	24.192	Middle Border of Intermittent Plug or slug flow and Annular dispersed flow
18	3.072	27.648	Border of Intermittent Plug or slug flow and Annular dispersed flow
19	3.328	29.952	Border of Intermittent Plug or slug flow and Annular dispersed flow
20	3.584	32.256	Border of Intermittent Plug or slug flow and Annular dispersed flow
21	3.84	34.56	Border of Intermittent Plug or slug flow and Annular dispersed flow
22	4.096	36.864	Annular dispersed flow
23	4.352	39.168	Annular dispersed flow
24	4.608	41.472	Annular dispersed flow